

LC-MS characterization of pigments in microalgae from different cultivation regimes

Ingunn Møgedal Stokkeland

Master's thesis in Pharmacy, May 2019

Acknowledgement

The work presented in this thesis was carried out at the Natural Products and Medicinal Chemistry Research Group, Department of Pharmacy (IFA), UiT The Arctic University of Norway in collaboration with the Norwegian College of Fishery Science (NFH) and Finnfjord AS in the period from August 2018 to May 2019. Supervisors were Associate Professor Terje Vasskog (IFA), PhD Candidate Jon Brage Svenning (NFH) and PhD Candidate Lars Dalheim.

First of all, I would like to thank my main supervisor Terje Vasskog. This thesis would not have been possible without your support, guidance and assistance throughout the period. Furthermore, I would like to thank Terkel Hansen for helping me with the Q Exactive.

I wish to express my gratitude to my external supervisors Jon Brage Svenning and Lars Dalheim for letting me participate in the cultivation and harvesting of microalgae at Finnfjord. A special thanks to the personnel at NFH who carried out the cultivation and harvesting of algae

Finally, I must show my appreciation to my family, boyfriend and friends for supporting and encouraging me throughout this period. Thank you!

Tromsø, May 2019

Ingunn Møgedal Stokkeland

Abstract

Background: The Arctic University of Norway entered a partnership with a smelting plant to reduce the factory fume CO₂-footprint by cultivation of microalgae (diatoms). The biomass produced from the microalgae is rich in lipids, proteins and pigments and can potentially function as fish feed for the aquaculture industry. Before the biomass can be utilized as e.g. fish feed, a thorough investigation of its constituents is important. In this thesis the main goals were to characterize the pigment composition in *Porosira glacialis* and investigate if different light regimes could affect the pigment composition.

Method: The microalgae, *Porosira glacialis*, cultivated in red, blue and white light regimes was included in the project. From freeze-dried algal biomass, the pigments were extracted with a mixture of methanol and acetone. Two different LC-MS techniques were investigated (Q-orbitrap and Q-TOF) for analyzing extracted pigments. Liquid chromatography coupled to Q Exactive with ESI in full scan mode was applied. A MS/MS mode was used to determine the fragmentation pattern of chlorophyll *a* and astaxanthin as well as identification of other pigments.

Results: Twelve pigments could be detected and identified in *P. glacialis*, where seven of them are carotenoids. The results suggest that light regimes can regulate the accumulation of different pigments in *P. glacialis*, especially carotene. The best light regime for accumulating chlorophyll *a* was white light.

Conclusion: The white light regime seems promising in cultivation of the microalgae, *P. glacialis*, in regards to the amount of pigments. It is however possible to induce a change in relative pigment composition by changing the color of the light during cultivation.

Table of Contents

1	Introduction	1
1.1	Background.....	1
1.2	Marine diatoms	2
1.3	Characteristics of algal pigments.....	4
1.3.1	Chlorophylls	5
1.3.2	Carotenoids.....	6
1.3.3	Phycobilins	7
1.4	Light effects on microalgal pigment content.....	8
1.5	Ultra-performance liquid chromatography (UPLC).....	9
1.6	Mass spectrometry	10
1.6.1	Ion source	11
1.6.2	Mass filter.....	12
1.7	Quantitative analysis.....	15
2	Aim of the thesis	17
3	Materials and method	18
3.1	Chemicals	18
3.1.1	Standards	18
3.2	Materials	19
3.3	Cultivation and harvesting of microalgae.....	19
3.3.1	Mass cultivation of microalgae at Finnfjord AS	20
3.3.2	Harvesting of microalgae at Finnfjord AS	20
3.4	Pigment extraction.....	21
3.4.1	Extraction method	21
3.4.2	Number of extractions needed.....	21
3.4.3	Extraction solvents	22
3.5	Calibration curves.....	23
3.5.1	Chlorophyll <i>a</i>	23
3.5.2	Astaxanthin.....	23
3.6	Analysis of extracted pigments.....	24
3.7	UPLC-MS analysis	25
3.7.1	UPLC.....	25
3.7.2	MS	29
3.8	Interpretation of chromatograms and mass spectra	32
3.9	Statistical analysis.....	32
4	Results and discussion.....	33

4.1	Extraction solvent	33
4.2	Extraction efficiency.....	36
4.3	Comparison of instruments and ion source	38
4.4	Evaluation of UPLC-MS method for pigment analysis.....	39
4.5	Pigment analysis of algal sample.....	40
4.6	MS/MS of chlorophyll <i>a</i>	45
4.7	MS/MS of astaxanthin	47
4.8	Effects of light regimes on pigment content.....	53
4.8.1	Chlorophyll <i>a</i> content in different light regimes	54
4.8.2	Relative amount of pigments.....	56
4.9	Limitations of the study	61
5	Conclusion and future perspective	63
	References	64
	Appendix	68
	Appendix 1: Summary of DHI pigment standards	68
	Appendix 2: Wavelengths of light conditions	74
	Appendix 3: Extraction test <i>P. glacialis</i>	75
	Appendix 4: Preparation of standard solutions	78
	Appendix 5: Calibration curves.....	79
	Appendix 6: t-SIM inclusion list.....	80
	Appendix 7: Extraction efficiency	81
	Appendix 8: Chromatograms of standard samples	82
	Appendix 9: Chromatograms of pigment extract.....	83
	Appendix 10: Chromatogram and mass spectra (t-SIM)	85
	Appendix 11: MS/MS of chlorophyll <i>a</i>	93
	Appendix 12: MS/MS of astaxanthin like compound.....	94
	Appendix 13: MS/MS of pigments	96
	Appendix 14: Q-test chlorophyll <i>a</i>	97

Abbreviations

ACN	Acetonitrile
APCI	Atmospheric pressure chemical ionization
AUX	Auxiliary
CI	Confidence interval
CID	Collision induced dissociation
Da	Dalton
DDA	Data dependent acquisition
DV	Divinyl
ESI	Electrospray ionization
eV	Electron volt
FA	Formic acid
HCD	Higher-energy collisional dissociation
LC	Liquid chromatography
MeOH	Methanol
MP	Mobile phase
MS	Mass spectrometry
MV	Monovinyl
m/z	Mass-to-charge ratio
PBR	Photobioreactor
PRM	Parallel reaction monitoring
Q	Quadrupole
RF	Radio frequency
RP	Reversed phase
RT	Retention time
SIM	Selected ion monitoring
TOF	Time of flight
t_R	Retention time
UPLC	Ultra-performance liquid chromatography
v/v	Volume/volume

1 Introduction

1.1 Background

The Arctic university of Tromsø (UiT) has entered a partnership with a smelting plant to reduce the CO₂-footprint from the company by cultivation of microalgae. Factory smoke from the smelting plant are lead through photobioreactors (PBR) containing microalgae, the smoke consist of large amounts CO₂, which microalgae through carbon fixations convert to organic carbon in form of carbohydrates, and oxygen is released. The reduction of CO₂ emission from the factory leads to increased algae biomass production. The biomass from the algae is rich in lipids, proteins and pigments and can e.g. potentially function as fish feed for the aquaculture industry.

Fish meal and fish oil are abundantly used in aquafeed due to their content of proteins and fatty acids (omega-3). However, decreasing fishmeal supply and increasing costs threaten the sustainability and growth of the aquaculture industry (1, 2). Consequently, alternative sources of nutrition is needed to solve this problem. In the middle of 2017, the EU commission voted to open the aquaculture feed market to insect-derived proteins. There are already new companies that have started developing insect-derived feed ingredients, e.g. InvertaPro (3, p. 19). Another commonly used ingredient in aquafeed is plant ingredients such as proteins from soy, beans and oils from rapeseed oil (4). It is important to find economical and sustainable alternative sources of proteins and lipids, and microalgae have the potential to be a part of the solution.

The project uses cold-water diatoms, *Porosira glacialis*, which is grown in photobioreactors. The diatoms were chosen because they are physiologically adapted to the northern conditions, i.e. the low naturally source of light due to winter darkness and the low temperature. *P. glacialis* is a large diatom species, which have small surface to volume ratio. This gives low self-shading levels and long light depth in the photobioreactor. This means cultivation tanks with large volume to surface area ratios can be employed, which is beneficial for mass production of microalgae in large scale.

Before the produced microalgae can be utilized as e.g. fish feed, a thorough investigation of its constituents is important. The project has so far focused on analyzing the lipid content of the

algae with focus on omega-3 polyunsaturated fatty acids. The algae have a favorable composition of fatty acids with a high content of polyunsaturated fatty acids (5). To continue the characterization of the microalgae the projects now seeks to develop methods for quantification of pigments by using LC-MS techniques (orbitrap and Q-TOF). This is somewhat challenging since pigments are easily oxidized and therefore short lived.

1.2 Marine diatoms

Diatoms are a major group of microalgae, within the Bacillariophyceae class. They have a siliceous skeleton and are found in almost every aquatic environment. Diatoms exist in different size groups from 2 μm to more than 5 mm and they consist of a frustule built as boxes with lids overlapping the lower part. It is estimated that there are more than 100 000 different species, whereas 1400-1800 species have been recorded from marine plankton. Diatoms can appear in colonies, but they are principally unicellular organism. The diatoms are divided in two different classes; centric and pennate diatoms. Centric diatoms have a circular circumference and the striae (= rows of areolae), radiate from a point, whereas the pennate diatoms are linear and the striae point to a line (Figure 1) (6, p. 112-114).

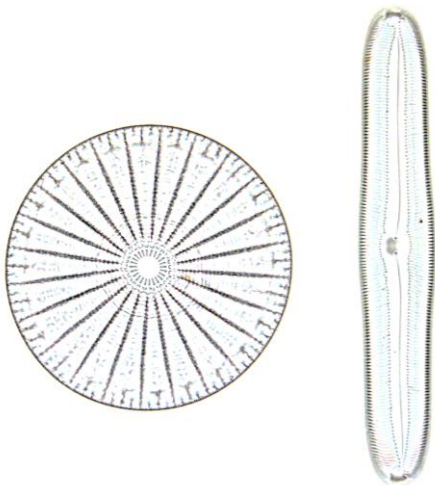


Figure 1 - Centric vs. pennate diatoms (7).

Mass cultivation of diatoms shows great potential, one of the reasons for this is due to their high growth rates. There are different factors affecting the growth and pigment production in

diatoms such as temperature, pH, nutrients, light and salinity (8, 9). Mass cultivation of diatoms occurs in closed systems, such as indoor/outdoor photobioreactors. In such bioreactors, diatoms are grown in highly selective conditions. Outdoor cultivation of diatoms is mainly devoted to the industry of aquaculture. Light is an essential resource for all algae, which drives the photosynthesis. Algae can utilize both solar and artificial light, however, a homogenous light intensity would be ideal to ensure that all algae cells are equally exposed to the light (10).

The project uses a strain called, *Porosira glacialis*, it is a large cold-water diatom with a diameter of 36-64 μm (Figure 2). *P. glacialis* is common in Norwegian coastal waters and is one of the main components in the plankton early in the spring bloom. *P. glacialis* is characterized by the unique valve structure - numerous strutted processes, the weak silification and the striae in a wave-like conformation (6, p. 130).

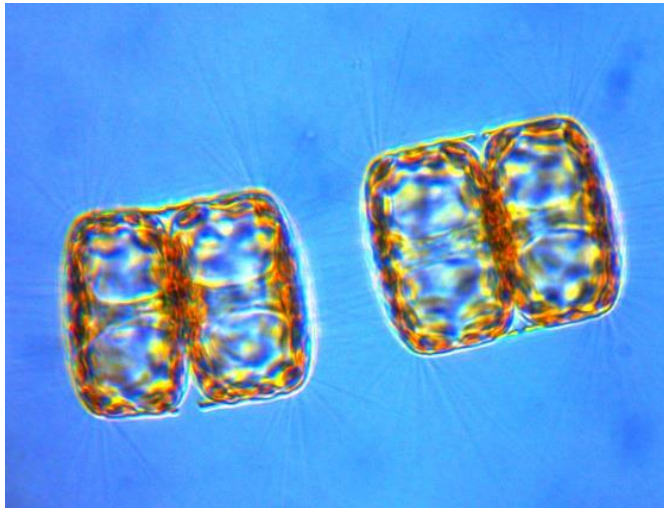


Figure 2 - *Porosira glacialis* (photo by Richard Ingebrigtsen).

The growth of diatoms is characterized by three phases, the lag phase, the exponential phase and the stationary phase. In the lag phase, there is little increase in cell density and this lag of growth may be the cause of physiological adaptations. The diatoms divide rapidly in the exponential phase. But when the physical and/or chemical factors such as space or nutrients begins to run out cell division slows down, this phase is called the stationary phase. In the exponential phase higher concentrations of light-harvesting pigments can be found compared to the stationary phase (11).

There are numerous commercial applications of algae. Algae are a rich source of proteins, vitamins, fatty acids and pigments, and can as an example be used to enhance the nutritional value in fish feed. There are several genera of microalgae used in the aquaculture as feed for larvae, rock scallops and oysters (e.g. *Chlorella*, *Spirulina*, *Thalassiosira* and *Dunaliella*) (12, 13).

Microalgae shows a great potential as feed in the aquaculture because, of their nutritional quality and potentially good availability. They are also a great source of naturally occurring pigments. The characteristic pink color of salmon flesh is obtained by carotenoid pigments from crustaceans they eat (e.g. shrimp). Synthetically produced carotenoids, e.g. astaxanthin, are added to the fish feed since farm-raised salmon do not have access to it (14). Studies of algae in fish diets shows positive effects, including increase in physiological activity, growth performance and disease resistance (1). Researchers at Nofima are investigating if microalgae used as fish feed could reduce the amount of sea lice on the salmon. The researchers says that oxylipids from omega-3 works deterrent on the sea lice (15).

Microalgae can also be utilized in the cosmetic industry. For instance, polysaccharides like alginate, fucoidan and laminaran found distributed in the cell walls of brown algae have antioxidative properties and can thus be applied in creams to prevent skin aging. Antioxidants can also be applied to cosmetic products to prevent lipid oxidation, avoiding changes in odor, flavor and appearance. Alginate can also be used as a thickening agent and stabilize emulsions. There is also an increasing demand for natural pigments, rather than chemically synthesized pigments. Carotenes and xanthophylls are used as natural color enhancers (16).

1.3 Characteristics of algal pigments

The pigments from microalgae are broadly used in different industries; food, cosmetic, nutraceutical and in the pharmaceutical aquaculture. There are three major classes of photosynthetic pigments in microalgae, they are chlorophylls, carotenoids and phycobiliprotein, which exhibit colors ranging from green, brown yellow to red. In diatoms chlorophylls and carotenoids are the most common pigments (8).

1.3.1 Chlorophylls

One of the most important bioorganic molecules are the chlorophylls; they are the principal pigments in photosynthesis. They comprise a group of more than 50 tetrapyrrolic pigments with common structural elements and function (17, 18). It is a pigment found in algae, phytoplankton and plants and makes them appear green because it reflects the green wavelengths found in sunlight. Several forms of chlorophylls have been identified in photosynthetic organisms, however, only two forms occur in diatoms: chlorophyll *a* (Figure 3, left) and chlorophyll *c* (*c*₁, *c*₂ and rarely *c*₃ have been identified). Chlorophyll *a* are found in various algae and plays a central role in the photochemical energy conversion, while chlorophyll *c* participates in photosynthesis as an accessory pigment. Chlorophyll *a*, exists in their monovinyl (MV) form (Figure 3, left) and in divinyl (DV) form. Chlorophyll *b* is found mainly in land and aquatic plants, however, in diatoms, instead of chlorophyll *b*, chlorophyll *c* have been identified (19, 20).

Chlorophylls are cyclic tetrapyrroles with a characteristic isocyclic five-membered ring with a magnesium (Mg^{2+}) ion as the central metal. There are chlorophylls that do not have the central Mg^{2+} , like pheophytins (Figure 3, right).

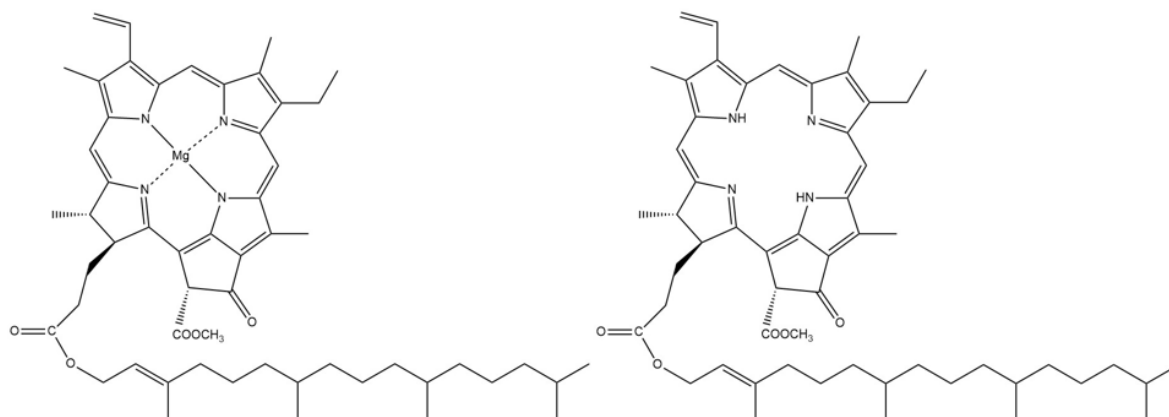


Figure 3 - Chlorophyll *a* (left) and pheophytin *a* (right)

1.3.2 Carotenoids

Carotenoids are naturally occurring pigments that serve a multitude of functions. They absorb light in the spectral region, in which the sun irradiates maximally and transfer the energy to chlorophylls, which in turn initiates the primary photochemical events of photosynthesis, and they also act as antioxidants. There are more than one thousand carotenoids, but only around 50 of them play a role in the photosynthesis (21, 22). Carotenoids consist of terpenoid pigments that are derived from a 40-carbon polyene chain and they may be complemented by cyclic groups and functional groups containing oxygen such as lutein (Figure 4) and astaxanthin (Figure 5) (8).

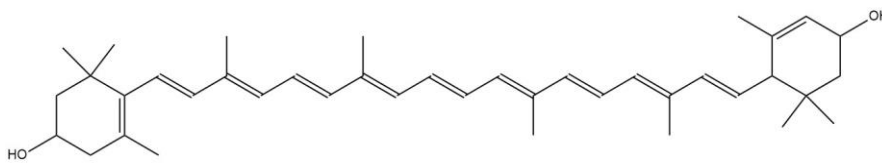


Figure 4 - Chemical structure of lutein

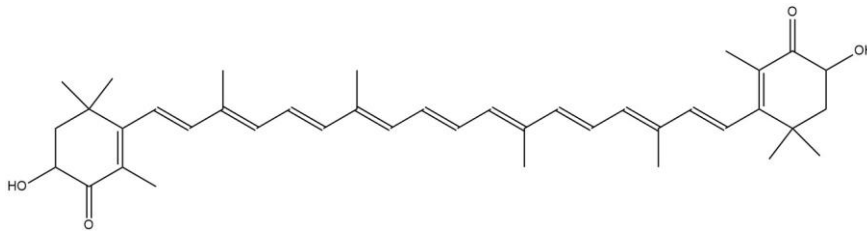


Figure 5 - Chemical structure of astaxanthin

Astaxanthin is a red pigment common to many marine animals, such as shrimp and salmon, contributing to the pink/red color of their flesh. Microalgae biosynthesize astaxanthin and function as the primary production level in the marine environment. Astaxanthin can also be synthesized by fungi, bacteria and plants. There has been a growing interest in the use of astaxanthin as natural feed additive for the aquaculture industry (23). Astaxanthin is also a precursor of vitamin A and have strong antioxidant properties. Therefore, astaxanthin also have potential in applications in human health and nutrition (23, 24).

1.3.3 Phycobilins

Phycobilins are found in the chloroplasts of red algae and in most cyanobacteria. These pigments are covalently bound to phycobiliproteins. Phycobilins consist of a chain of four pyrrole-like rings, e.g. tetrapyrrole. They are assembled in phycobilisomes, which are located on the surface of the photosynthetic membrane; the thylakoids. In most cyanobacteria, C-phycoerythrin (Figure 6), is the main phycobiliprotein (8).

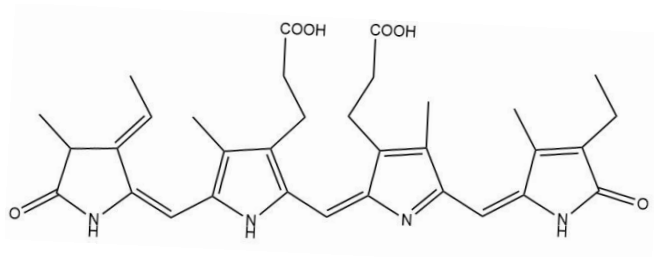


Figure 6 - Chemical structure of C-phycoerythrin

Phycobiliproteins are being used as natural dyes, for example can they replace synthetic pigments in food and makeup. Such as the blue color of phycoerythrin could be used as colorant in chewing gums, drinks and dairy products (25). A phycobilin called phycoerythrin (Figure 7) has yellow fluorescence properties and can therefore be used as a second color in fluorescent-labeling antibodies (8).

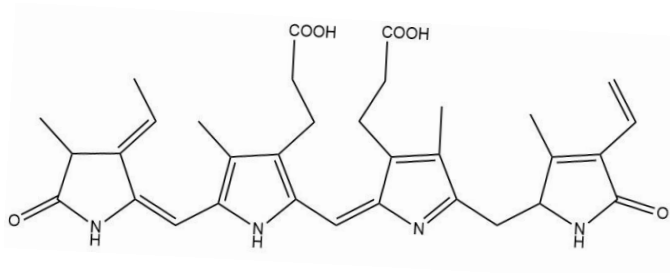


Figure 7 - Chemical structure of phycoerythrin

1.4 Light effects on microalgal pigment content

Algal growth is affected by several parameters, but the role of light is very important. Darkness, light, light limitation, photoperiod and irradiance are important factors for algal growth, lipid and pigment accumulation and reproduction. Algae contains light harvesting chlorophylls and other accessory pigments, which is vital for photosynthesis (26). Generally, microalgae utilize light of wavelengths from 400 to 700 nm for photosynthesis, in addition, the amount of light absorbed depends upon the pigment composition and concentration in the algae. Depending on the species, microalgae absorb different wavelengths, for example, green microalgae absorb light through chlorophylls in the range of 450-475 nm and 630-675 nm and through accessory pigments, carotenoids, in the range of 400-550 nm (27).

In the green algae, *Dunaliella salina*, it has been shown that when cultured under high light intensities (32.43 $\mu\text{molphoton}/\text{m}^2/\text{sec}$, white light) both chlorophyll and β -carotene accumulation was low compared to low light intensities (11.28 $\mu\text{molphoton}/\text{m}^2/\text{sec}$, white light) (8, 28). However, it has been reported that intense light illuminating can induce oxidative stress resulting in an increase of carotenoid content (29). When the green microalgae, *Haematococcus pluvialis*, was illuminated with intense light intensities (350 $\mu\text{molphoton}/\text{m}^2/\text{sec}$, fluorescent light) the astaxanthin accumulation increased by at least 4-fold compared to lower light intensities (75 $\mu\text{molphoton}/\text{m}^2/\text{sec}$, fluorescent light). This is most likely an reaction, by which astaxanthin protects against photooxidative damage (30).

In another green microalgae, *Chlorella vulgaris*, the maximum amount of chlorophyll *a* was obtained with green light (0.241 mg/ml), followed by white light (0.164 mg/ml), blue light (0.118 mg/ml) and red light (0.092 mg/ml). The amount of astaxanthin was highest when cultured under blue light (0.036 mg/ml) and lowest under red light (0.018 mg/ml). However, the optimal growth of *Chlorella vulgaris* occurred under red light (31). This opens for the possibility of manipulation of environmental factors in cultivation of microalgae with focus on improving content of high value compounds, like pigments.

1.5 Ultra-performance liquid chromatography (UPLC)

In theory both HPLC and GC can be used for separation and identification of pigments, but due to the low stability and volatility of pigments, HPLC is a better choice than GC. There are several developed liquid chromatography (LC) methods described in the literature for separating and measuring pigments since the 1980s. Separation of pigments are usually conducted with use of reversed phase (RP) conditions and columns packed with stationary phases having an aliphatic chain length of C₈, C₁₈ or C₃₀ (32). There are some differences regarding column performance with regards to the aliphatic chain length. For example, C₈ columns makes it possible to separate chlorophylls from their divinyl forms (32, 33). Columns with C₁₈ stationary phase have also been reported to yield sufficient separations of several pigments, especially the carotenoids (32, 34-36). Ethylene bridged hybrid (BEH) C18 columns have also been successful to separate several pigments (36).

In this thesis ultra-performance liquid chromatography (UPLC) with a reverse phase column was used. UPLC are systems capable of running at very high pressure and employs particles smaller than 2 μm in diameter. The LC system consist of three main parts; the solvent delivery, the separation column, which is where the separation occurs and lastly the detector (Figure 8). The mobile phase is pumped at a constant flow through the column and separation of the analytes occurs based on affinity for the stationary phase.

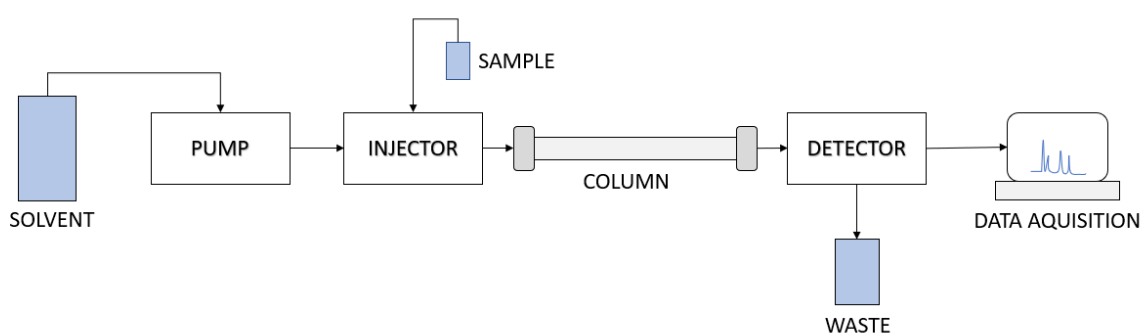


Figure 8 - Overview of a liquid chromatograph

In reversed phase (RP) chromatography the main separation mechanism is hydrophobic interactions. Consequently, polar analytes will elute earlier in the chromatogram and nonpolar analytes are retained strongly and elutes therefore late. The mobile phases used for RP chromatography consist of one or more water miscible organic solvents and water. The strength

of the mobile phase will also play a role in determining the retention of analytes, e.g. increasing the amount of organic solvents increase the strength of the mobile phase and retention of analytes decreases (37).

1.6 Mass spectrometry

A mass spectrometer can be used as a detector for liquid chromatography. Mass spectrometry (MS) is an analytical method for measuring molecular mass of chemical compounds and/or their fragments, it can be used for both quantitative analysis and identification. A mass spectrometer consists of a sample inlet, an ion source, one or more mass filters, a detector and a data system (Figure 9). First the sample enters the mass spectrometer through the inlet, molecular ions are formed in the ion source, which might further be decomposed into smaller fragment ions. The mass filter separates the ions according to their mass-to-charge ratio, m/z , then a detector measures the abundance of the separated ions and the signals are recorded by a data system. The computer displays the signals graphically as a mass spectrum where m/z is plotted against relative intensity.

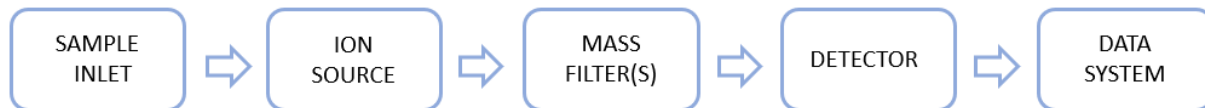


Figure 9 - Overview of a mass spectrometer.

Previously, the most conventional method for quantification of pigments relied on ultraviolet (UV) detection. However, in recent years there has been a widespread use of mass spectrometry (MS), which has led to considerable new advantages in pigment analysis. MS allows us to distinguish between co-eluting pigments and it also provides data on isomers, which conventional LC-UV systems could not achieve (22). MS analysis also provides exact mass measurements and fragmentation information from both chlorophylls and carotenoids, which we would not achieve with UV alone (38). Many carotenoids exhibit similar UV-Vis spectra (e.g. α -cryptoxanthin and zeinoxanthin), MS has permitted the discrimination of pigments that exhibit indistinguishable UV/Vis spectra (34). LC-MS/MS provides more confirmative information, which is needed due to the complexity of the algae samples.

1.6.1 Ion source

In order for the analytes to be detected by the MS, the molecules must be charged. The charged intact ions are called protonated/deprotonated molecular ions in the case of protonation/deprotonation as ionization method. This molecular ion might be further decomposed into smaller fragment ions. Several ionization techniques have been used for MS analysis of chlorophylls and carotenoids, including fast atom bombardment (FAB), matrix-assisted laser desorption/ionization (MALDI), electrospray ionization (ESI) and atmospheric pressure chemical ionization (APCI). In pigment analysis on LC-MS, atmospheric pressure ionization techniques such as APCI and ESI are most widely used (34, 39).

However, electron ionization has been used in analyzing carotenoids in mass spectrometry. But it has several limitations due to that the technique requires the sample to vaporize, which is a huge disadvantage when analyzing thermally labile and non-volatile pigments like carotenoids. Additionally, spectra acquired from electron ionization have minor or absent molecular ions, hence, a second ionization technique like FAB, which is a softer ionization technique, is required to use to provide molecular information (39).

1.6.1.1 Electrospray ionization

Electrospray ionization takes place under atmospheric pressure outside the vacuum region of the MS. ESI uses electrical energy to assist the transfer of ions from solution into gaseous phase. The mobile phase from the UPLC column passes through a narrow capillary. A fine aerosol is formed at the end of the capillary by nitrogen gas flowing along the tip (nebulizing gas). Between the capillary tip and the sampling cone, a voltage is applied. A fine aerosol is formed at the end of the capillary by nitrogen gas flowing along the tip (nebulizing gas). The aerosol consists of several small droplets, the surface of the droplets containing the ionized analytes becomes charged due to the potential difference between the capillary and the sampling cone. The small droplets will shrink by evaporation of the mobile phase and the charge density increases. This leads to repulsion forces between the charges until the droplet undergoes coulombic explosion. The charged analyte ions are extracted into the vacuum area of the mass spectrometer for further analysis by the mass filter (37, 39).

1.6.1.2 Atmospheric pressure chemical ionization

In atmospheric pressure chemical ionization (APCI) the analytes (eluent) is introduced into the interface using a capillary, similar in design to the ESI source. In APCI no potential is applied to the capillary, instead the solution emerges from the capillary surrounded by a flow of nebulizing gas into a heated, vaporizing region. The combination of gas and heat converts the solution into an aerosol that begins to rapidly evaporate. The analytes are then ionized by a corona discharge with a high potential (5-10 kV) applied and produces an electrical discharge, which ionizes the analytes within the aerosol. Like the ESI source, it can generate both positive and negative ions. It is a relatively soft ionization technique, and mainly molecular ions are formed (37).

1.6.2 Mass filter

A mass filter separates the ions according to their mass-to-charge ratio (m/z). Mass filters commonly used in LC-MS instruments are quadrupole (Q), ion trap, orbitrap and time of flight (TOF). Many instruments also feature several mass filters coupled together and the quadrupole has become an integral part of some of the most sophisticated mass spectrometers, such as Q-TOF and Q-Orbitrap. Such instruments are often referred to as a “hybrid” mass spectrometer. Generally, the goal in the design of a hybrid instrument is to combine different performance characteristics offered by various types of filters into one instrument. Such performance characteristics may include the ion kinetic energy for collision-induced dissociation, mass resolving power and speed of analysis.

A quadrupole mass filter is made up of four parallel rods to which are applied both a constant voltage and a radio frequency (RF) oscillating voltage (Figure 10). The electric field deflects ions in trajectories as they pass through the quadrupole. By varying voltages on the electrodes, only selected ions will pass through and reach the detector. Other ions collides with the rods and do not reach the detector (37, p. 250-251).

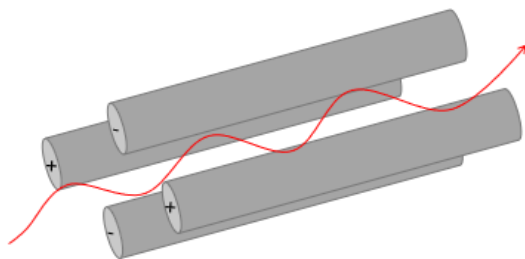


Figure 10 - Quadrupole mass filter

Mass spectrometers can either be set to scan over a mass range or to detect specific masses. When using *full scan mode*, a wide mass range is scanned. By choosing to set the mass spectrometer to detect specific masses, only certain m/z values reach the detector, this is called *selected ion monitoring (SIM)*. It is common to operate the mass spectrometer in SIM when performing quantitative measurements. If SIM does not give adequate sensitivity or specificity, tandem mass spectrometry (MS/MS) mode can be applied (37, p. 254-255).

1.6.2.1 Quadrupole orbitrap

In this thesis a quadrupole coupled to an orbitrap was used to analyze extracted pigments from algae (Figure 11). The instrument is termed “Q Exactive” and is a Fourier Transform based hybrid instrument. This hybrid instrument combines the sensitivity and speed of the quadrupole with the high mass accuracy and high resolution of orbitrap. The quadrupole mass filter allows transfer of specific m/z ions into the C-trap for accumulation, thus improving sensitivity for MS/MS experiments. The orbitrap consists of a small electrostatic device into which packets of ions are injected at high energies to orbit around a central, spindle shaped electrode. Image current signals are converted into frequencies by Fourier transformation. The frequencies, which are characteristic of each ion m/z value, are finally converted into a mass spectrum (40).

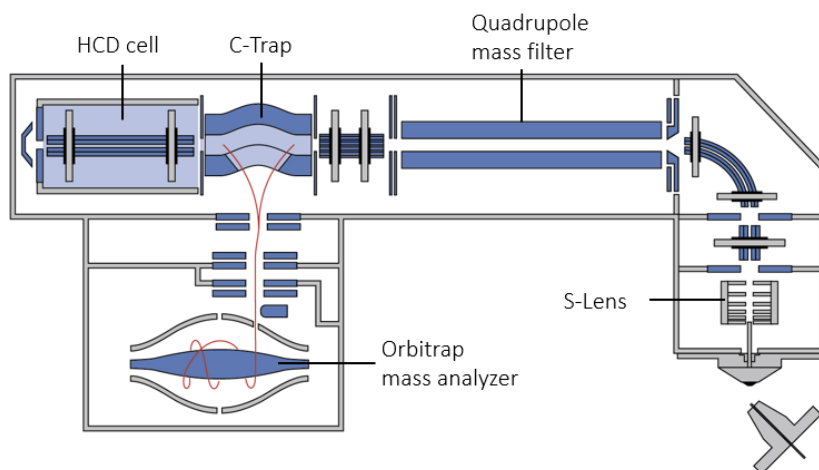


Figure 11 - Schematic overview of the Q Exactive. This instrument incorporates an S-lens, a quadrupole, an HCD collision cell directly interfaced to the C-trap and an orbitrap mass analyzer (41).

To better understand the structural composition of a molecule, a dissociation technique is used to fragment the analyte into smaller constituents. In the Q Exactive fragmentation is obtained by higher-energy collisional dissociation (HCD) cell, which uses higher RF voltage to retain fragment ions in the C-trap where they are cooled and stored. Ions are then injected from the C-trap into and separated inside the orbitrap based on their rotational frequency differences (Figure 11) (41).

1.6.2.2 Quadrupole time of flight (Q-TOF)

Pairing a quadrupole (and collision cell) with a time-of-flight mass filter, allows high-resolution, high mass accuracy analysis of all ions simultaneously. The principle of TOF is that ions are formed in the ion source and accelerated in pulses by means of an electrical potential imposed on a back plate right in the back of the ion source. All the ions are accelerated to the same kinetic energy ($\frac{1}{2} * mv^2$), which means that the lighter ions will travel faster than the heavier ions. The flight time in the flight tube is then used to determine the m/z value of the ions.

Fragmentation via tandem mass spectrometry (MS/MS) can be achieved with collision induced dissociation (CID). In the Q-TOF, precursor ions are selected in the quadrupole and sent to the collision cell where the ions form fragments. The produced product ions are then separated and their m/z value are measured by the TOF analyzer.

1.7 Quantitative analysis

A general method for determining the concentration of an unknown sample is the use of a standard curve. The standard curve is a plot that shows how the detector response changes with the concentration of the target analyte. Standard solutions are prepared from stock solutions with known concentration. The concentration range should be the same as or preferably wider than the expected concentration range of the analyte. When plotting the detector response of the standard solutions along the y-axis and the concentration along the x-axis typically yields a linear relationship that fit the equation $y = ax + b$, where a is the slope and b is the intercept. From this equation the unknown analyte concentration, x , could be calculated. With a linear regression analysis, the coefficient of determination (R^2 value), is given. The R^2 value is a statistical measurement of how close the data are to the fitted regression, and hence the uncertainty of the concentration calculated from the standard curve. The R^2 value is given as a number between 0 and 1, where 1 indicates that the model explains all the variability of the response data around its mean. In general, the higher the R^2 value, the better the model fits your data.

Quantitative analysis is typically carried out using either external or internal standards. For external standards, a standard curve is produced to show the relationship between concentration and peak size (area) or peak intensity for the analyte. Then, the sample is run separately from the standard. This is a simple analysis to carry out, however, the precision is limited by changes that may take place between runs and there is no compensation for losses of sample during sample preparation (42). Airs and Keely determined the concentration of chlorophyll *a* and pheophytin *a* using the peak area (43), however, no studies could be found where the concentration of pigments were determined from peak intensity. Nonetheless, peak intensity have been used for quantification of peptides and carboxylic acid metabolites in other studies (44, 45).

Quantification with internal standard (IS) will correct for uncontrolled loss of analyte, during sample preparation or analysis. The internal standard is a substance which is added in the same sample as the analyte of interest, allowing the measurements to be taken simultaneously. Instead of basing the results on the absolute response of the analyte, they are based on the ratio of responses to the analyte and the IS. An internal standard would be beneficial where there are

multiple sample preparation steps, in which volumetric recovery may vary to decrease the accuracy of the results (46).

2 Aim of the thesis

The main aim of this master thesis was to characterize the pigment composition in *Porosira glacialis* and investigate if different light conditions could affect the pigment composition. To achieve this the following sub goals were set:

- Investigate different cultivation conditions (light).
- To develop a separation method on UPLC-MS.
- To develop optimized methods on different MS instruments, for comparing analytical methods on algal pigments.
- Test different pigment extraction methods.
- Use the optimized methods on extracts from microalgae cultivated with different light conditions.

3 Materials and method

3.1 Chemicals

Table 1 - Chemicals and solvents

Substance	Purity	CAS-number	Supplier
2-propanol (isopropanol)	100.0%	67-63-0	VWR International S.A.S., Fontenay-sous-Bois, France
Acetone	≥99.5%	67-64-1	Merck, Darmstadt, Germany
Acetonitrile	≥99.9%	75-05-8	VWR chemicals, Fontenay- sous-Bois, France
Formic acid	98-100 %	64-18-6	Merck, Darmstadt, Germany
Milli-Q Water			Merck Millipore, Billerica, MA, USA
Methanol	≥99.9%	67-56-1	Merck, Darmstadt, Germany
Midazolam			Available in solution at UiT, origin unknown

3.1.1 Standards

The pigment standards were purchased from DHI (Hørsholm, Denmark), the content was a mixture of phytoplankton pigments in 90% acetone (1 mL vials). The mixture contains more than 20 different pigments; chlorophyll c_3 , chlorophyll c_2 , divinyl protochlorophyllide (Mg-DVP), chlorophyllide a , peridinin, peridinin isomer, 19'-but-fucoxanthin, fucoxanthin, neoxanthin, prasinoxanthin, violaxanthin, 19'-hex-fucoxanthin, astaxanthin, diadinoxanthin, alloxanthin, diatoxanthin, zeaxanthin, lutein, DV chlorophyll b , chlorophyll b , crocoxanthin, DV chlorophyll a , chlorophyll a , pheophytin a , alpha + beta carotene. The concentration of the individual pigments in the mixture is unknown, except for chlorophyll a , that has a concentration of 3.31 mg/L. All standards were stored frozen, below -20 °C, in the sealed vial. The molecular formula and structure of the pigments are listed in Appendix 1: Summary of DHI pigment standards.

A pure standard of astaxanthin (*all-trans-Astaxanthin*) as powder, was purchased from Merck (Darmstadt, Germany).

3.2 Materials

Table 2 - Materials used for pigment extraction

Description	Name of equipment	Supplier
Analytical balance	Sartorius Entris 224I-1S	Sartorius, Göttingen, Germany
Brown glass vials	Amber vials, screw top	Merck, Darmstadt, Germany
Filter	Acrodisc 13 mm minispice with 0.2 μm GHP	Pall Corporation, Puerto Rico
Finntip pipettes in different sizes		Thermo Fisher Scientific, Vantaa, Finland
Freeze dryer	Labconco 12 port freeze dry system	Labconco Corporation, Kansas City, MO, USA
Glass Pipettes	Glass Pasteur pipettes 150 mm	VWR International, West Chester, PA, USA
LC-MS vials	12x32 mm glass screw neck vial, silicone/PTFE septa	Waters, Milford, MA, USA
Nitrogen evaporator	Stuart sample concentrator, SBHCONC/1	Cole-Parmer, UK
Ultrasonic bath	2231 Branson	Branson ultrasonics, Danbury, USA
Vortexer	Vortex 1	IKA Works, Staufen, Germany

3.3 Cultivation and harvesting of microalgae

All cultivations were performed by personnel at the Norwegian College of Fishery Science (NFH). See Bjørnstads bachelor thesis for a detailed description of cultivation parameters (47).

Briefly, cultivation of *P. glacialis* was performed in parallel triplicates of 4 liter polycarbonate bottles (Nalgene, Thermo Scientific) using filtered and pasteurized (70 °C) seawater added 4 mL/L Guillard's F/2 medium and 12.32 μM sodium metasilicate nonahydrate ($\geq 98\%$). Constant illumination was provided using LED strips (North Light, Clas Ohlson) calibrated to a scalar irradiance of 32 $\mu\text{molphoton m}^{-2} \text{ s}^{-1}$ set to white, blue and red light for each triplicate, respectively. Culture growth was monitored by daily cell counts ($n=4$ for each replicate) and *in vitro* chlorophyll *a* measurements and calculated as the specific growth rate (μ ; doublings hour⁻¹). The cultures were harvested by filtration through a plankton net (KC Denmark, Silkeborg, Denmark) and subsequent storage at -80 °C prior to pigment extraction. See Appendix 2: Wavelengths of light conditions for further information about the wavelength for red, blue and white light.

The specific growth rate for each irradiance type was calculated from the cell counts using the 1st order differential equation for exponential growth:

$$\mu = \ln(X/X_0)/t \quad (1)$$

Where X is the cell count at time t, X₀ is the initial cell count and t is the time in hours.

3.3.1 Mass cultivation of microalgae at Finnfjord AS

The microalgae, *Porosira glacialis*, was cultivated in a nutrient replete environment in a 6 000 L fiberglass tank at the factory facilities at Finnfjord AS. The tank was supplied with seawater from Finnfjordbotn, which were filtered prior to addition. The algae cell count was maintained at approximately 9 000 000 cells/L, at a temperature of 8.0 °C and a pH of 8.6. The algae culture was illuminated by a 200 W LED light (JM Hansen, Norway) placed in the center of the tank. In order to prevent sedimentation of the algae, air was continuously added from the bottom of the tank.

3.3.2 Harvesting of microalgae at Finnfjord AS

Algal biomass was harvested in the exponential growth phase by filtrating 500 liters of algal culture through a 20 µm pore size plankton net at a flow of 6 L/min. The filtered algal sample was then centrifuged at 3500 rpm (Rotina 380, Hettich Zentrifugen) for 5 minutes. After centrifugation, the supernatant was discarded and only the algal biomass was taken for further investigation. Finally, the algal biomass was filled in containers and wrapped in aluminum foil, then stored in a biofreezer at -80 °C. The algae was harvested in order to be analyzed on an optimal method for pigment analysis.

3.4 Pigment extraction

Disruption of the cell wall is necessary to extract the pigments from algae; it can be done either chemically, mechanically (ultrasound) or physically (freeze-thaw cycles). The pigment extraction procedure was carried out under dim light to prevent photooxidation of pigments. Different extraction solvents (Table 3) and number of extractions were tested on samples of *Porosira glacialis*. Prior to pigment extraction, all algae samples were freeze-dried for two days and crushed with a mortar into a fine powder.

3.4.1 Extraction method

Approximately 10 mg of pulverized sample material was weighed into a brown vial (exact mass was noted). 2 mL of extraction solvent was added to the sample (see Table 3). The sample was shaken for a few seconds, then vortexed for another few seconds. The sample was placed in a glass container filled with crushed ice and the container was placed in an ultrasonic bath for 30 minutes. The extract was pipetted out with a glass pipette into a container and filtered (0.2 μ m) into a LC vial prior to analysis to remove cells and cell debris. Then the vial was placed in a freezer until analysis. The same sample was re-extracted two more times with the same procedure (i.e. three extractions in total on the same pellet).

3.4.2 Number of extractions needed

The number of extractions needed was studied by analyzing each extraction done by the extraction method described. Since the standard mix from DHI was solubilized in 90% acetone, this solution was used as extraction solvent in the preliminary extractions. A sample of *P. glacialis* was re-extracted three times and analyzed on the Q Exactive mass spectrometer.

Three extractions were tested on the same algae sample. Figure 12 displays extracted ion chromatogram of chlorophyll *a* that shows a high relative abundance in all three extractions. Additional examples of other pigments extracted ion chromatograms can be found in Appendix 3: Extraction test *P. glacialis*.

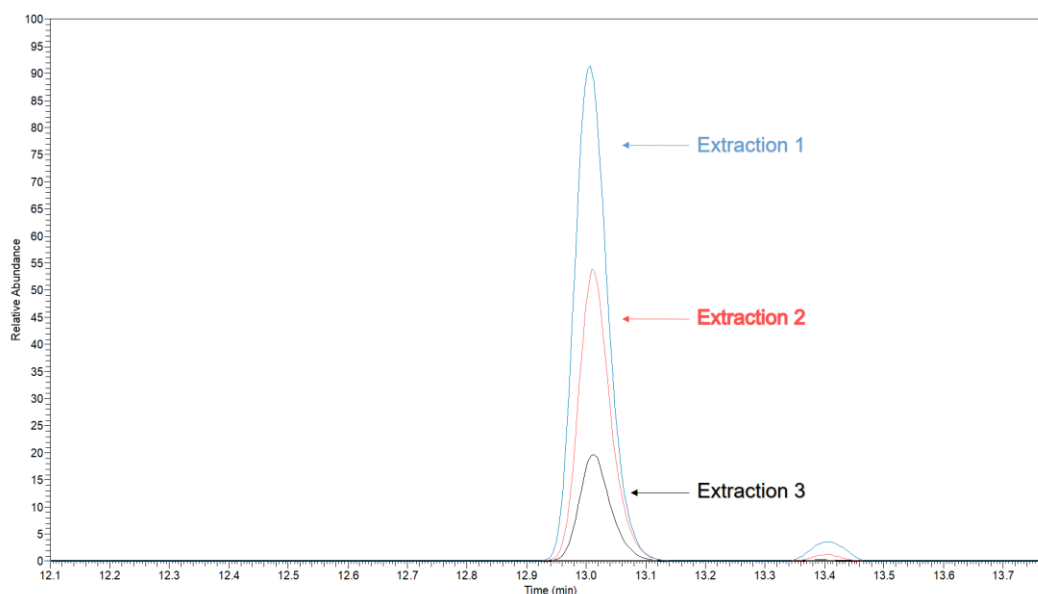


Figure 12 - Extracted ion chromatogram of chlorophyll a in extraction 1-3.

3.4.3 Extraction solvents

Four different extraction solvents were tested on samples of *P. glacialis* (Table 3), three parallels were made for each solvent. Due to time limitations only one extraction was carried out for these samples to test the extraction efficiency. The samples were extracted and analyzed on the Q Exactive mass spectrometer on the same day.

Table 3 - Extraction solvents tested for pigment extraction from *P. glacialis*.

Extraction solvent	Acetone (%)	Methanol (%)	Isopropanol (%)	Milli-Q (%)
1	90			10
2	50	50		
3	50		50	
4	33.3	33.3	33.3	

3.5 Calibration curves

Calibration curves were set up for quantification of chlorophyll *a* and astaxanthin. The samples were run with increasing concentration to minimize carry-over effects (when going from highest to lowest concentration, two blank samples were run to avoid carry-over). Two calibration curves were set up for both pigments, one where the area of the peak was plotted against the concentration and one where the intensity of the peaks was plotted against the concentration (see Appendix 5: Calibration curves). It was desirable to investigate whether peak intensities provided equally reproducible data as peak area.

3.5.1 Chlorophyll *a*

Chlorophyll *a* was quantified with the standard mix from DHI (DHI-mix). The standard solution concentration of chlorophyll *a* was 3.31 $\mu\text{g/mL}$. An aliquot of 1000 μL was evaporated under nitrogen and re-dissolved in 100 μL MeOH:Acetone (1:1), giving a concentration of 33.1 $\mu\text{g/mL}$. The standard solution was diluted into the following concentrations: 16.55, 3.31, 1.655, 0.331 and 0.0331 $\mu\text{g/mL}$. The preparation of each standard solution is shown in Appendix 4: Preparation of standard solutions.

3.5.2 Astaxanthin

A stock solution of astaxanthin (Stock 1, 10 000 $\mu\text{g/mL}$) was made from astaxanthin powder from Merck and dissolved in MeOH:acetone (1:1, v/v). Further a second stock solution was made from stock 1, with a concentration of 100 $\mu\text{g/mL}$ (stock 2). Seven different concentration levels were prepared (10, 5, 1, 0.5, 0.1, 0.05 and 0.01 $\mu\text{g/mL}$), however, only the concentration range 5-0.01 $\mu\text{g/mL}$ was used for making the calibration curve. The preparation of each standard solution is shown in Appendix 4: Preparation of standard solutions.

3.6 Analysis of extracted pigments

For each sample of *P. glacialis* cultivated in different light conditions, three parallels were prepared. An aliquot of the extracted pigments were diluted 1:20 in order for chlorophyll *a* to come within the range of the calibration curve. For quantitative analysis, each parallel was injected three times on UPLC-MS. Two blank samples were run between each parallel to avoid carry-over and when going from diluted to undiluted samples. See flowchart (Figure 13) for the sample preparation process.

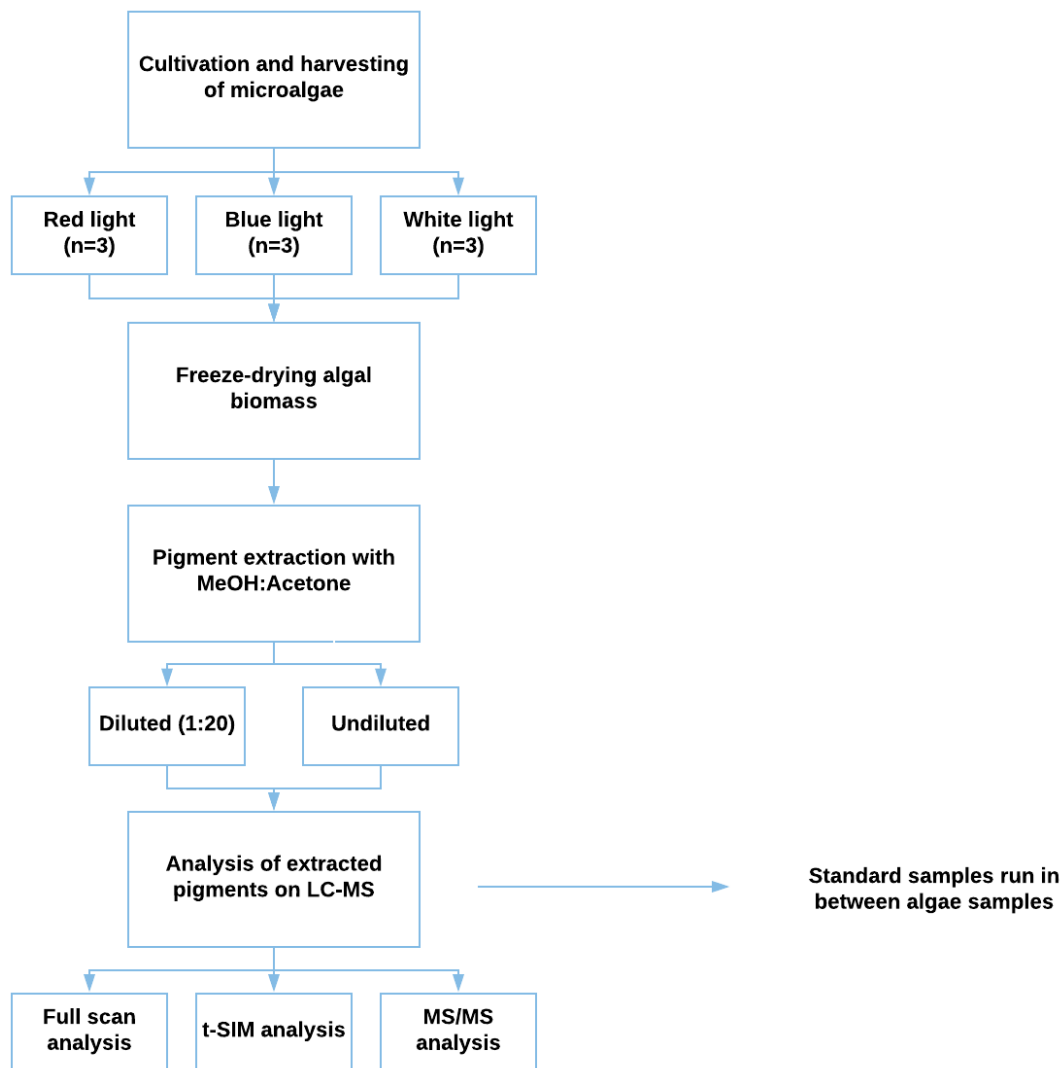


Figure 13 - Flowchart of sample preparation process.

3.7 UPLC-MS analysis

Pigments from standards and extracted from *P. glacialis* were studied using two different UPLC-MS techniques.

UPLC-MS analyses were performed using an Acquity UPLC (Waters, MS Technologies, UK) coupled to a Q Exactive mass spectrometer (Thermo Fisher Scientific, USA) equipped with an electrospray ionization (ESI) source in positive mode. The chromatographic system consisted of a binary pump (Binary Solvent Manager, Waters) and an autosampler (Sample Manager, Waters). Five microliters of sample were injected into a Waters Acquity UPLC® BEH C18 column (2.1x100mm, 1.7µm).

UPLC-MS analyses were also performed on a Waters Acquity I-Class UPLC (Waters, MS Technologies, UK) coupled to a Waters Xevo G2 Q-TOF (Waters, MS Technologies, UK) equipped with an atmospheric pressure ion source (APCI) in both positive and negative mode. The chromatographic system consisted of a binary pump (Binary Solvent Manager, Waters I-Class) and an autosampler (Sample Manager, Waters). Five microliters of sample were injected into a Waters Acquity UPLC® BEH C18 column (2.1x100mm, 1.7µm).

Electrospray ionization was initially tested on both Waters G2 Q-TOF and Waters Xevo Vion Q-TOF, however neither ionized the pigments at all and further testing was not performed.

3.7.1 UPLC

It is important to optimize chromatographic conditions prior to quantitative analysis. The accuracy of quantification is influenced by the resolution of the peaks and the noise level surrounding the peaks of interest. Well separated peaks can easily be integrated reproducibly, while peaks eluting on noisy baselines can be difficult to integrate in a reproducible manner. Peaks with tailing are also difficult to integrate reproducibly.

Various gradient profiles were therefore tested with extracted pigments from *P. glacialis* to achieve acceptable chromatographic separations. All tests were performed using reversed-phase chromatography on an Acquity UPLC BEH C18 1.7 µm (2.1 x 100 mm) column and on a Q Exactive mass spectrometer with ESI⁺. The mobile phase (MP) consisted of solvent A:

Milli-Q:ACN (60:40, v/v) + 0.1% formic acid and solvent B: Isopropanol:ACN (90:10, v/v) + 0.1% formic acid. Injection volume was set to 5 μ l and the temperature in the sample manager was set at 5 $^{\circ}$ C \pm 25. The column temperature was initially tested at 60 $^{\circ}$ C \pm 2, which is the standard column temperature at the research laboratory that was used.

Problems with exceeding the pressure limit of the LC pump, led to using a lower flow compared to analyses done with a combination of water and acetonitrile as mobile phase. However, with method one (flow one and flow two), the pressure exceeded the LC pump limit (see Table 4).

Table 4 - Gradient elution method 1. Same gradient tested with two different flow rates. MP A: Milli-Q:ACN (60:40, v/v) + 0.1% FA. MP B: isopropanol:ACN (90:10, v/v) + 0.1% FA. The column temperature was set to 60 $^{\circ}$ C \pm 2.

Time (min)	Flow (ml/min)		A (%)	B (%)
	Flow 1	Flow 2		
Initial	0.450	0.400	80	20
10.00	0.450	0.400	5	95
10.10	0.450	0.400	80	20
13.00	0.450	0.400	80	20

It was not desirable to lower the flow rate any further, due to increased risk of band broadening leading to poor resolution and chromatographic separations. The Acquity UPLC BEH columns can operate up to 90 $^{\circ}$ C, but operating at such high temperatures (e.g. >70 $^{\circ}$ C) may result in shorter column lifetimes (48). Increasing the column temperature will lead to reduced back pressure due to lower viscosity. When increasing the column temperature from 60 $^{\circ}$ C to 65 $^{\circ}$ C \pm 2 the pressure limit of the LC pump was not exceeded.

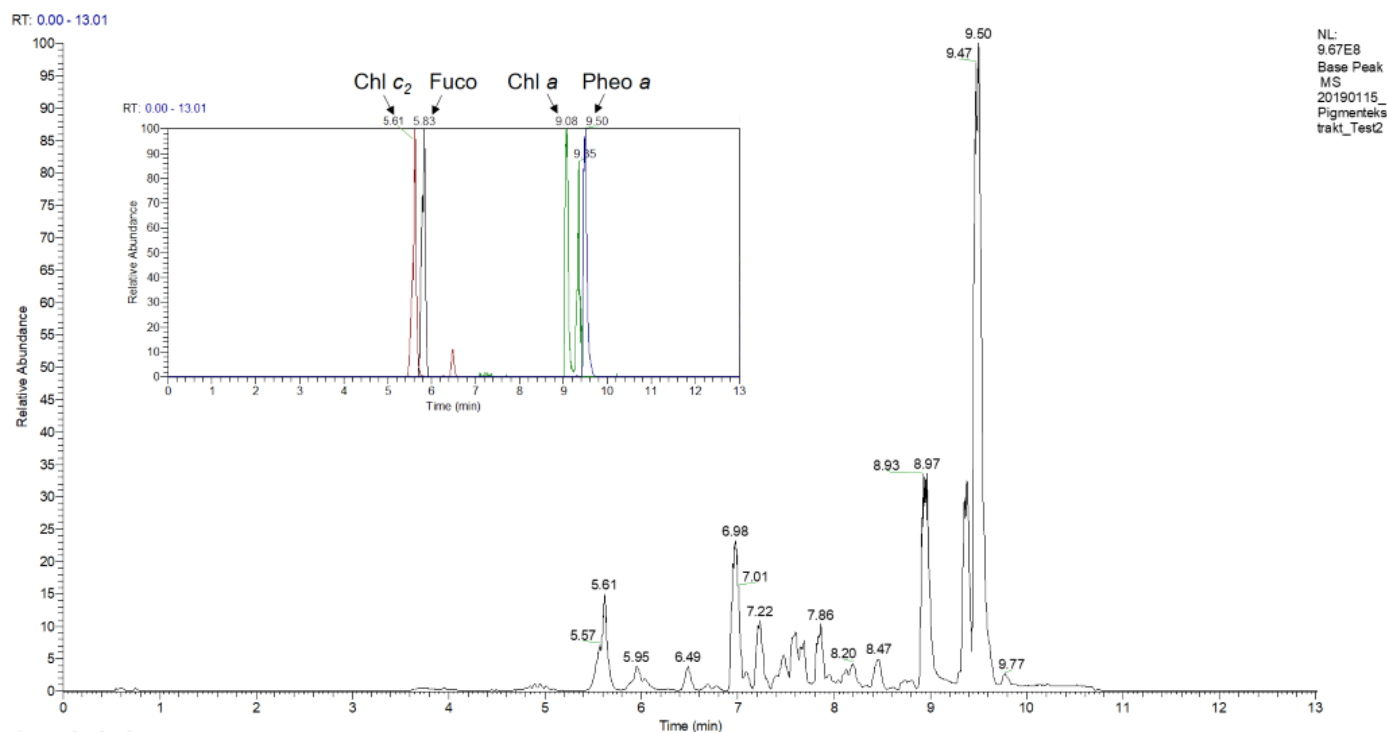
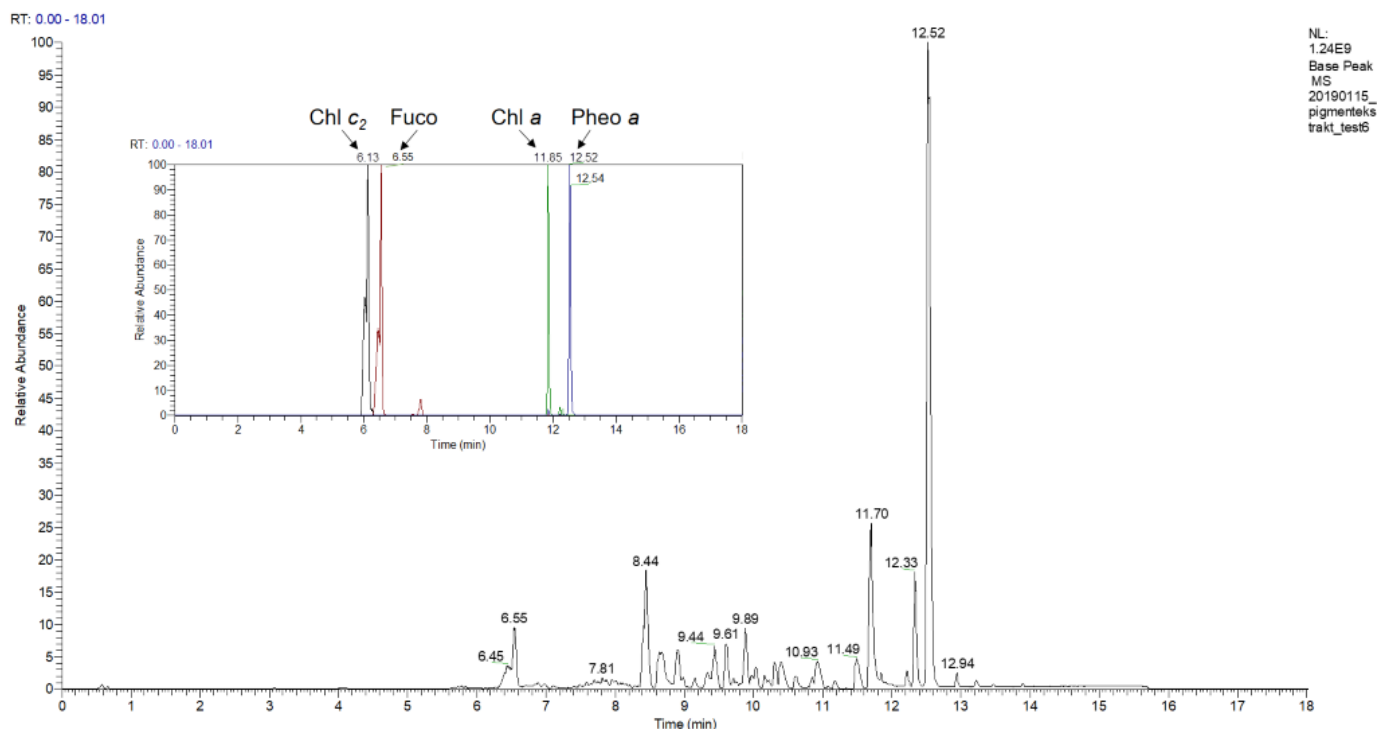


Figure 14 – Base peak chromatogram from gradient profile listed in Table 4 with column temperature 65 °C and flow rate 0.400 ml/min. Extracted ion chromatogram of chlorophyll c_c (chl c₂), fucoxanthin (fuco), chlorophyll a (chl a) and pheophytin a (pheo a).

However, the chromatogram showed poor separation of the analytes, like chlorophyll a and pheophytin a (Figure 14). In order to solve this problem, the gradient time was increased from 10 minutes to 15 minutes. The initial conditions of mobile phase A was also increased from 80% to 90% (Table 5).

Table 5 - Gradient elution method 2 on pigment extracts from *Porosira glacialis*. MP A: Milli-Q:ACN (60:40, v/v) + 0.1% FA. MP B: isopropanol:ACN (90:10, v/v) + 0.1% FA. Flow rate 0.400 mL/min and column temperature 65 °C ± 2.

Time (min)	Flow (mL/min)	A (%)	B (%)
Initial	0.400	90	10
15.00	0.400	5	95
15.10	0.400	90	10
18.00	0.400	90	10



NL:
1.24E9
Base Peak
MS
20190115_
pigmenteks
trakt_test6

Figure 15 - Chromatogram from gradient elution with method two. Extracted ion chromatogram of chlorophyll *c*₂ (*chl c*₂), fucoxanthin (*fuco*), chlorophyll *a* (*chl a*) and pheophytin *a* (*pheo a*).

Adjusting the chromatographic run from 10 to 15 minutes improves separation of the pigments (Figure 15). However, now it takes over six minutes before the first pigment, chlorophyll *c*₂, elutes in the chromatogram. Consequently, there is six minutes of “unused” space in the beginning of the chromatogram that only helps prolong the analysis. Changing the initial starting conditions back to 80% mobile phase A and 20% mobile phase B will lead to earlier elution of the first pigments.

Table 6 - Gradient elution method 3 on pigment extracts from *Porosira glacialis*. Gradient profile used in pigment separation. MP A: Milli-Q:ACN (60:40, v/v) + 0.1% FA. MP B: isopropanol:ACN (90:10, v/v) + 0.1% FA. Column temperature was set to 65 °C ± 2.

Time (min)	Flow (mL/min)	A (%)	B (%)
Initial	0.400	80	20
12.00	0.400	30	70
15.00	0.400	5	95
15.10	0.400	80	20
18.00	0.400	80	20

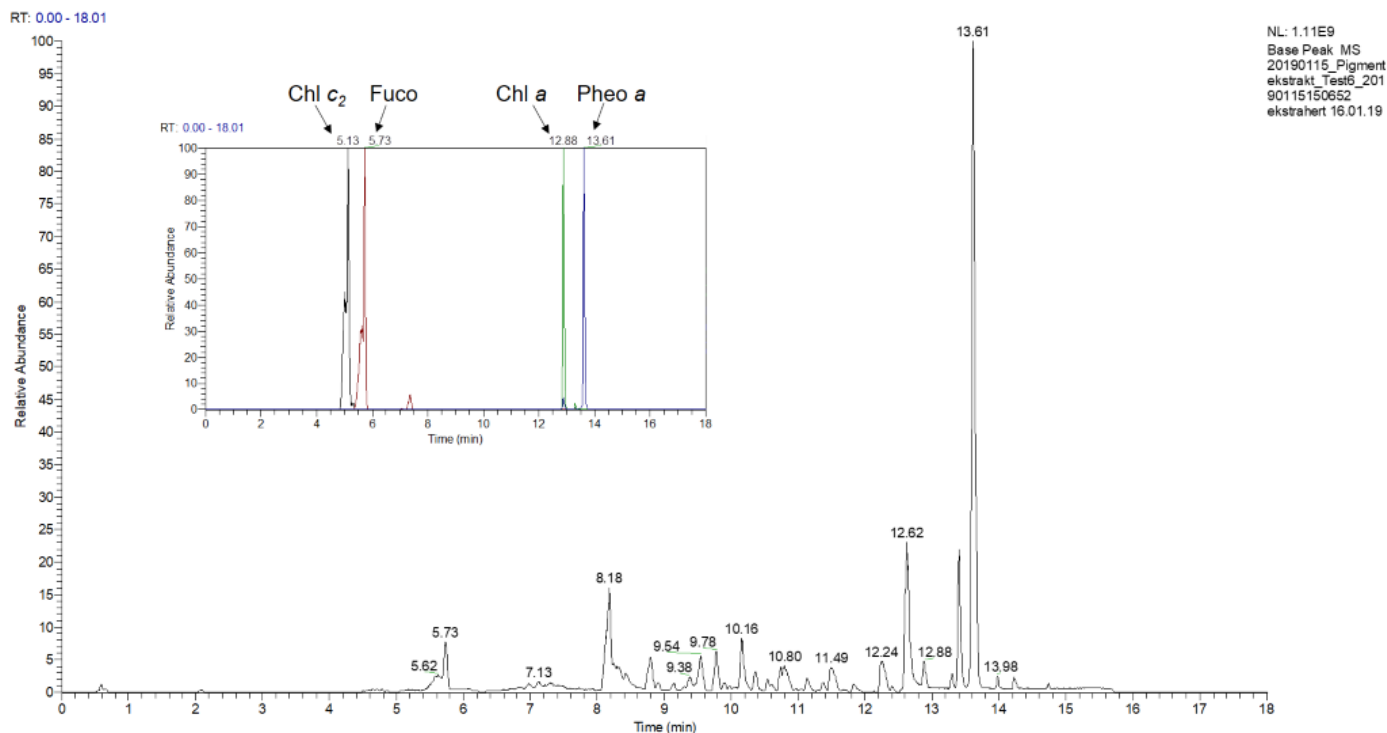


Figure 16 - Chromatogram from gradient elution with method three. Extracted ion chromatogram of chlorophyll c_2 (chl c_2), fucoxanthin (fuco), chlorophyll a (chl a) and pheophytin a (pheo a).

Table 6 shows the final gradient profile for analyzing extracted pigments from *P. glacialis*. Adjusting the gradient profile of the mobile phase provided better resolution and chlorophyll c_2 eluted one minute earlier and pheophytin a eluted one minute later compared with method two (Figure 16). Both mobile phases A and B were added 0.001% (v/v) midazolam from a 100 $\mu\text{g/mL}$ solution that was used as lock mass.

3.7.2 MS

To optimize the LC-MS method different key parameters were tuned for both Q-TOF with APCI and Q Exactive with ESI on pigment standards from DHI to optimize the sensitivity for both instruments. Initially an ESI ion source was tested in positive mode on both Waters G2 Q-TOF and Waters Xevo Vion Q-TOF, where neither ionized the pigments at all. Both tested- and optimal MS conditions for pigment analyses are listed in Table 7 and Table 8.

Table 7 - Summary of MS and MS/MS conditions examined for Q Exactive ESI

MS conditions	Values/settings examined						Optimal conditions
	Positive						
Polarity	Positive						Positive
Sheat gas flow rate	40	50	60	80			60
AUX gas flow rate	5	10	15				10
Sweep gas flow rate	0	3	10				3
Spray voltage (kV)	0.6	1.5	3	3.5	4	5	3.5
Aux gas heater temp. (°C)	200	300	400				300
Capillary temp. (°C)	350						350
S-lens RF level	50						50

Since the Waters ESI source did not ionize the pigments, a APCI source was tested, which successfully ionized the pigments in the DHI standard mix in positive mode. Both positive and negative mode were investigated for G2 Q-TOF with APCI, where positive mode gave best results. The MS Q-TOF conditions with APCI as ion source are listed in Table 8.

Table 8 - Summary of MS conditions examined for Q-TOF APCI.

MS conditions	Values/settings examined					Optimal conditions
	Positive	Negative				
Polarity	Positive	Negative				Positive
Current corona (kV)	5					Not used
Voltage corona (kV)	0.3	0.5	1			0.5
Sampling cone	25	35	45	55		55
Extraction cone	2					2
Temperature source (°C)	100	130	150			100
Temperature desolvation (°C)	400	550	650	700	750	650
Cone gas (L/h)	20					20
Desolvation gas (L/h)	400	600	800	1000	1200	800

In this thesis, the Q Exactive with electrospray ionization in positive mode gave the most prominent results in comparison to the Q-TOF with APCI. Because of time limitations, only the Q Exactive MS was chosen to conduct further investigations on samples from *P. glacialis*.

3.7.2.1 Scan mode

All standard samples for the calibration curves and all algae samples were analyzed in full scan mode. Calibration curves were analyzed on the Q Exactive instrument. A targeted selected ion monitoring (t-SIM) mode was developed for both standard and algae samples, it acquires scans based on a specified inclusion list (see Appendix 6: t-SIM inclusion list). A MS/MS method was developed (data dependent acquisition (DDA)) and used on both standard samples and pigment extracts with a 2.0 Da isolation window to acquire information about the pigments fragmentation pattern. Further a parallel reaction monitoring (PRM) scan was developed for improved screening and qualitative confidence for astaxanthin. Fragmentation was obtained by using an HCD cell. MS parameters for all developed scan modes are listed in Table 9.

Table 9 – Different scan modes used for analyzing standard samples and pigments extracted from *P. glacialis*.

	Full scan	t-SIM	DDA	PRM
Mass (<i>m/z</i>)	250-1200	*	250-1200	597.3948
Time (min)	0-18	0-18	0-18	0-18
Resolution	70 000 and 140 000	70 000	70 000	70 000
Maximum IT (ms)	100	250	200	200
AGC target	3e6	1e5	2e5	2e5
Isolation window (Da)		4.0	2.0	0.4
Collision energies (V)			10, 20 and 30	10, 20 and 30

*See Appendix 6: t-SIM inclusion list

3.8 Interpretation of chromatograms and mass spectra

Identification of pigments separated on UPLC are done by (1) comparison of retention time (t_R) values with those of standards and from the certificate of the DHI-Mix standard provided by the manufacturer and (2) using the mass spectra and comparing MS/MS spectra with known standards and literature (see (3) and lastly using exact masses.

3.9 Statistical analysis

The data for pigment content was analyzed using Microsoft Excel®. An independent samples t-test was used to determine whether there is a statistically significant difference in mean pigment content in blue and red light compared to white light samples. Significance level was set to 0.05. A Q-test was used to identify statistical outliers in the data, the decision level was set at a 95% confidence interval.

4 Results and discussion

4.1 Extraction solvent

The intensity of seven different pigments were measured and compared using four different extraction solvents (see Table 3). Based on exact mass the peak intensity of chlorophyll c_2 , fucoxanthin, carotene, lutein, astaxanthin, chlorophyll a and pheophytin a was measured. The selection of an extraction solvent is important since it determines the degree of affinity to the chemical composition of the substances to be extracted. Apart from the dissolution ability towards the pigments to be extracted and quantified, the solvent also plays an important role in cell lysis.

For all carotenoids investigated, except for astaxanthin, the most effective extraction solvent was 90% acetone (fucoxanthin (Figure 18), carotene (Figure 19) and lutein (Figure 20)). For chlorophyll c_2 extraction, 90% acetone was also the most effective solvent, followed by acetone:MeOH (1:1, v/v)(Figure 17).

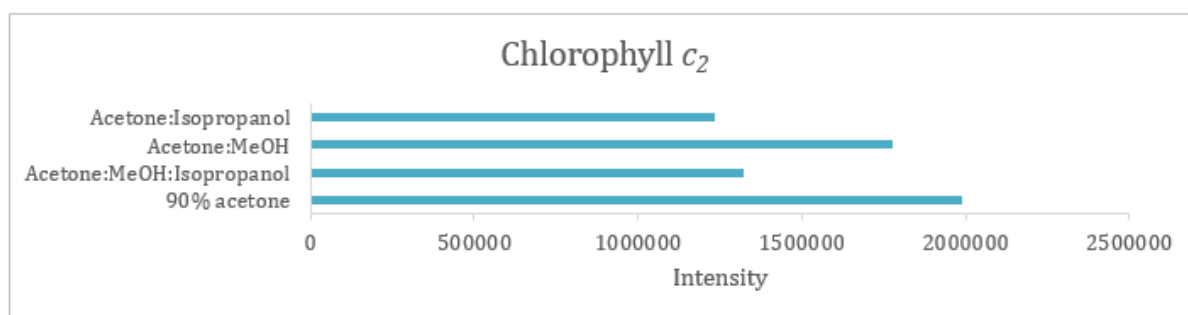


Figure 17 - Comparison of chlorophyll c_2 peak intensity with different extraction solvents.

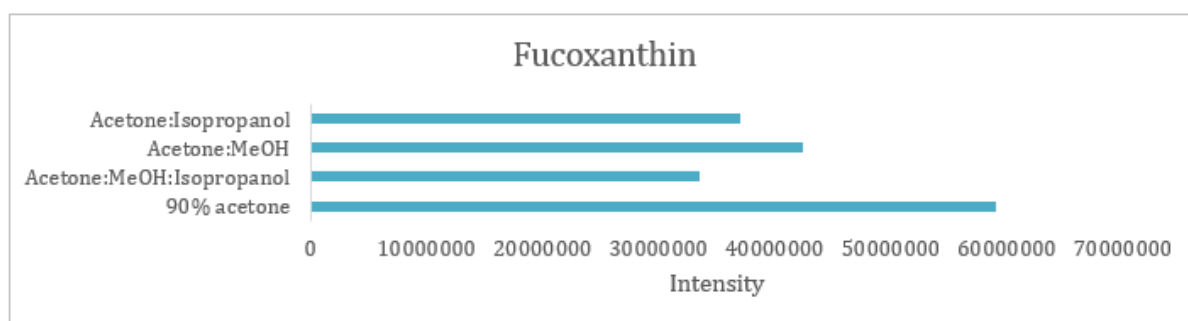


Figure 18 - Comparison of fucoxanthin peak intensity with different extraction solvents.

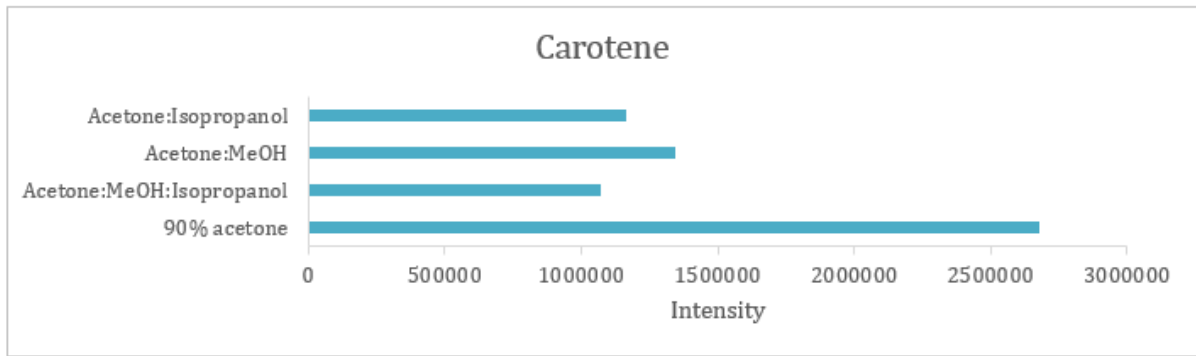


Figure 19 - Comparison of carotene peak intensity with different extraction solvents.

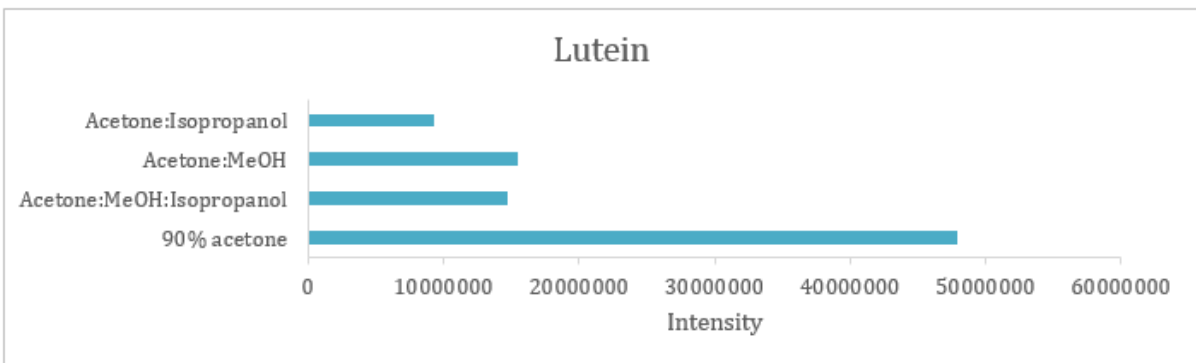


Figure 20 - Comparison of lutein peak intensity with different extraction solvents.

The intensity of astaxanthin was lowest when using 90% acetone as extraction solvent (Figure 21). The most effective extraction solvent for analyzing astaxanthin in *P. glacialis* is a mixture of acetone and methanol (1:1, v/v), followed by acetone:MeOH:isopropanol (1:1:1, v/v/v) and acetone:isopropanol (1:1, v/v). Pheophytin *a* also shows high intensities when extracted in acetone:MeOH (1:1, v/v) (Figure 23), while the mixture of acetone and isopropanol (1:1, v/v) gave the highest intensity for chlorophyll *a* (Figure 22).

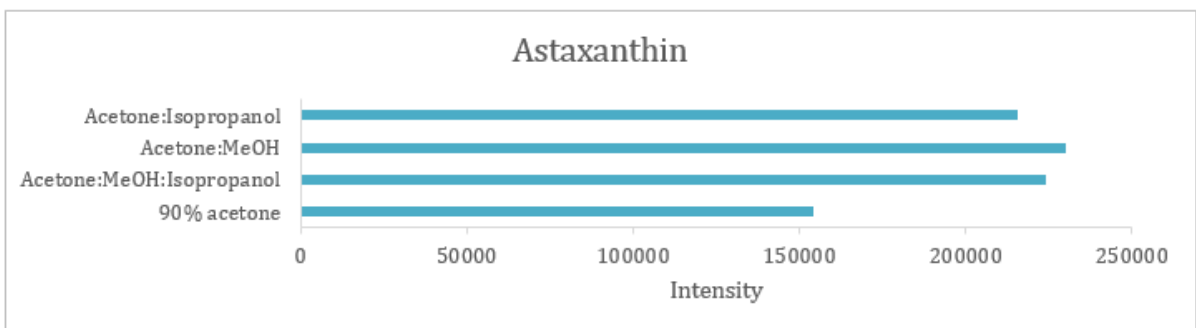


Figure 21 - Comparison of astaxanthin peak intensity with different extraction solvents.

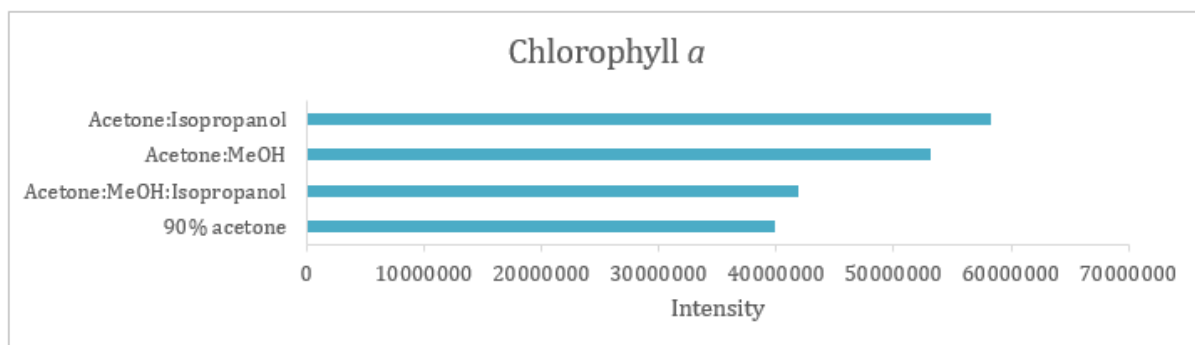


Figure 22 - Comparison of chlorophyll *a* peak intensity with different extraction solvents.

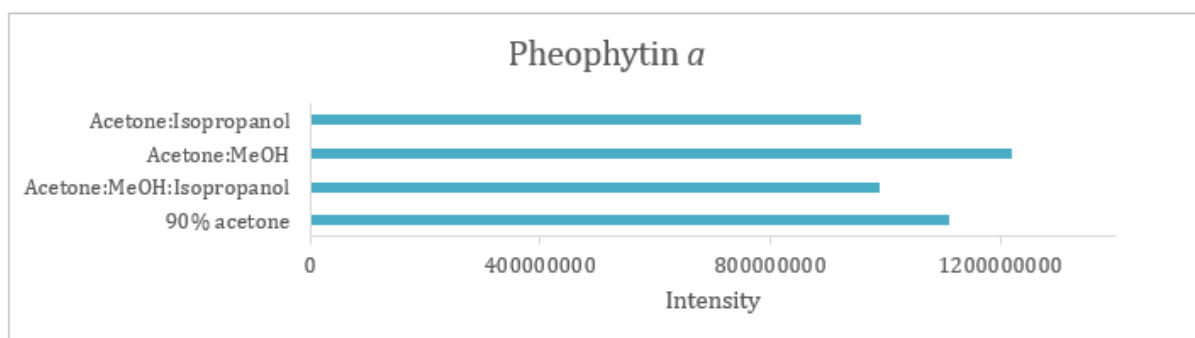


Figure 23 - Comparison of pheophytin *a* peak intensity with different extraction solvents.

Both chlorophyll *a* and astaxanthin were of great interest. Chlorophyll *a* is commonly used as an indirect measure of overall algal biomass world-wide and could provide interesting data (20). Since it could be interesting to use the microalgal biomass in fish feed, the pigment astaxanthin is of high value as it colors the flesh of the salmon. Preliminary analysis shows low quantities of astaxanthin compared to several of the other pigments, therefore, the extraction efficiency was weighted heavily for astaxanthin. The combination of acetone and methanol was chosen as extraction solvent since it gave high intensities for both chlorophyll *a* and astaxanthin compared to other extraction solvents.

4.2 Extraction efficiency

Each algae sample was extracted three times and injected on the UPLC-MS. In order to evaluate the accuracy of extraction and reproducibility of the instrument the extraction efficiency was calculated. The extraction efficiency in red algae samples was estimated for chlorophyll *a*, pheophytin *a*, fucoxanthin and carotene. These pigments were chosen because of their high intensities in the algae samples, and because it was interesting to investigate both chlorophyll and carotenoid pigments. The extraction efficiency for chlorophyll *a* and fucoxanthin is displayed in Figure 24 and Figure 25.

Figure 24 displays the extraction efficiency between three extractions for three parallels for the mean of chlorophyll *a* measured in peak area for algae samples cultivated in red light. The results are normalized to extraction one that is set to 1, and the results from extraction two and three are normalized to this to give an impression of the amount of compound in extraction one, two and three. A table for the extraction efficiency with standard deviation and relative standard deviation are shown in Appendix 7: Extraction efficiency

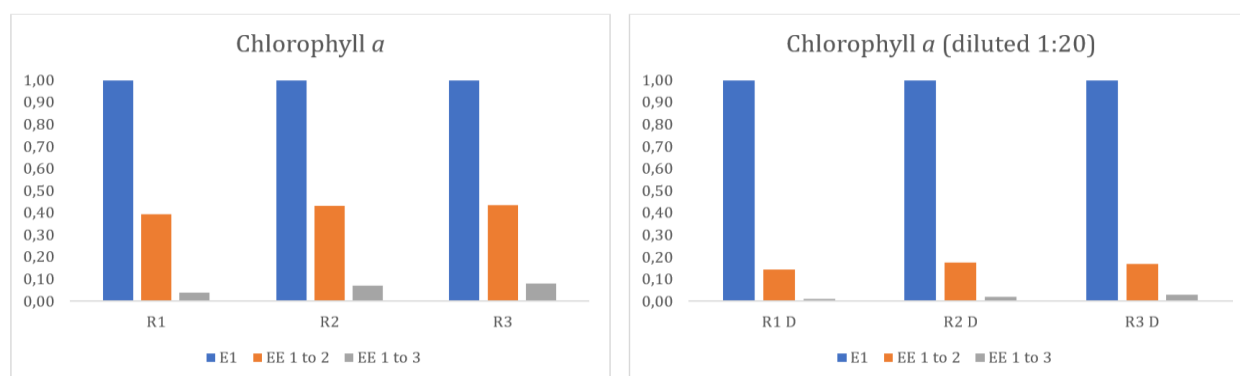


Figure 24 - Extraction efficiency between parallels for both undiluted (left) and diluted 1:20 (right) pigment samples from *P. glacialis* cultivated in red light. The results are based on peak areas (mean, $n=3$) of chlorophyll *a*. The numbers are normalized, and the extraction efficiency in percentages can be found in Appendix 7: Extraction efficiency.

The algae samples were diluted 1:20 in order to come within the standard curve and the linear range. In the undiluted sample (Figure 24, left) chlorophyll *a* falls outside the linear range and shows lower extraction efficiency for extraction one, since the extraction efficiency for extraction two and three is higher relative to extraction one. Therefore, the extraction efficiency for the diluted sample is more correct. This trend was also seen in blue and white light samples of *P. glacialis*. However, for fucoxanthin the extraction efficiency was similar for both

undiluted and diluted samples cultivated in red light (Figure 25). This could also be seen in blue and white light for fucoxanthin. Pheophytin *a* and carotene exhibited also the same trend as fucoxanthin.

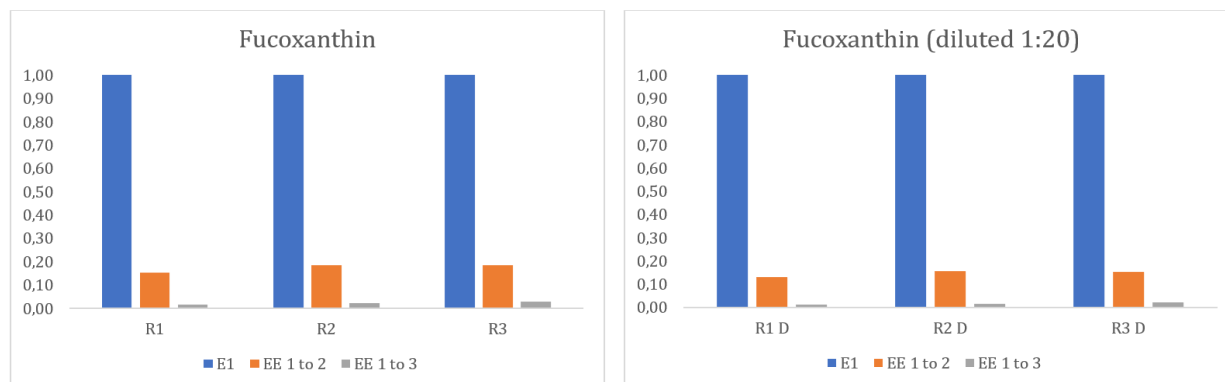


Figure 25 - Extraction efficiency between parallels for both undiluted (left) and diluted 1:20 (right) pigment samples from *P. glacialis* cultivated in red light. The results are based on peak areas (mean, $n=3$) of fucoxanthin. The numbers are normalized, and the extraction efficiency in percentages can be found in Appendix 7: Extraction efficiency.

4.3 Comparison of instruments and ion source

With the Q-Exactive MS and electrospray as ion source lower concentrations could be detected compared with the Q-TOF with APCI as ion source. As displayed in Figure 27, the sensitivity for carotenoids was low when ionized with chemical ionization (APCI). Both the carotenoids, fucoxanthin and astaxanthin could not be detected with APCI. However, from the literature it is described that APCI is one of the most widely used ionization techniques for carotenoids (22, 34).

Concentration (µg/ml) of chl <i>a</i>	Pheophytin <i>a</i>		Chlorophyll <i>a</i>		Carotene		Chlorophyll <i>c</i> ₂		Fucoxanthin		Astaxanthin	
	ESI	APCI	ESI	APCI	ESI	APCI	ESI	APCI	ESI	APCI	ESI	APCI
3.31	Signal	Signal	Signal	Signal	Signal	Signal	Signal	Signal	Signal	Signal	Signal	No signal
0.331	Signal	Signal	Signal	Signal	Signal	No signal	Signal	Signal	Signal	No signal	Signal	No signal
0.0331	Signal	Signal	Signal	No signal	Signal	No signal	No signal	Signal	No signal	No signal	No signal	No signal
0.00331	Signal	No signal	No signal	No signal	No signal	No signal	No signal	No signal	No signal	No signal	No signal	No signal
0.000331	No signal	No signal	No signal	No signal	No signal	No signal	No signal	No signal	No signal	No signal	No signal	No signal
0.0000331	No signal	No signal	No signal	No signal	No signal	No signal	No signal	No signal	No signal	No signal	No signal	No signal

Figure 26 - Comparison of two different ion sources with six selected pigments (from DHI standard mix).

Interestingly we noticed differences between suppliers (Waters and Thermo) electrospray ion sources. Both Waters G2 Q-TOF and Waters Xevo Vion Q-TOF with ESI as ion source could not ionize the pigments at all. However, the Waters Xevo Vion Q-TOF was equipped with UV, where some pigments could be confirmed present in the standard sample. When trying Thermo’s ESI source coupled with the Q Exactive, pigments were detected on the first run.

4.4 Evaluation of UPLC-MS method for pigment analysis

To determine the pigment content in *Porosira glacialis* a LC-MS method was developed. Different approaches were tested with standard samples on RP-UPLC coupled to the Q Exactive with ESI as ion source (positive mode) and RP-UPLC coupled to the Q-TOF, which was tested with both ESI (positive mode) and APCI (positive and negative mode). The method yielding the best results was the one with the Q Exactive with ESI in positive ionization mode, where 12 different pigments were detected in samples from *P. glacialis* cultivated in red, blue and white light conditions.

A t-SIM scan mode was developed to see if lower amounts of pigments could be detected compared to a full scan mode. A t-SIM scan mode and a full scan mode was tested on a dilution series of a DHI-mix standard sample ranging from 33.1-0.00331 $\mu\text{g/mL}$. A difference could be seen in the sample diluted three times (0.331 $\mu\text{g/mL}$ chlorophyll *a*), where the full scan mode detected five pigments and the t-SIM mode detected eight pigments. For both full scan and t-SIM mode, only pheophytin *a* was detectable in the lower ranges. Since the pigments in the chromatogram vary some in retention time from run to run it was difficult to develop a reproducible method with t-SIM, however, for future work this should be tested further.

The Q Exactive has a resolving power up to 140 000, in this thesis both 70 000 and 140 000 in resolving power was tested on both DHI-mix standard samples and extracted pigment samples from red, blue and white light. When increasing the resolving power two things happens: (1) the peaks looks narrower and (2) fewer data points can be seen over the peak. More than 10 data points are desirable and needed for reproducible quantitation. For chlorophyll *a* in DHI-mix standard sample (16.55 $\mu\text{g/mL}$) with a resolving power of 70 000, 30 data points over the peak was obtained. With a resolving power of 140 000, only 15 data points over the chlorophyll *a* peak was obtained. The same trend can be seen for carotene; 42 data points with resolving power 70 000 and 22 data points with resolving power 140 000. Although a resolution of 140 000 in theory gives enough data points over the peaks, more data points are desirable, and since no interesting findings came from increasing the resolving power considering astaxanthin, there was no need to do any further analyses with a resolving power of 140 000.

4.5 Pigment analysis of algal sample

Chromatograms of pigments extracted from algae are often very complex and contains several peaks, as seen in Figure 27. The chromatogram of *P. glacialis* cultivated in white light (Figure 27) shows 12 different pigments, where seven of them are carotenoids. The same pigments were also found in algae cultivated in red and blue light regimes (Appendix 9: Chromatograms of pigment extract). For red, blue and white light samples of *P. glacialis* the major carotenoids detected were fucoxanthin, lutein and carotene based on peak area and peak intensity. There were also several peaks in the chromatogram that could not be identified in this project. Elucidation of pigments was done using t_R obtained from DHI, exact masses and MS/MS spectra, which was compared to theoretical fragments and fragments obtained from the standard sample (DHI) (Appendix 13: MS/MS of pigments).

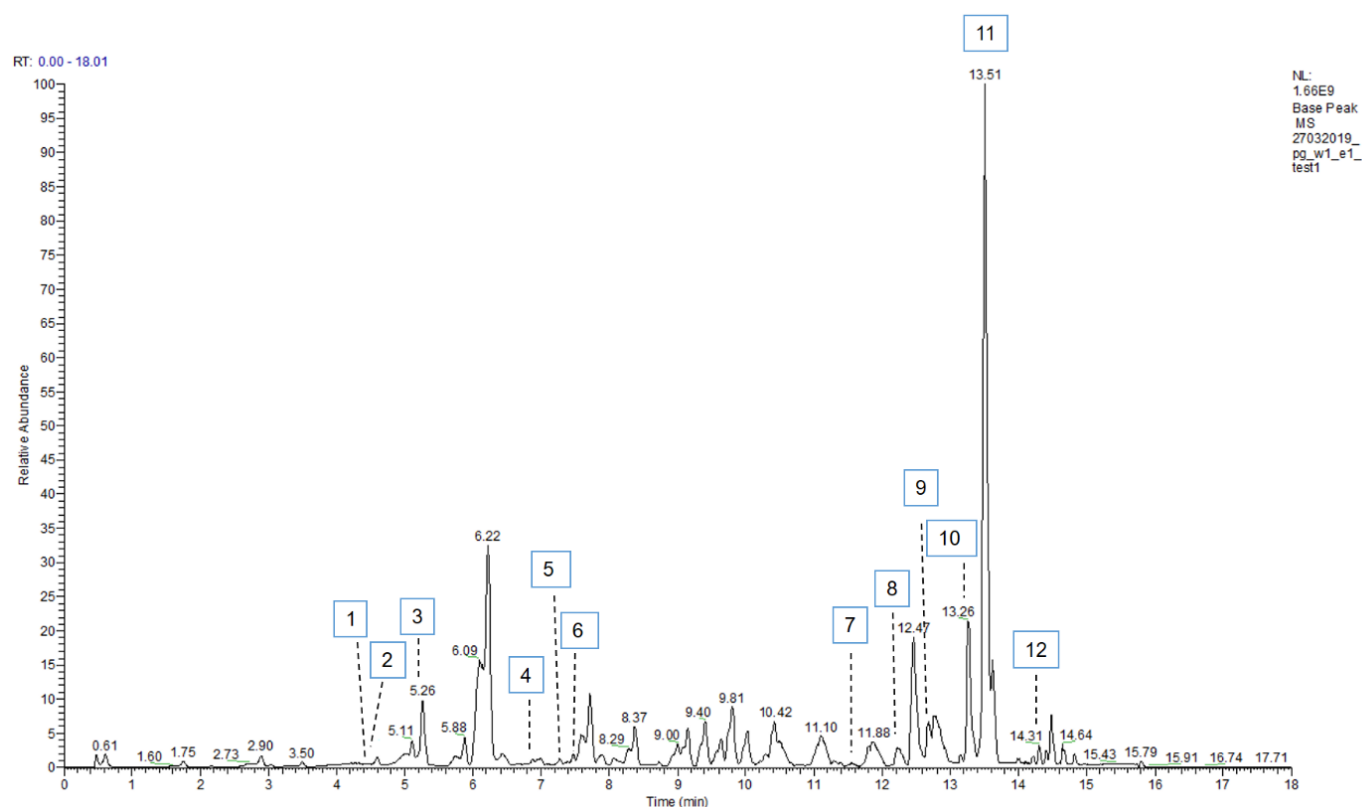


Figure 27 – Base peak chromatogram of extracted pigments cultivated in white light. 1=Chlorophyll c_2 , 2=Mg-DVP, 3=Fucoxanthin, 4=Diadinoxanthin, 5=Alloxanthin, 6=Diatoxanthin, 7=Zeaxanthin, 8=DV chlorophyll a, 9=Chlorophyll a, 10=Lutein, 11=Pheophytin a and 12=Carotene.

Chlorophylls and carotenoids are generally fat soluble molecules and can be extracted with organic solvents. However, an research paper claims that peridinin are water soluble and need to be extracted from algae after the extraction of chlorophyll and carotenoids with organic

solvent (49). In samples illuminated with red, blue or white light, neither of them exhibited peridinin in the chromatogram. Nevertheless, a research paper on separation of chlorophylls and carotenoids, successfully extracted peridinin with 95% methanol as extraction solvent, in a dinoflagellate, *Alexandrium minutum* (50). Based on peridinin's chemical structure, it is unlikely that peridinin will not be extracted with the combination of methanol and acetone. It is more likely that peridinin is not a common carotenoid in diatoms and is more seen in dinoflagellates (50-52).

According to Airs and Keely, chlorophylls exhibit low ionization efficiency in metallized form (43). The nitrogen atoms provide a suitable site for protonation, especially when magnesium is not present, resulting in higher ionization efficiency. Pheophytins, which lack the central magnesium (Mg^{2+}) ion, have therefore higher ionization efficiency compared to chlorophylls. Pheophytin *a* have a higher intensity than chlorophyll *a* in the DHI-mix standard sample and in the algae samples. The difference in response could relate to differences in the efficiency of ionization of pheophytins and chlorophylls, but it could also be explained by differences in concentration. The concentration of pheophytin *a* is not known in the standard mix from DHI, and a standard with a known concentration of pheophytin *a* is needed to resolve this matter.

In the standard sample 19 pigments were resolved. However, the pigments prasinoxanthin, violaxanthin and neoxanthin have the same exact mass and came out as one peak in the chromatogram (Appendix 10: Chromatogram and mass spectra (t-SIM), Figure 73). These pigments are present in the standard sample from DHI, however, the intensity for these pigments were not high enough for activation of DDA when conducting MS/MS analysis. Thus it was not possible to determine which pigment was present. In addition to this diadinoxanthin co-eluted with prasinoxanthin/violaxanthin/neoxanthin in the standard sample. In the algae samples cultivated under different light conditions (red, blue and white), neither prasinoxanthin, violaxanthin nor neoxanthin could be detected. Because they were not detected in the algae samples, no further investigation of structure determination was conducted for prasinoxanthin, violaxanthin and neoxanthin

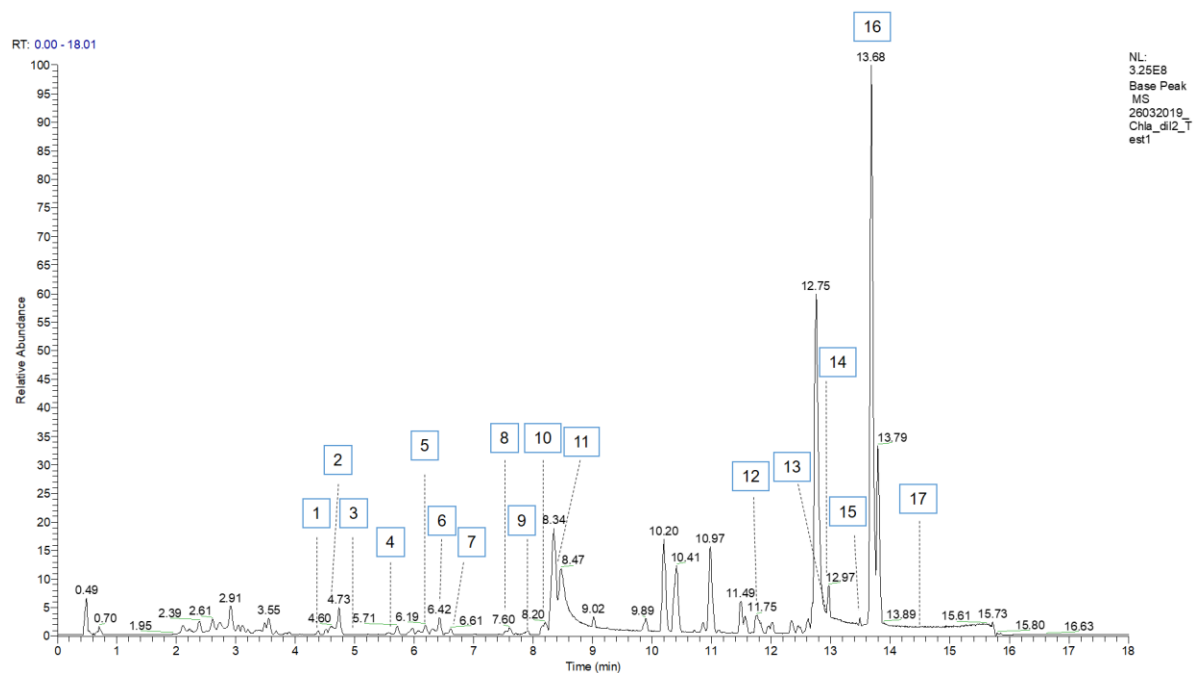


Figure 28 – Base peak chromatogram of DHI-mix standard sample (16.55 $\mu\text{g}/\text{mL}$ chlorophyll *a*). 1=Peridinin, 2=Mg-DVP, 3=Chlorophyll *c*₂, 4=19-but-fucoxanthin, 5=Prasinoxanthin/violaxanthin/neoxanthin and diadinoxanthin, 6=19-hex-fucoxanthin, 7=Astaxanthin, 8=Alloxanthin, 9=Diatoxanthin, 10=Zeaxanthin, 11=Crococanthin, 12=DV chlorophyll *b* and chlorophyll *b*, 13= DV chlorophyll *a*, 14=Chlorophyll *a*, 15=Lutein, 16=Pheophytin *a* and 17=Carotene.

In the DHI-mix standard sample both monovinyl and divinyl chlorophyll *b* (Figure 29) co-eluted. However, neither MV nor DV chlorophyll *b* could be detected in the algae samples. The amount of chlorophyll *b* could be too low to be detected by the developed method, however, in diatoms, chlorophyll *c* can be found instead of chlorophyll *b*. It is normal to find chlorophyll *b* in land and aquatic plants, but not in diatoms (20).

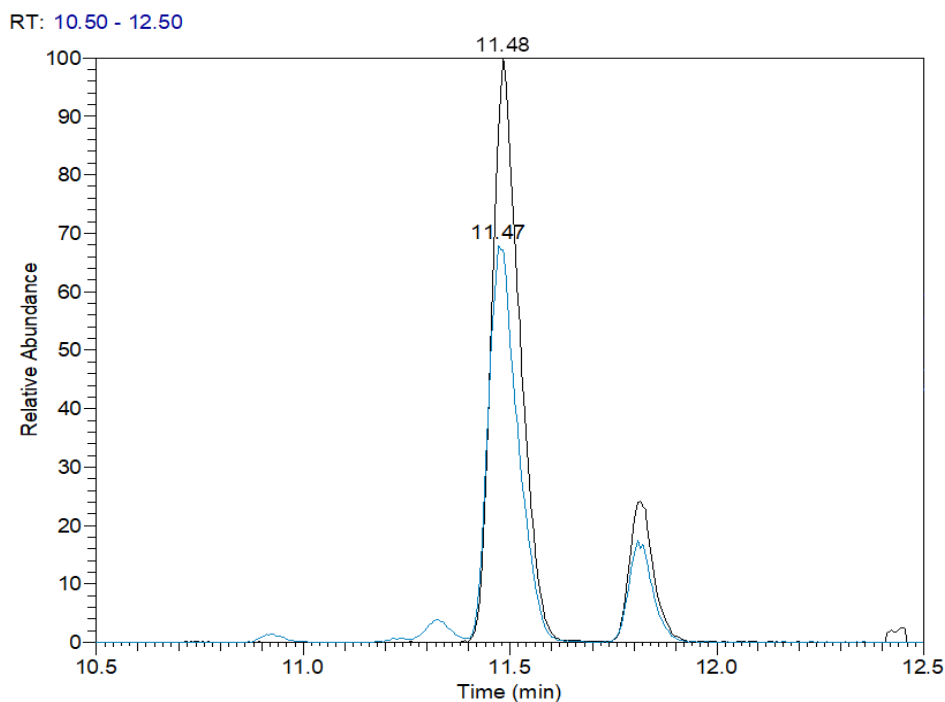


Figure 29 – Overlapping chromatogram of chlorophyll *b* (black) and DV chlorophyll *b* (blue) from standard sample (DHI) (16.55 $\mu\text{g}/\text{mL}$ chlorophyll *a*).

In the standard sample both β -carotene and α -carotene were present in the sample according to the certificate from DHI, but showed a single peak in the chromatogram. The two carotenes, β -carotene and α -carotene are isomers with the same exact mass. They did not separate from each other with the developed UPLC-MS method, and showed a single peak in the chromatogram (see Appendix 10: Chromatogram and mass spectra (t-SIM), Figure 65) for both the DHI-mix standard sample and in the extracted pigment analysis. However, Kuczynska et al. reports that diatoms possess β -carotene of the two carotenes, this may also be the case for *P. glacialis* (20).

Monovinyl and divinyl chlorophyll *a* overlapped in the chromatogram from DHI-mix standard sample (Figure 31, A). However, in the chromatogram from the algae samples cultivated in different light conditions (red, blue and white), MV and DV chlorophyll *a* did not co-elute because DV chlorophyll *a* have a shorter t_R (Figure 31, B). This could be explained by the conversion of chlorophylls to C*-epimers (Figure 30), which could have happened under the extraction process (18, 53). The presence of a DV chlorophyll *a* epimer could explain the different retention time in the algae sample compared to the standard sample. However, it is unlikely that all the DV chlorophyll *a* molecules has formed C*-epimers, since the literature only describes a conversion of a small amount of chlorophylls to their C*-epimer form (18, 53).

In addition to this, MV chlorophyll *a* did not form any epimer, which would have been expected if DV chlorophyll *a* did form epimers under the extraction process. An explanation for the shift in t_R could just be explained by the lack of reproducible t_R throughout the pigment analysis.

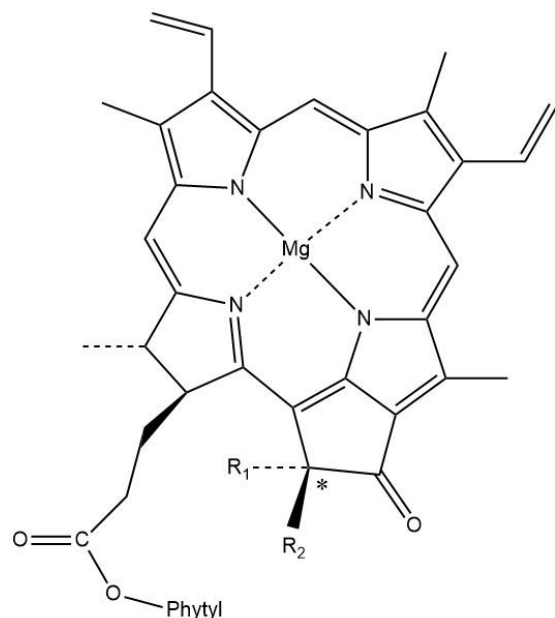


Figure 30 - Structure formula for DV chlorophyll *a* ($R_1=COOCH_3$, $R_2=H$) and C*-epimer ($R_1=H$, $R_2=COOCH_3$).

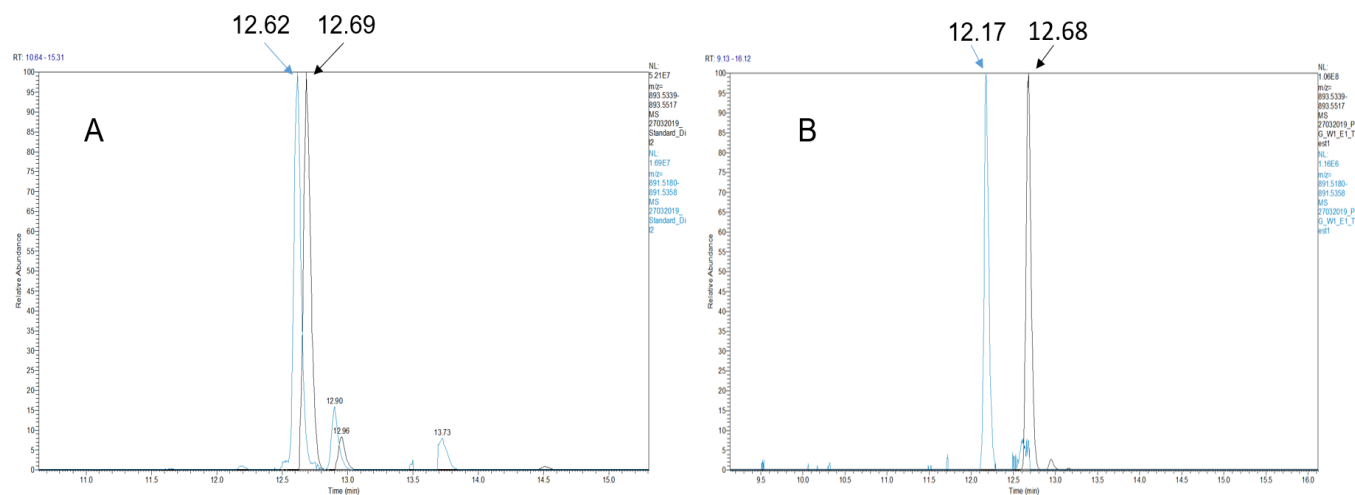


Figure 31 – Chromatogram of chlorophyll *a* (black) and DV chlorophyll *a* (blue) from A. standard sample (DHI-mix) (16.55 $\mu\text{g}/\text{mL}$ chlorophyll *a*) and B. *P. glacialis* illuminated with white light.

4.6 MS/MS of chlorophyll *a*

A DDA scan mode was developed to obtain the fragmentation pattern of different pigments present in the algae and standard sample, among the photosynthetic pigment chlorophyll *a*. The molecular ion of chlorophyll *a* was obtained at m/z 893.5 with ESI in positive mode. As seen in Figure 32, there is a fragmentation pattern that leads to the loss of a phytyl chain ($[M-C_{20}H_{38}+H]^+$, 278 Daltons (Da)) at m/z 615.2 (Figure 33). The fragment ion from the loss of the phytyl chain from the molecular ion to chlorophyll *a*, correspond to chlorophyllide *a* ($C_{35}H_{34}MgO_5N_4$), which is a known algae pigment. Apart from the high peak due to loss of phytyl group, two other high intensity peaks are detected at m/z 583.2 and at m/z 555.2 (base peak). The fragment at m/z 583.2 could be due to loss of phytyl group (at chain A) and a methoxide (CH_3O) at chain B, or it could be due to loss of $[M-C_{20}H_{38}O_2+H]^+$. The base peak, m/z 555.2, could be due to the loss of phytyl group and the loss of methyl formate at chain B ($COOCH_3$).

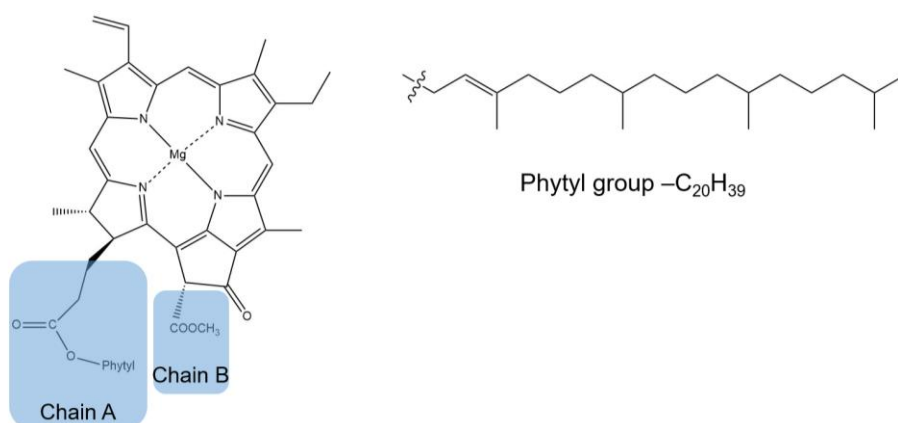


Figure 32 - Chemical structure of chlorophyll *a*, showing the phytyl group.

All MS/MS spectra of *P. glacialis* cultivated under red, blue and white light shows the same fragmentation pattern as the standard sample of chlorophyll *a*. The MS/MS spectrum from white light samples can be seen in Figure 34 and MS/MS spectrum from samples cultivated in blue and red light are shown in Appendix 11: MS/MS of chlorophyll *a*. The MS/MS spectrum obtained from chlorophyll *a* was easy to interpret and showed the same fragmentation pattern, as can be seen in the literature (36, 39).

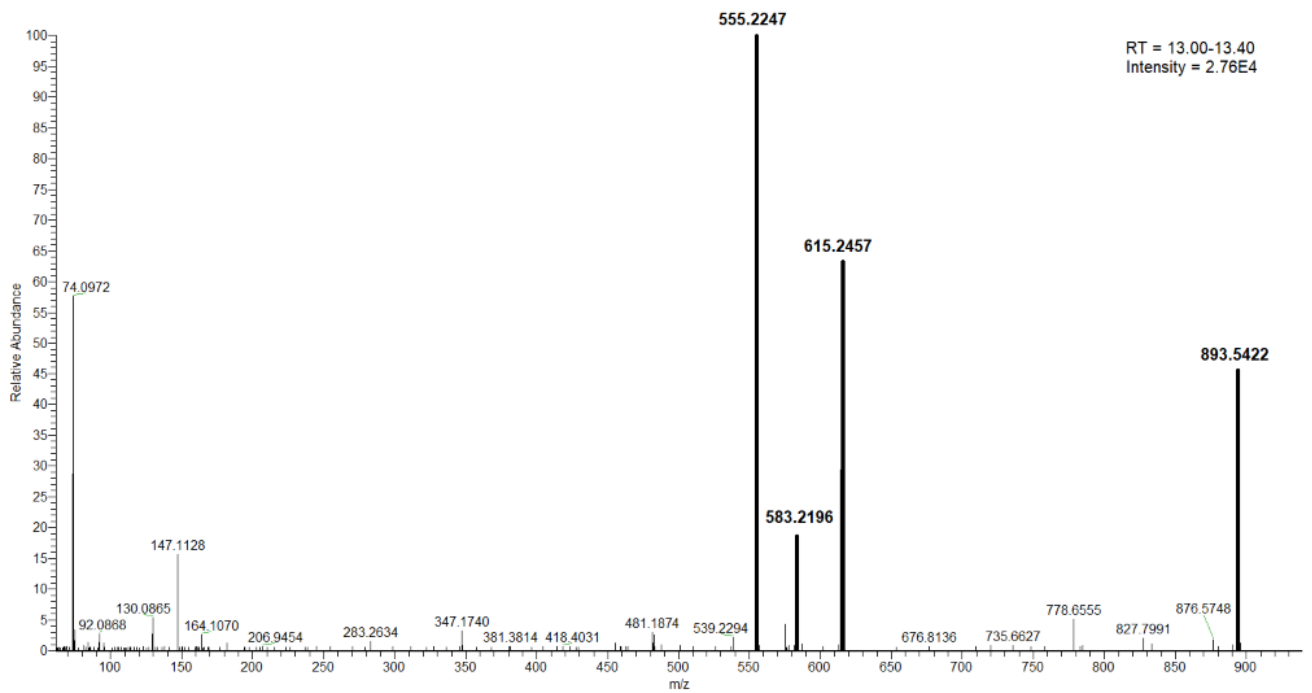


Figure 33 - MS/MS spectrum of chlorophyll a from DHI-mix standard.

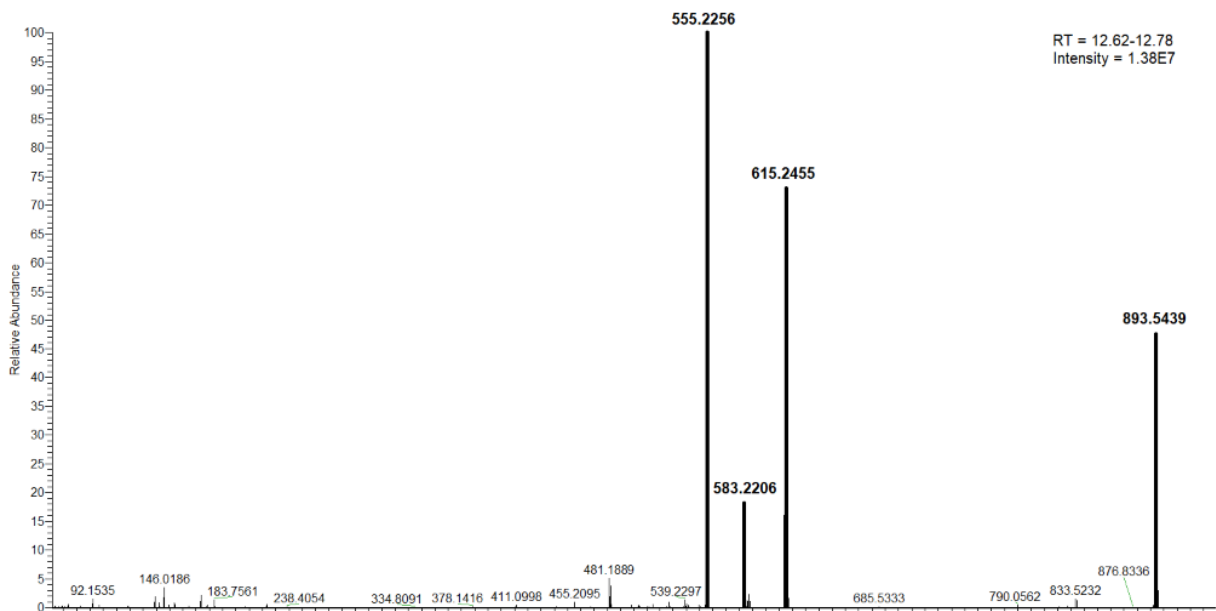


Figure 34 - MS/MS spectrum of chlorophyll a from samples of *P. glacialis* cultivated under white light.

4.7 MS/MS of astaxanthin

Determining whether astaxanthin was present in *P. glacialis* was difficult due to ambiguous results. Some earlier samples of red light indicated in the MS/MS spectrum (DDA scan) indicates the presence of astaxanthin, but in small amounts. However, when analyzing the same samples a few days later with a PRM method with a smaller isolation window, clear evidence of astaxanthin was not seen.

An MS/MS mass spectrum of astaxanthin obtained from DHI-mix standard is shown in Figure 36. For direct comparison MS/MS mass spectrum was collected of what might be astaxanthin from samples of *P. glacialis* cultivated in red (Figure 37 and Figure 82), blue (Figure 83) and white (Figure 38) light conditions. All samples were analyzed with the Q Exactive MS with ESI in positive ionization mode.

The fragmentation pattern of astaxanthin was characterized by the loss of one (fragment m/z 579.4) and two (fragment m/z 561.4) hydroxyl groups (H_2O). The fragment ion at m/z 147.1 is the base peak ion, van Breemen et al. suggested that the fragment corresponds to a dehydrated terminal ring with cleavage between carbon seven and eight (Figure 35) (54).

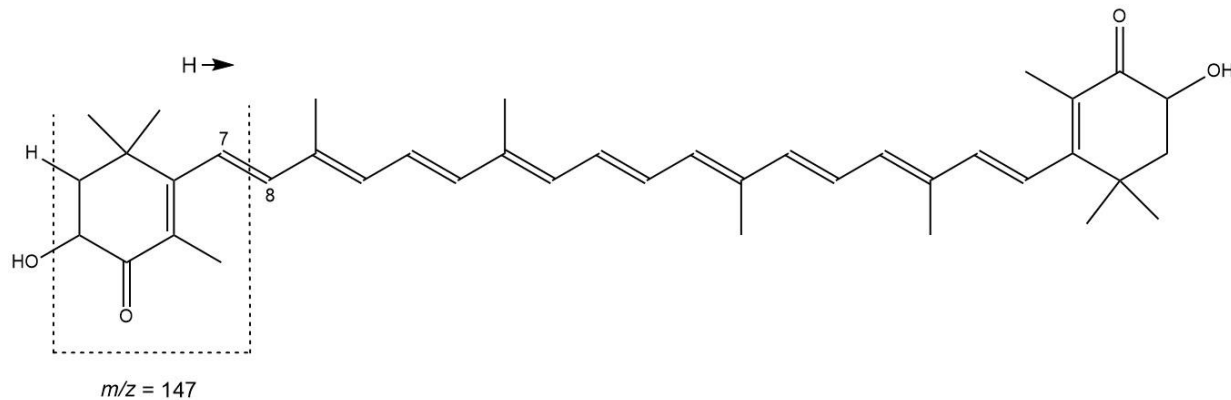


Figure 35 – Suggested fragmentation for astaxanthin fragment ion at m/z 147.1165

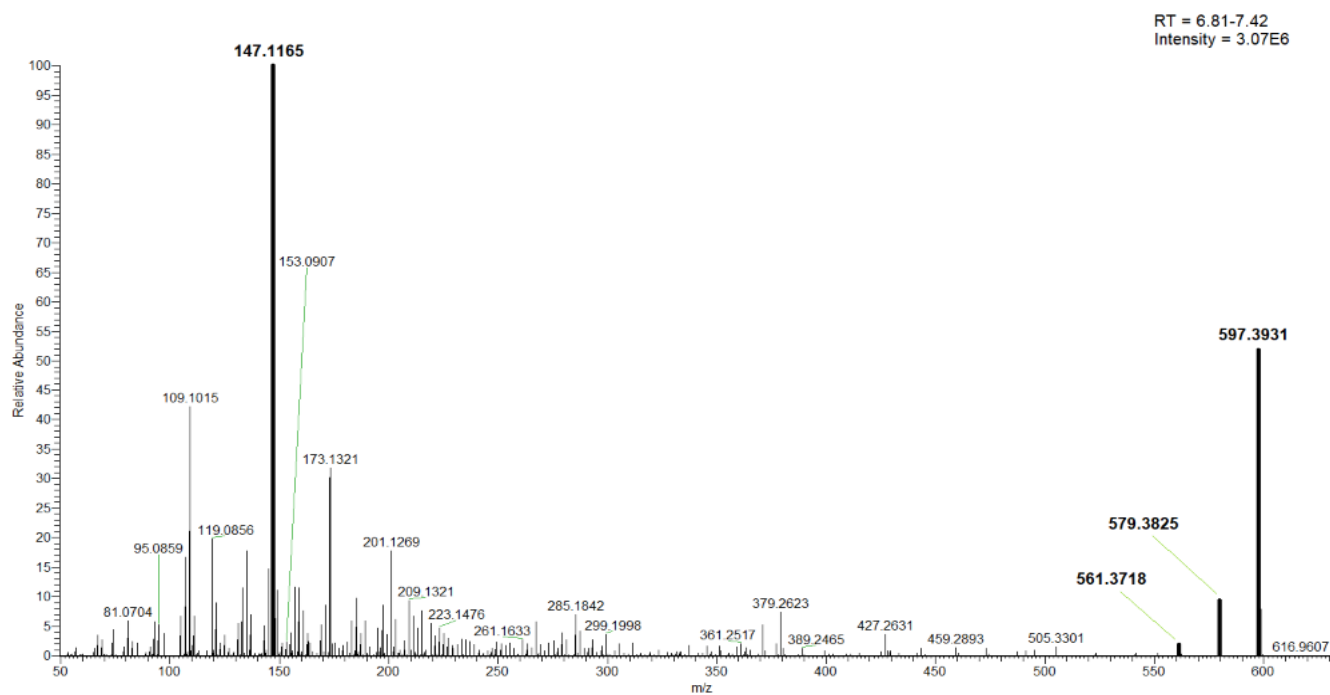


Figure 36 – MS/MS spectrum of astaxanthin from DHI-mix standard.

When developing the DDA method, both DHI-mix standard samples and another batch of *P. glacialis* cultivated under red light was tested. The old batch of red light showed promising MS/MS spectrum of astaxanthin, with the fragment ion at m/z 147.1 having a 35% relative abundance (Figure 37). The fragment ion corresponding to the loss of a hydroxyl group at m/z 579.4 was also present.

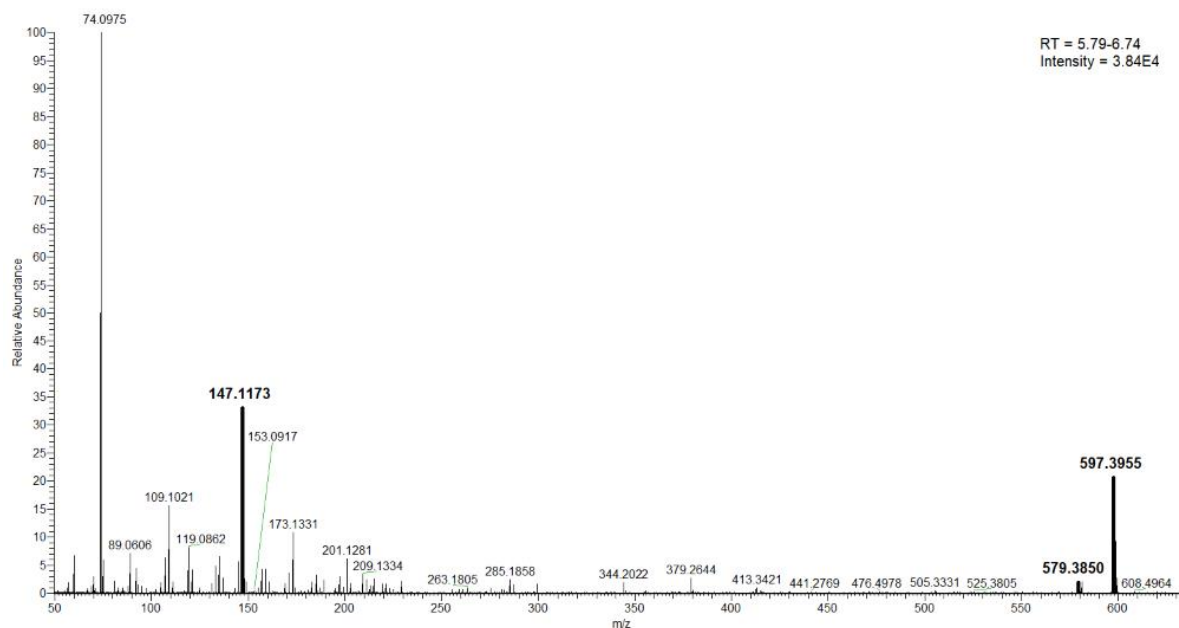


Figure 37 – MS/MS spectrum of astaxanthin from testing DDA scan mode on samples cultivated under red light.

However, the MS/MS spectrum of new batches of *P. glacialis* cultivated in red and blue light lacked the fragment ion corresponding to the loss of two hydroxyl groups, m/z 561.4, but was present in white light samples in small amounts and could be just noise (Figure 38). In addition to this, the base peak ion (m/z 147.1) seen in the MS/MS spectrum of the astaxanthin standard, have now a relative abundance around 2-6% in the algae samples and could possibly be just noise. Samples from red and white light conditions have a base peak ion at m/z 74.1, and blue light at m/z 255.2 (Appendix 12: MS/MS of astaxanthin like compound).

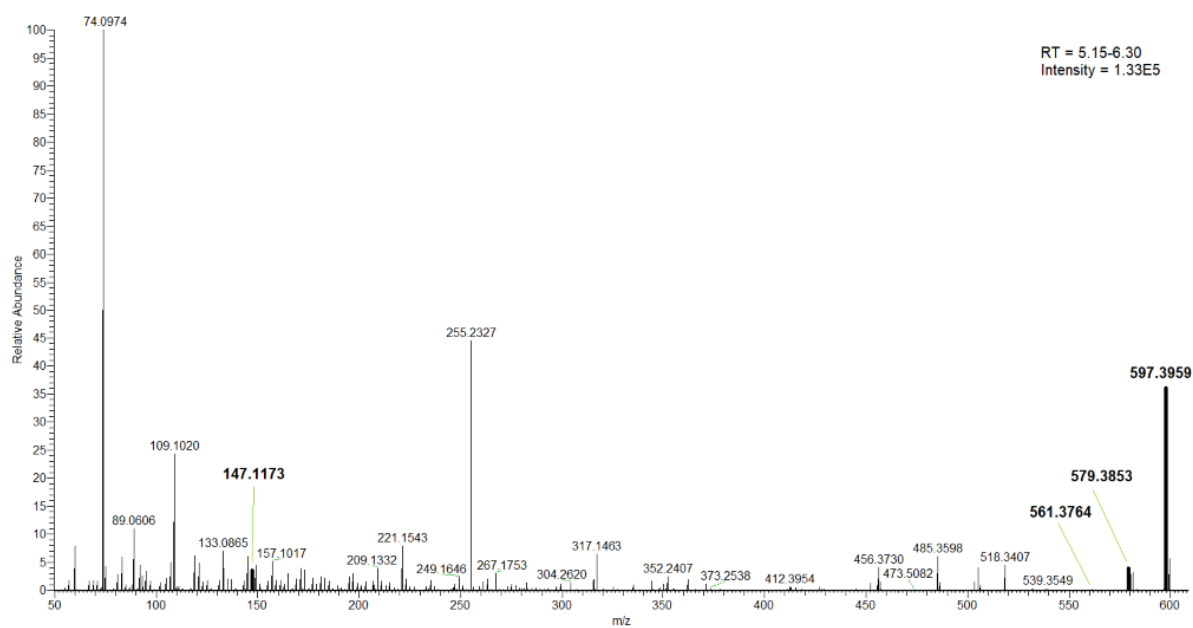


Figure 38 – MS/MS spectrum of astaxanthin from samples cultivated under white light.

When looking closer in the MS/MS spectrum of red, blue and white light samples, it looks like something is co-eluting with astaxanthin and have similar m/z values and fragments as astaxanthin. For improved screening and quantitative confidence in determining whether or not astaxanthin is present a PRM scan mode was developed with a narrower isolation window (0.4 Da), as well as a full scan mode with a resolving power of 140 000.

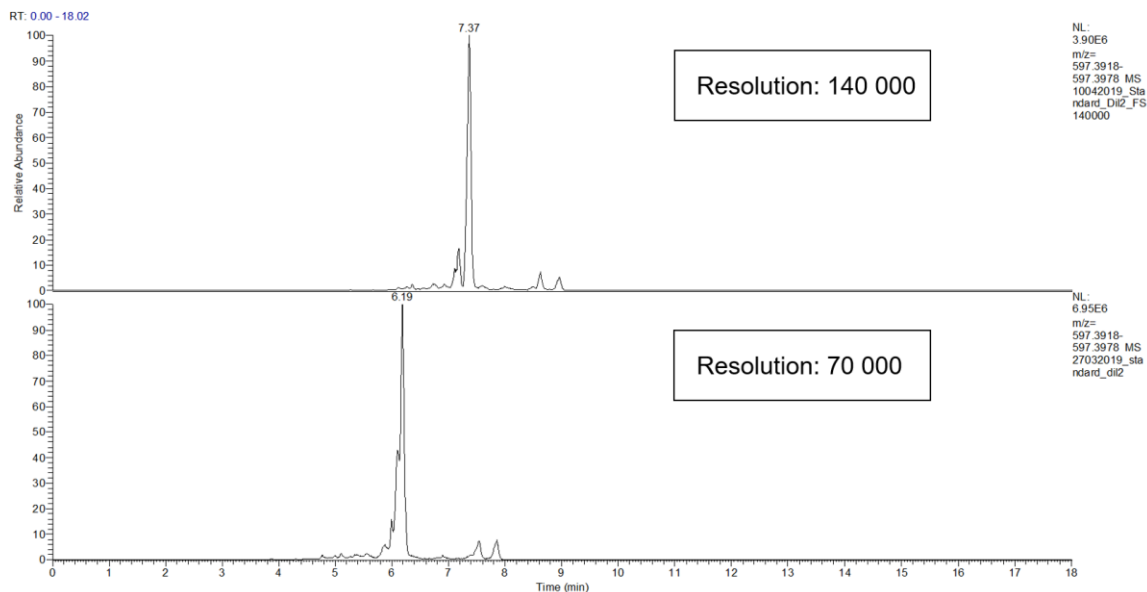


Figure 39 – Extracted ion chromatogram of astaxanthin from DHI-mix standard in resolving power of 140 000 and 70 000.

The standard and algae samples were first analyzed with a resolving power of 70 000, where the results were difficult to interpret due to the presence of some analytes very similar to astaxanthin. In an attempt to obtain more accurate identification of astaxanthin, the same standard samples and algae samples were analyzed 14 days later with a resolving power of 140 000. However, the pigments proved it difficult to obtain reproducible retention times and the extracted ion chromatogram of astaxanthin from the same standard sample (DHI) analyzed 14 days apart shows that the t_R shifted from 6.19 to 7.37 (Figure 39). With a shift in t_R a co-eluting peak was separated from astaxanthin (resolution 140 000). Nonetheless, no extra information came out from increasing the resolving power for the algae samples, and it is uncertain whether astaxanthin actually is present in the samples.

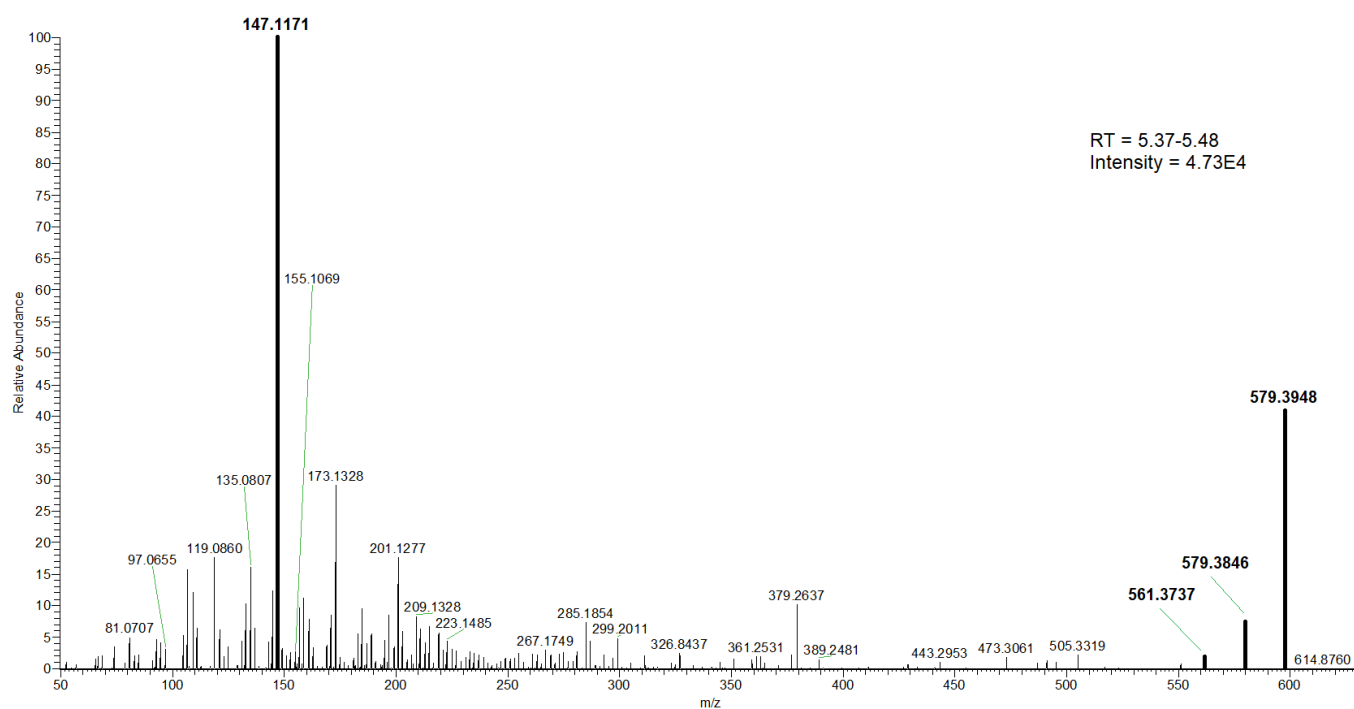


Figure 40 - MS/MS spectrum of astaxanthin from DHI-mix standard (PRM)

The MS/MS spectrum of astaxanthin from DHI-mix standard shows the same fragmentation pattern with the PRM scan mode (Figure 40) as the DDA scan mode (Figure 36). The MS/MS spectrum from two different peaks in white light samples of *P. glacialis* (Figure 41) did not show the same fragmentation pattern as the astaxanthin in the DHI-mix standard did at all. Nor the MS/MS spectrum of *P. glacialis* cultivated in red and blue light conditions showed the same fragmentation pattern as the DHI-mix standard sample did (Appendix 12: MS/MS of astaxanthin).

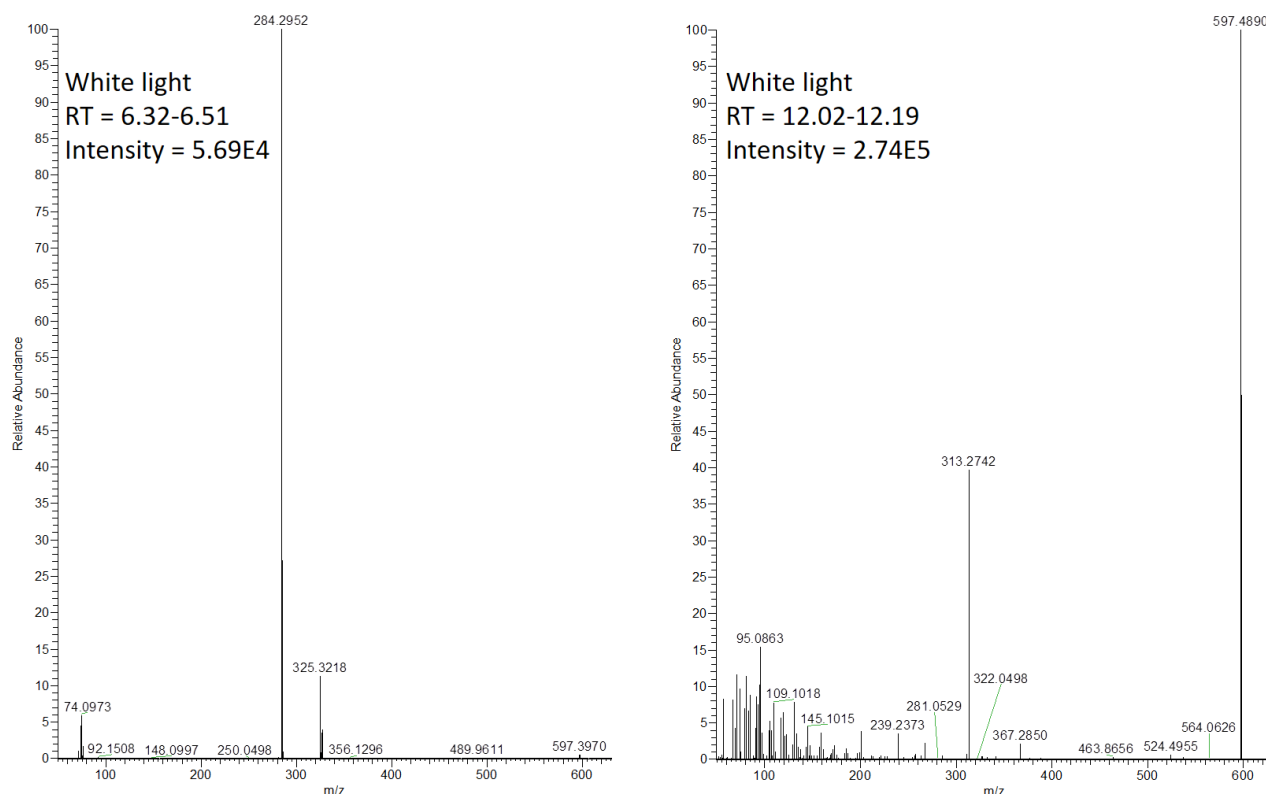


Figure 41 – MS/MS spectrum of two peaks from *P. glacialis* illuminated with white light (PRM).

4.8 Effects of light regimes on pigment content

To understand the effect of different light conditions on the pigments in microalgae it is important to identify and quantify chlorophyll and carotenoids. To estimate the pigment content a method was developed to identify and quantify chlorophyll *a* and astaxanthin with external standards. Other pigments were also identified and quantified relative to chlorophyll *a*.

For samples of *P. glacialis* cultivated under red, blue and white light, three parallels of each light regime were made. For each sample three extractions were carried out and injected three times on UPLC-MS (Q-Exactive with ESI⁺). Chromatograms of each light condition are shown in Appendix 9: Chromatograms of pigment extract.

4.8.1 Chlorophyll a content in different light regimes

Table 10 and Table 11 presents the variations in the amount of chlorophyll *a* in *P. glacialis* illuminated with different wavelengths of light with different methods for calculating the concentrations. The concentration of chlorophyll *a* was calculated based on both peak area and peak intensity from the standard curves in Appendix 5: Calibration curves. The R² values were 0.9871 for peak area and 0.9828 for peak intensity. The maximum values of chlorophyll *a* in extraction one was measured to 233.8 µg/mL (peak area) and 206.1 µg/mL (peak intensities) in cultures illuminated with white light.

For concentrations based on peak area (Table 10), there was a statistic significant difference in amount of chlorophyll *a* between samples cultivated under red and white light (p=0.042) in extraction one. However, there was no significant difference between samples cultivated under blue and white light conditions (p=0.162) in extraction one. Red light was least effective in accumulation of chlorophyll *a* compared to white and blue light conditions. The same effects of different lights on chlorophyll *a* accumulation was also seen in the green microalgae, *Chlorella vulgaris* (31).

Table 10 - Concentrations of chlorophyll *a* cultivated in different lights. Concentrations are obtained with peak area.

Extraction 1			
	Concentration (µg/mL)	SD	RSD (%)
Red light	182.89*	21.53	11.77
Blue light	206.54	6.95	3.36
White light	233.81	20.58	8.80
Extraction 2			
	Concentration (µg/mL)	SD	RSD (%)
Red light	21.99*	0.04	0.16
Blue light	23.00	5.47	23.76
White light	34.72	1.90	5.46
Extraction 3			
	Concentration (µg/mL)	SD	RSD (%)
Red light	2.86	0.94	32.69
Blue light	4.34	1.37	31.64
White light	5.15	1.12	21.73

* Statistically significant difference between light conditions (t-test, 95% CI, $\alpha=0.05$, n=3)

When calculating concentration of chlorophyll *a* based on peak intensities (Table 11), there was a significant difference between red and white light samples ($p=0.007$), but no significant difference between blue and white light samples ($p=0.073$).

Table 11 - Concentrations of chlorophyll *a* cultivated in different lights. Concentrations are obtained with peak intensity.

Extraction 1			
	Concentration ($\mu\text{g/mL}$)	SD	RSD (%)
Red light	177.99*	22.12	12.43
Blue light	184.57	8.64	4.68
White light	206.11	18.54	8.99
Extraction 2			
	Concentration ($\mu\text{g/mL}$)	SD	RSD (%)
Red light	22.02*	0.51	2.32
Blue light	20.07*	4.98	24.81
White light	30.51	1.79	5.86
Extraction 3			
	Concentration ($\mu\text{g/mL}$)	SD	RSD (%)
Red light	2.86	0.91	31.90
Blue light	3.90	1.30	33.26
White light	4.55	0.95	20.93

* Statistically significant difference between light conditions (t-test, 95% CI, $\alpha=0.05$, $n=3$).

The amount of chlorophyll *a* has been used as a measurement of algal biomass, and the results may indicate that the algae grow best under white light conditions. However, the specific growth rate for *P. glacialis* calculated from the cell count shows different results.

The specific growth rates and the statistical subgroups as calculated from an All Pair Tukey Test for each irradiance type is presented in Table 12. Blue light gave highest growth overall, but the only statistical difference was observed between cells grown under blue light compared to cells grown under white light ($p=0.03$) (47). This suggest that using the amount of chlorophyll *a* as an index for algal biomass, might be an unreliable method.

Table 12 - Specific growth rates \pm standard deviation for each irradiance type. Labels a-b denote homogenous subsets (47).

Irradiance	μ (doublings h^{-1})
Blue	0.0260 ± 0.0032^a
Red	0.0225 ± 0.0037^b
White	0.0230 ± 0.0015^{ab}

When weighing out the algae samples for analysis, an analytical weighing balance with four decimals was used. For the analysis 10.0 mg of dry algal biomass was weighed out, the exact mass weighed was mostly 10.0 mg, however a couple of samples was weighed out to be 9.9 mg and 10.1 mg. Since the weight variance of 0.1 mg was so small, it was not taken into account when calculating concentration of chlorophyll *a*.

4.8.2 Relative amount of pigments

The pigment content in red, blue and white light regimes was estimated for pheophytin *a*, fucoxanthin and carotene. These pigments were chosen because of their high intensities in the algae samples, and because it was interesting to investigate the effect of light on chlorophyll and carotenoid content. The figures (Figure 42, Figure 44 and Figure 46) displayed are the total amount (mean peak area and mean peak intensity) of all three extractions for pheophytin *a*, fucoxanthin and carotene in red, blue and white light regimes. The selected pigments were also displayed as a relative amount compared to chlorophyll *a* (Figure 43, Figure 45 and Figure 48).

The amount of pheophytin *a* in *P. glacialis* was measured as both peak area and peak intensity. The effect of different light regimes, e.g. red, blue and white light, on total amount of pheophytin in *P. glacialis* is shown in Figure 42. Looking at peak area, there is a statistically significant difference between white light conditions compared to blue light ($p=0.002$) and red light ($p=0.007$). However, when looking at peak intensity, there was no significant difference between white light and red light ($p=0.299$), but there was a significant difference between white and blue light ($p=0.032$). The trend is similar for both area and intensity even though not equally significant when using signal intensity.

The relative standard deviation (RSD) was low for all light intensities both in peak area and peak intensity for pheophytin *a* (red: 2.6% and 2.4%, blue: 2.7% and 3.6%, white: 1.2% and 3.8%), meaning the SD is small and the data is tightly clustered around the mean.

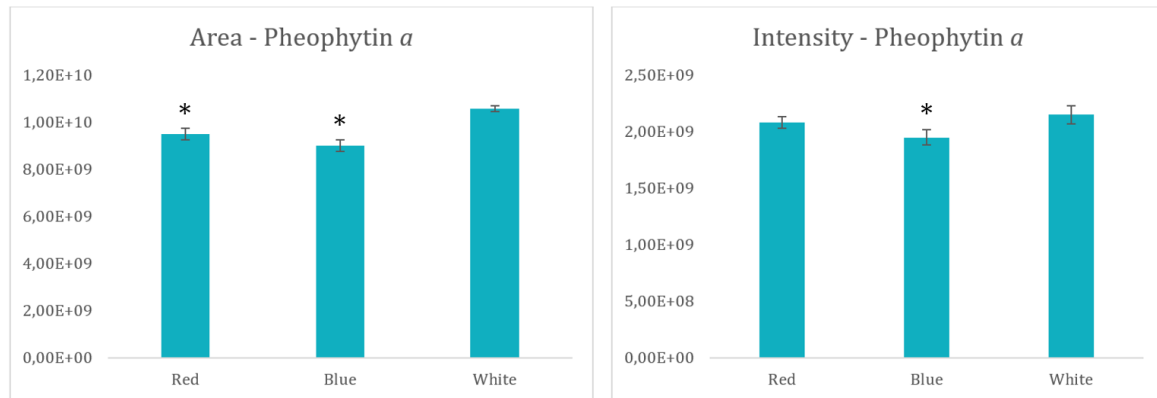


Figure 42 - Effects of red, blue and white light on amount of pheophytin *a* in *P. glacialis*. Displayed with both peak area and peak intensity with respective standard deviations. *Statistically significant difference between red and blue light compared to white light conditions (t-test, 95% CI, $\alpha=0.05$, $n=3$)

Figure 43 shows the relative amount of pheophytin *a* (mean peak area and peak intensity) compared to chlorophyll *a* (mean peak area and peak intensity). There was no statistically significant difference of the relative amount of pheophytin *a* compared to chlorophyll *a* in red, blue and white light regimes (independent sample t-test, $\alpha=0.05$).

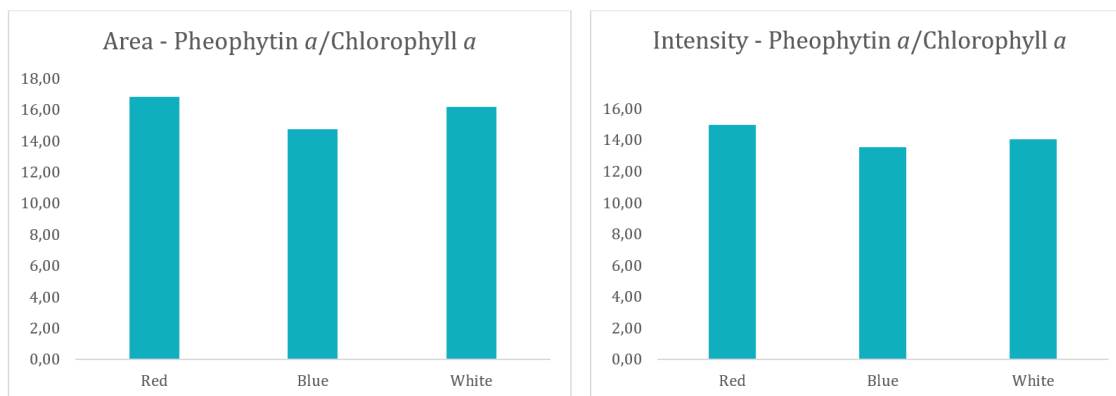


Figure 43 - Relative amount of pheophytin *a* compared to chlorophyll *a*, with regard to both peak area (left) and peak intensity (right) ($n=3$).

The amount of the carotenoid, fucoxanthin, was also significantly higher when *P. glacialis* was cultivated under white light compared to blue light for peak area ($p=0.006$) and for peak intensity ($p=0.027$). However, there was no significant difference between red and white light for both peak area ($p=0.091$) and peak intensity ($p=0.105$). This is due to the large standard

deviation for the red light sample as seen in Figure 44 and overlapping confidence intervals (CI).

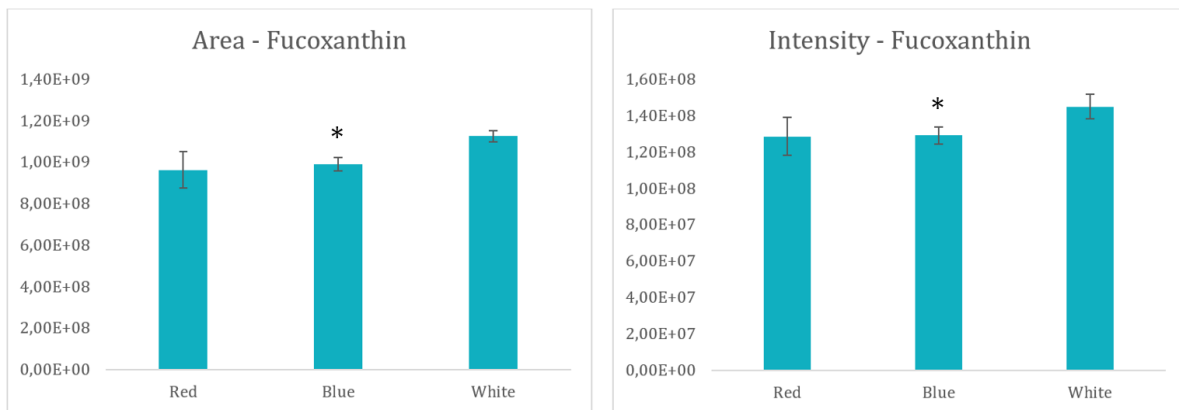


Figure 44 - Effects of red, blue and white light on amount of fucoxanthin in *P. glacialis*. Displayed with both peak area and peak intensity with respective standard deviations. *Statistically significant difference between red and blue light compared to white light conditions (t-test, 95% CI, $\alpha=0.05$, $n=3$).

The relative amount of fucoxanthin compared to chlorophyll *a* was very similar for all light conditions (red, blue and white) (Figure 45). An independent samples t-test ($\alpha=0.05$) showed that there was no statistical significant difference of the relative amount of fucoxanthin compared to chlorophyll *a* in red, blue and white light regimes.

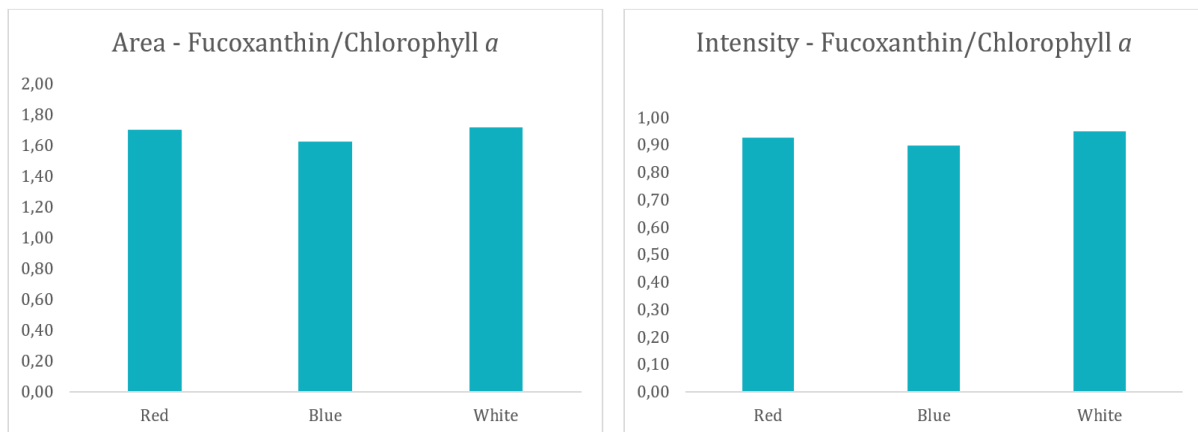


Figure 45 - Relative amount of fucoxanthin compared to chlorophyll *a*, with regard to both peak area (left) and peak intensity (right) ($n=3$).

Significantly higher amounts of carotene was seen when cultivating *P. glacialis* in white light conditions compared to blue ($p=0.006$) and red light ($p=0.005$) for peak area (Figure 46). The

same trend was also seen for peak intensities, hence red light was much less effective in accumulation of carotene in *P. glacialis*.

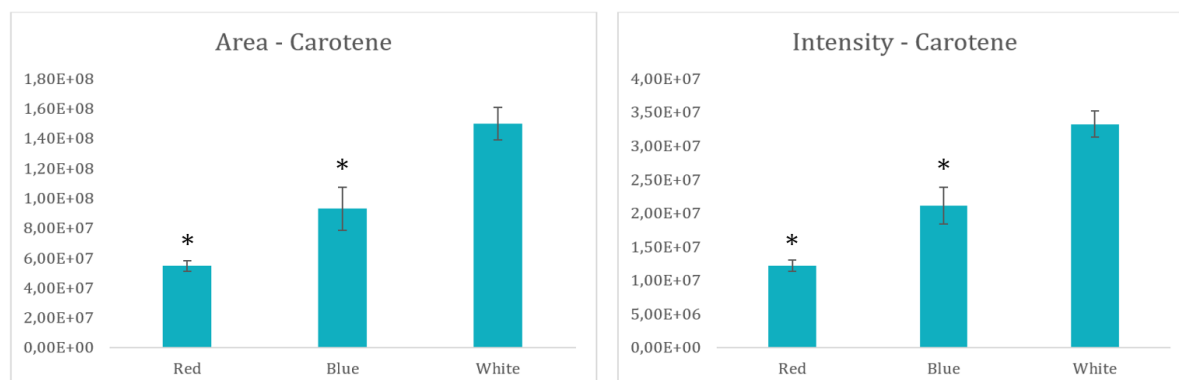


Figure 46 - Effects of red, blue and white light on amount of carotene in *P. glacialis*. Displayed with both peak area and peak intensity with respective standard deviations. *Statistically significant difference between red and blue light compared to white light conditions (*t*-test, 95% CI, $\alpha=0.05$, $n=3$)

This trend can also be seen in the chromatogram, where the amount of carotene increases from red to white light condition (Figure 47). In addition to this, the problem with non-reproducible retention times are also shown in the figure. The t_R shifted 0.16 min and 0.32 min for carotene and chlorophyll *a*, respectively, when comparing samples cultivated in white and red light.

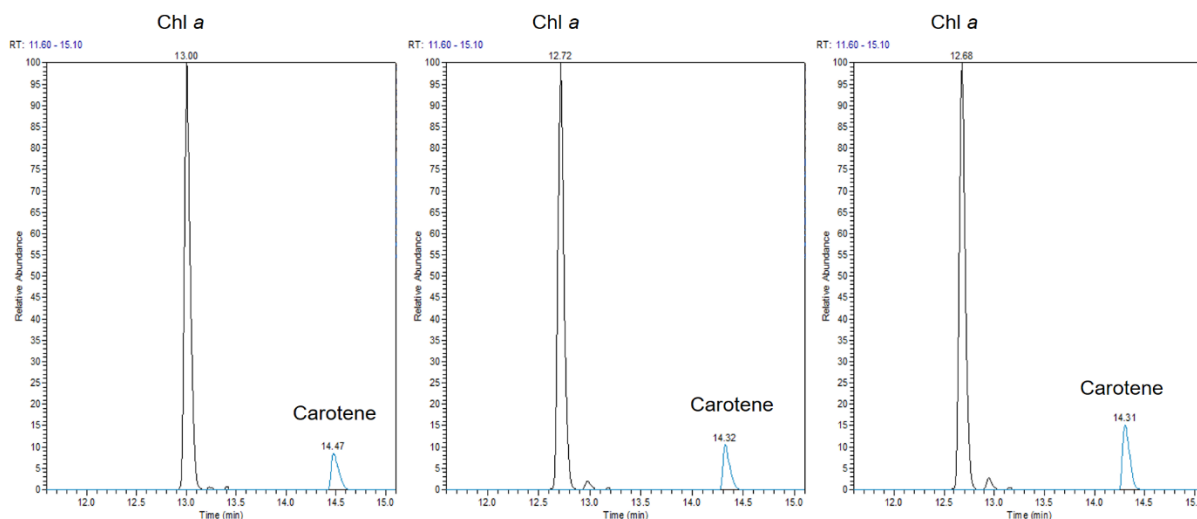


Figure 47 - Extracted ion chromatogram of chlorophyll *a* and carotene in red, blue and white samples, respectively.

When comparing relative amounts of carotene to chlorophyll *a*, the same trend is shown in both peak area and peak intensity (Figure 48). The results shows a significant difference of the relative amount of carotene compared to chlorophyll *a* in the different light regimes. The relative amount of carotene compared to chlorophyll *a* was low in samples cultivated under red

light conditions and high in samples cultivated under white light. Hence, white light is the most effective light for accumulating carotene in *P. glacialis*.

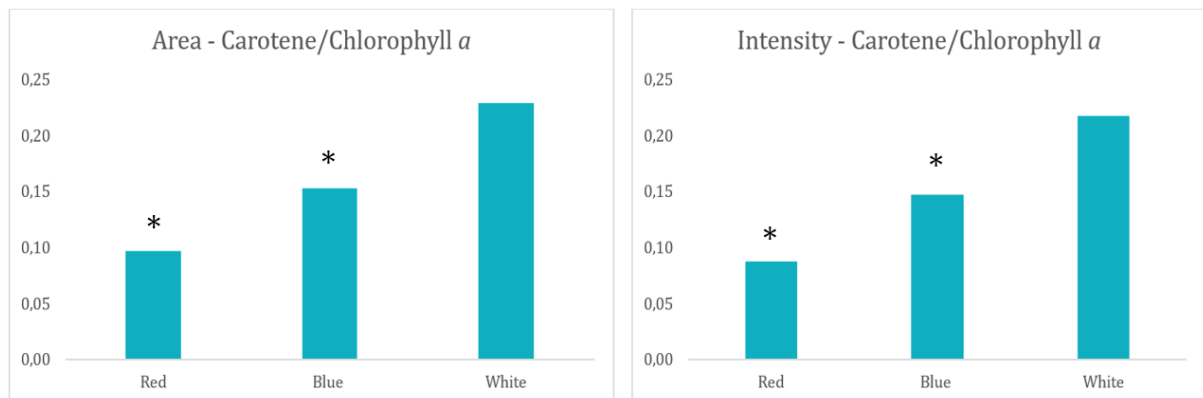


Figure 48 - Relative amount of carotene compared to chlorophyll a, with regard to both peak area (left) and peak intensity (right) (t-test, 95% CI, $\alpha=0.05$, $n=3$).

Pigments that are red/orange, like carotene, would absorb white and blue light and reflect the red light. When the algae is irradiated with red light, carotene would not be able to utilize the light and it becomes excessive. This just shows that the algae can regulate the production of the pigments they need given the conditions they are exposed to.

4.9 Limitations of the study

It is plausible that several limitations might have influenced the results of estimating the content of chlorophyll *a* and determining the pigment content in *P. glacialis*.

When testing the different extraction solvents, due to the time limitations only one extraction was carried out for each algae sample. Two more extractions should have been carried out on the same algae sample to avoid random errors in the results.

In the chromatogram of the standard samples and algae samples some pigments needed manually integration to determine the peak area, e.g. fucoxanthin, due to peak shouldering/splitting. This did not apply to chlorophyll *a* and did not affect the standard curve. Astaxanthin exhibited peaks which needed some manually integration and could have affected the standard curve. However, the standard curve from astaxanthin was not used to calculate concentrations for astaxanthin since it could not be detected in the algae samples.

The chromatography of the DHI-mix standard sample and algae sample exhibited reproducibility issues because of the shift in the retention time. This was seen for all pigments in both the standard sample (DHI) and algae samples, where inter-day variations were larger than intra-day variations. This made it difficult to develop a reproducible t-SIM method, which showed promising results compared to full scan analysis. An example of the disadvantage the variable t_R came with can be seen in the Appendix 10: Chromatogram and mass spectra (t-SIM) for e.g. alloxanthin (Figure 67) and chlorophyll c_2 (Figure 72), where the t_R of the pigments have shifted so that a part of the peak falls outside the retention window. For optimal sensitivity and due to the limited scan speed of the Q Exactive a limited number of t-SIM methods should have overlapping retention windows, and hence it was not ideal to expand the windows to avoid the problem.

Pigments are difficult to work with, due to that light, oxygen and heat causes destruction of pigment extracts (49). To minimize this, the extracts were kept and worked with in the lowest possible light throughout the extraction procedure. Nevertheless, some pigments may still have degraded. The pigments stability was not tested thoroughly in this project, which is something that must be done in future studies.

There were rather few parallels for the estimation of chlorophyll *a* content and pigment composition in red, blue and white light regimes (n=3). This could have led to type II errors in hypothesis testing the effect of light regimes on selected pigments. Type II error is the probability of failing to reject the null hypothesis when in fact it is wrong. In order for these estimates to be more representative for the actual chlorophyll *a* content and the effect of light regimes on the microalgae, several rounds of cultivation are needed. When the sample size gets larger, the standard error gets smaller and the probability of type II error decreases.

In parallel one, injection two for red, blue and white algae samples there were several values that potentially could be outliers. These were tested using Q-test in Excel®, the results can be found in Appendix 14: Q-test chlorophyll *a* (extraction one). However, since some of the high values for parallel one, injection two, could not be rejected with the Q-test, it was decided that no values were removed from the data set. The outliers did not greatly affect the results; for algae samples cultivated in white light (extraction one, peak area), the difference in chlorophyll *a* content was 3.9% when the potential outliers were removed.

Only samples cultivated in laboratory scale was analyzed in this thesis. Algae harvested from Finn fjord AS was intended to be analyzed on an optimal UPLC-MS analysis. However, due to the lack of time left on this project these samples were not tested.

5 Conclusion and future perspective

Porosira glacialis was cultivated in laboratory scale to investigate the pigment composition and the influence of different light regimes (red, blue and white) on pigment accumulation. Twelve different pigments were identified in *P. glacialis*, where seven of them are carotenoids.

The results suggest that different light regimes could regulate the accumulation of different pigments in *P. glacialis*. Especially the carotenoid, carotene, showed significant difference in various light regimes, where red light was much less effective in accumulation of carotene than blue and white light. Overall, the accumulation of chlorophyll *a*, pheophytin *a*, fucoxanthin and carotene was highest when samples of *P. glacialis* was illuminated in white light. Future work should calculate the relative amount of the other identified pigments in *P. glacialis* compared to chlorophyll *a*.

Whether astaxanthin actually is present in *P. glacialis* is uncertain with the current light regimes (32 $\mu\text{molphoton}/\text{m}^2/\text{sec}$). However, it has been reported that intense light illumination (350 $\mu\text{molphoton}/\text{m}^2/\text{sec}$) of algae can induce oxidative stress resulting in an increase of photoprotective carotenoid content, e.g. astaxanthin (30). This is something that would be interesting to look further into.

UPLC coupled to the MS Q Exactive with electrospray ionization in full scan mode appeared to be useful for determination of molecular ions of different pigments. This method provided better sensitivity compared to UPLC coupled to MS Q-TOF with APCI. The t-SIM mode showed promising results, however, the retention time of the pigments should be more stable.

References

1. Norambuena F, Hermon K, Skrzypczyk V, Emery JA, Sharon Y, Beard A, et al. Algae in fish feed: performances and fatty acid metabolism in juvenile Atlantic Salmon. *PloS one*. 2015;10(4):e0124042-e.
2. Senroy S, Pal R. *Microalgae in Aquaculture: A Review with Special References to Nutritional Value and Fish Dietetics* 2014.
3. *The Norwegian aquaculture analysis 2017*. Ernst & Young AS; 2018.
4. Ytrestøyl T, Aas TS, Åsgård T. Utilisation of feed resources in production of Atlantic salmon (*Salmo salar*) in Norway. *Aquaculture*. 2015;448:365-74.
5. Ramskjell M. Large scale cultivation of microalgae at Finnfjord AS: The effect of addition of CO₂ and flue gas on lipid production and fatty acid composition Tromsø: The arctic university of Norway; 2018.
6. Throndsen J, Hasle GR, Tangen K. *Phytoplankton of Norwegian coastal waters*. Oslo: Almater forl.; 2007.
7. Botany Do. Centric vs. pennate [13.01.2019]. Available from: <http://botit.botany.wisc.edu/Resources/Botany/Heterokonts/Diatoms/Centric%20vs%20pennate.jpg.html>.
8. Begum H, Yusoff FMD, Banerjee S, Khatoon H, Shariff M. Availability and Utilization of Pigments from Microalgae. *Critical Reviews in Food Science and Nutrition*. 2016;56(13):2209-22.
9. Schnurr PJ, Allen DG. Factors affecting algae biofilm growth and lipid production: A review. *Renewable and Sustainable Energy Reviews*. 2015;52:418-29.
10. Lebeau T, Robert JM. Diatom cultivation and biotechnologically relevant products. Part I: cultivation at various scales. *Applied microbiology and biotechnology*. 2003;60(6):612-23.
11. Ruivo M, Amorim A, Cartaxana P. Effects of growth phase and irradiance on phytoplankton pigment ratios: implications for chemotaxonomy in coastal waters. *Journal of Plankton Research*. 2011;33(7):1012-22.
12. Pulz O, Gross W. Valuable products from biotechnology of microalgae. *Applied microbiology and biotechnology*. 2004;65(6):635-48.
13. Yaakob Z, Ali E, Zainal A, Mohamad M, Takriff MS, Yaakob Z. An overview: biomolecules from microalgae for animal feed and aquaculture. *Journal of biological research (Thessalonike, Greece)*. 2014;21(1):1-10.
14. Asche F, Bjørndal T. *The Economics of Salmon Aquaculture: Improved feed quality*. 2 ed. Somerset: Wiley; 2011.
15. Bremnes E. Kan algefôr gi mindre lusepåslag hos laks? Nofima 2018 [updated 06.02.2019]. Available from: <https://nofima.no/nyhet/2018/11/kan-algefôr-gi-mindre-lusepåslag-hos-laks/>.
16. Wang HD, Chen CC, Huynh P, Chang JS. Exploring the potential of using algae in cosmetics. *Bioresource technology*. 2015;184:355-62.
17. *Chlorophylls and Bacteriochlorophylls: Biochemistry, Biophysics, Functions and Applications*. Dordrecht: Springer Netherlands, Dordrecht; 2006.
18. Milenković SM, Zvezdanović JB, Anđelković TD, Marković DZ. The identification of chlorophyll and its derivatives in the pigment mixtures: HPLC-chromatography, visible and mass spectroscopy studies. *Adv Technol*. 2012;1(1):16-24.
19. Brodie JA, Lewis J. *Unravelling the algae : the past, present, and future of algal systematics*. Boca Raton: CRS Press; 2007.

20. Kuczynska P, Jemiola-Rzeminska M, Strzalka K. Photosynthetic Pigments in Diatoms. *Mar Drugs*. 2015;13(9):5847-81.
21. Polivka T, Frank HA. Molecular factors controlling photosynthetic light harvesting by carotenoids. *Accounts of chemical research*. 2010;43(8):1125-34.
22. Rivera SM, Christou P, Canela-Garayoa R. Identification of carotenoids using mass spectrometry. *Mass spectrometry reviews*. 2014;33(5):353-72.
23. Yuan JP, Peng J, Yin K, Wang JH. Potential health-promoting effects of astaxanthin: a high-value carotenoid mostly from microalgae. *Molecular nutrition & food research*. 2011;55(1):150-65.
24. Cuellar-Bermudez SP, Aguilar-Hernandez I, Cardenas-Chavez DL, Ornelas-Soto N, Romero-Ogawa MA, Parra-Saldivar R. Extraction and purification of high-value metabolites from microalgae: essential lipids, astaxanthin and phycobiliproteins. *Microbial biotechnology*. 2015;8(2):190-209.
25. Newman DJ, Cragg GM, Grothaus P. *Chemical Biology of Natural Products*. 1 ed 2017.
26. Singh SP, Singh P. Effect of temperature and light on the growth of algae species: A review. *Renewable and Sustainable Energy Reviews*. 2015;50:431-44.
27. Blair MF, Kokabian B, Gude VG. Light and growth medium effect on *Chlorella vulgaris* biomass production. *Journal of Environmental Chemical Engineering*. 2014;2(1):665-74.
28. Eloranta P. Paper chromatography as a method of phytoplankton community analysis. *Annales Botanici Fennici*. 1986;23(2):153-9.
29. Salguero A, de la Morena B, Vigarra J, Vega JM, Vilchez C, León R. Carotenoids as protective response against oxidative damage in *Dunaliella bardawil*. *Biomolecular Engineering*. 2003;20(4):249-53.
30. Wang B, Zarka A, Trebst A, Boussiba S. Astaxanthin accumulation in *Haematococcus pluvialis* (chlorophyceae) as an active photoprotective process under high irradiance. 2003:1116-24.
31. Kendirlioğlu Şimşek G, Cetin A. Effect of Different Wavelengths of Light on Growth, Pigment Content and Protein Amount of *Chlorella vulgaris*. *Fresenius Environmental Bulletin*. 2017;26:7974-80.
32. Bidigare R, Van Heukelem L, C. Trees C. *Algal Culturing Techniques: Analysis of Algal Pigments by High-Performance Liquid Chromatography*. Andersen RA, editor. Amsterdam: Elsevier; 2005. 327-45 p.
33. Mendes CR, Cartaxana P, Brotas V. HPLC determination of phytoplankton and microphytobenthos pigments: comparing resolution and sensitivity of a C18 and a C8 method. *Limnology and Oceanography: Methods*. 2007;5(10):363-70.
34. Rivera SM, Canela-Garayoa R. Analytical tools for the analysis of carotenoids in diverse materials. *Journal of chromatography A*. 2012;1224:1-10.
35. van Leeuwe MA, Villerius LA, Roggeveld J, Visser RJW, Stefels J. An optimized method for automated analysis of algal pigments by HPLC. *Marine Chemistry*. 2006;102(3):267-75.
36. Juin C, Bonnet A, Nicolau E, Bérard J-B, Devillers R, Thiéry V, et al. UPLC-MS^E profiling of Phytoplankton metabolites: application to the identification of pigments and structural analysis of metabolites in *Porphyridium purpureum*. *Marine drugs*. 2015;13(4):2541-58.
37. Hansen S, Pedersen - Bjergaard S, Rasmussen K. *Introduction to Pharmaceutical Chemical Analysis*. Chichester, UK: Chichester, UK: John Wiley & Sons, Ltd; 2011.

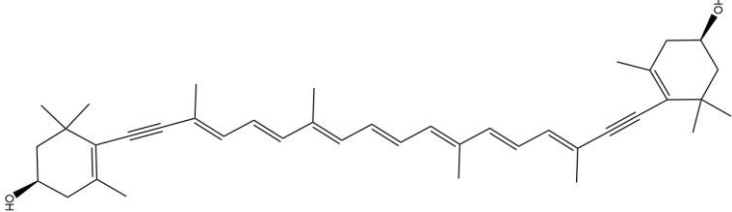
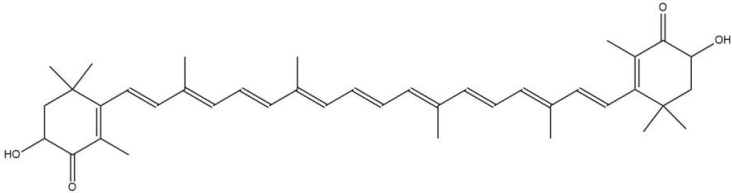
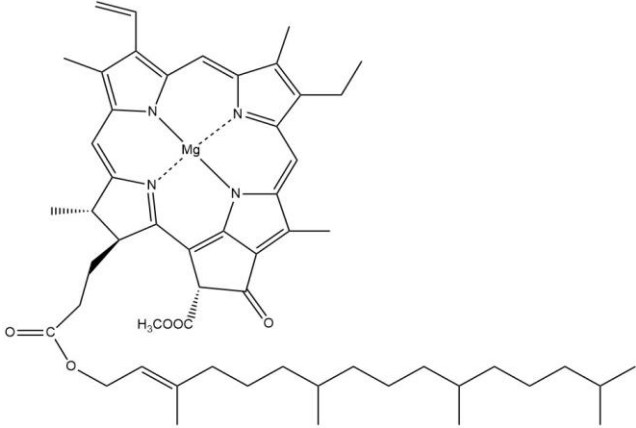
38. Fu W, Magnusdottir M, Brynjolfson S, Palsson BO, Paglia G. UPLC-UV-MS(E) analysis for quantification and identification of major carotenoid and chlorophyll species in algae. *Anal Bioanal Chem.* 2012;404(10):3145-54.
39. Airs RL, Garrido JL. Liquid chromatography-mass spectrometry for pigment analysis. In: Llewellyn CA, Egeland ES, Johnsen G, Roy S, editors. *Phytoplankton Pigments: Characterization, Chemotaxonomy and Applications in Oceanography.* Cambridge Environmental Chemistry Series. Cambridge: Cambridge University Press; 2011. p. 314-42.
40. Kalli A, Smith GT, Sweredoski MJ, Hess S. Evaluation and optimization of mass spectrometric settings during data-dependent acquisition mode: focus on LTQ-Orbitrap mass analyzers. *Journal of proteome research.* 2013;12(7):3071-86.
41. ThermoFisherScientific. Molecular Dissociation Technology Overview [16.03.2019]. Available from: <https://www.thermofisher.com/no/en/home/industrial/mass-spectrometry/mass-spectrometry-learning-center/mass-spectrometry-technology-overview/dissociation-technique-technology-overview.html>.
42. Usher KM, Hansen SW, Amoo JS, Bernstein AP, McNally MEP. Precision of internal standard and external standard methods in high performance liquid chromatography. *LCGC.* 2015.
43. Airs RL, Keely BJ. A novel approach for sensitivity enhancement in atmospheric pressure chemical ionisation liquid chromatography/mass spectrometry of chlorophylls. *Rapid Communications in Mass Spectrometry.* 2000;14(3):125-8.
44. Matzke MM, Brown JN, Gritsenko MA, Metz TO, Pounds JG, Rodland KD, et al. A comparative analysis of computational approaches to relative protein quantification using peptide peak intensities in label-free LC-MS proteomics experiments. *Proteomics.* 2013;13(3-4):493-503.
45. Lamos SM, Shortreed MR, Frey BL, Belshaw PJ, Smith LM. Relative quantification of carboxylic acid metabolites by liquid chromatography-mass spectrometry using isotopic variants of cholamine. *Analytical chemistry.* 2007;79(14):5143-9.
46. Dolan JW. When should an internal standard be used? *LCGC North America.* 2012;30(6):474-80.
47. Bjørnstad EA. Understanding how excitation wavelengths influence algal growth phenotypes and phytopigment content: Norwegian College of Fishery Science; 2019.
48. Waters. ACQUITY UPLC BEH Columns Care and Use Manual [24.03.2019]. Available from: <http://www.waters.com/waters/support.htm?lid=10008685&type=USRM>.
49. Alam DT. Extraction of Natural Pigments from Marine Algae. *Journal of Agricultural and Marine Sciences.* 2019;23:81-91.
50. Zapata M, Rodríguez F, Garrido J. Separation of chlorophylls and carotenoids from marine phytoplankton: A new HPLC method using a reversed phase C8 column and pyridine-containing mobile phases. *Marine Ecology Progress series.* 2000;195:29-45.
51. Cerón-García MC, González-López CV, Camacho-Rodríguez J, López-Rosales L, García-Camacho F, Molina-Grima E. Maximizing carotenoid extraction from microalgae used as food additives and determined by liquid chromatography (HPLC). *Food Chemistry.* 2018;257:316-24.
52. Buchaca T, Felip M, Catalan J. A comparison of HPLC pigment analyses and biovolume estimates of phytoplankton groups in an oligotrophic lake. *Journal of Plankton Research.* 2005;27(1):91-101.
53. Watanabe T, Nakazato M, Mazaki H, Hongu A, Konno M, Saitoh S, et al. Chlorophyll a epimer and pheophytin a in green leaves. *Biochimica et Biophysica Acta (BBA) - Bioenergetics.* 1985;807(2):110-7.

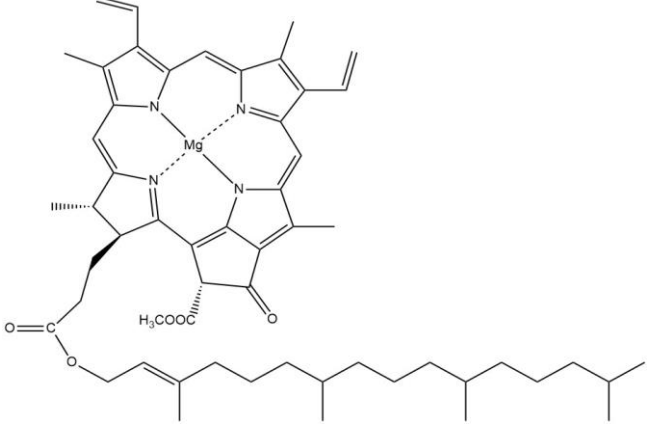
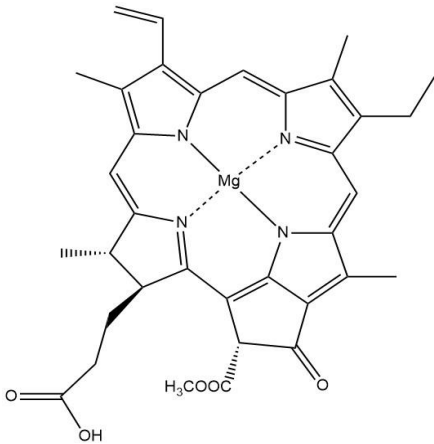
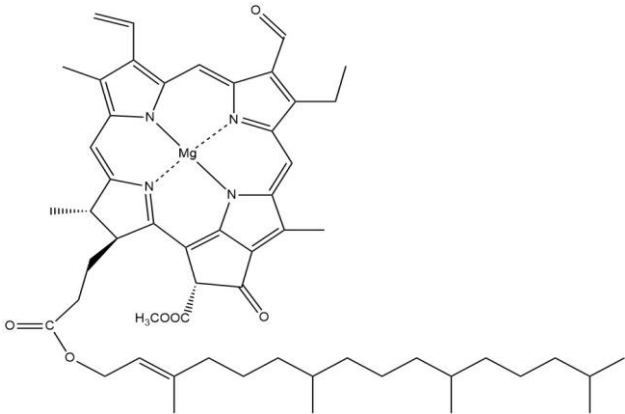
54. van Breemen RB, Dong L, Pajkovic ND. Atmospheric Pressure Chemical Ionization Tandem Mass Spectrometry of Carotenoids. *International journal of mass spectrometry*. 2012;312:163-72.
55. Rajauria G, Foley B, Abu-Ghannam N. Characterization of dietary fucoxanthin from *Himantalia elongata* brown seaweed. *Food Research International*. 2017;99:995-1001.
56. Jiao G, P M Hui J, W Burton I, Thibault M-H, Pelletier C, Boudreau J, et al. Characterization of Shrimp Oil from *Pandalus borealis* by High Performance Liquid Chromatography and High Resolution Mass Spectrometry. *Marine drugs*. 2015;13(6):3849-76.
57. Sommella E, Conte G, Salviati E, Pepe G, Bertamino A, Ostacolo C, et al. Fast Profiling of Natural Pigments in Different *Spirulina (Arthrospira platensis)* Dietary Supplements by DI-FT-ICR and Evaluation of their Antioxidant Potential by Pre-Column DPPH-UHPLC Assay. *Molecules*. 2018;23:1152.
58. Rivera S, Vilaro F, Canela R. Determination of carotenoids by liquid chromatography/mass spectrometry: effect of several dopants. *Anal Bioanal Chem*. 2011;400(5):1339-46.

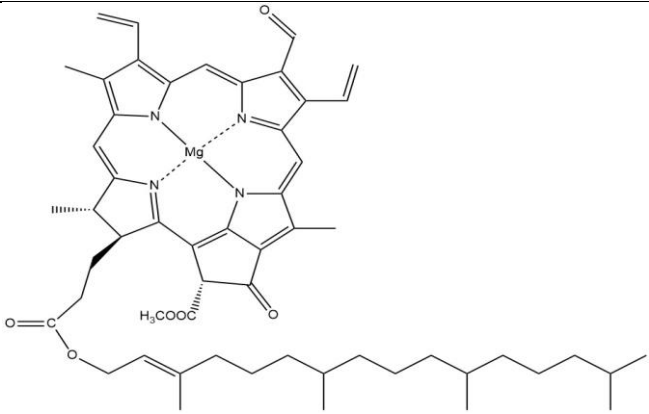
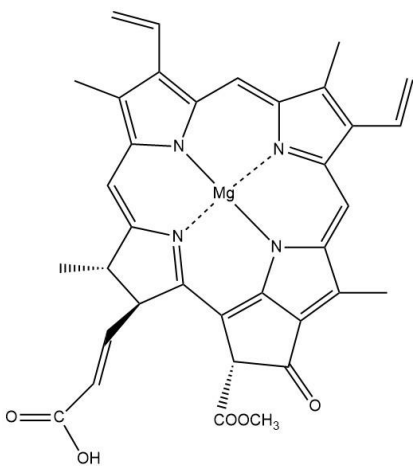
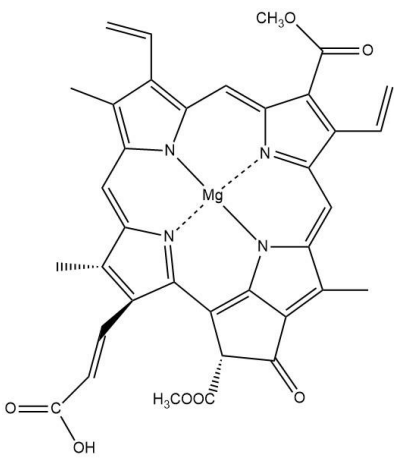
Appendix

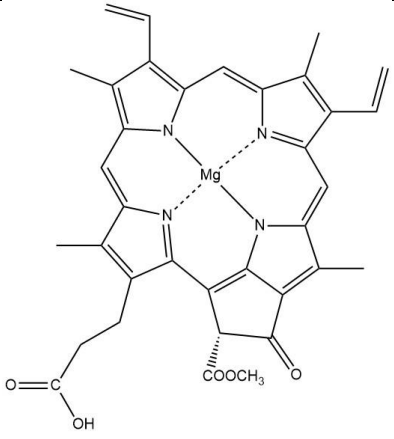
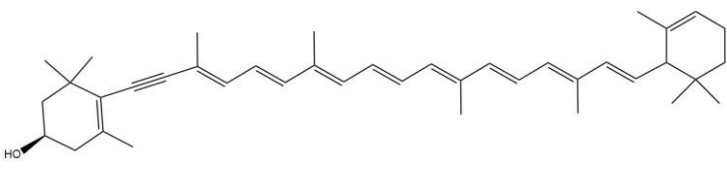
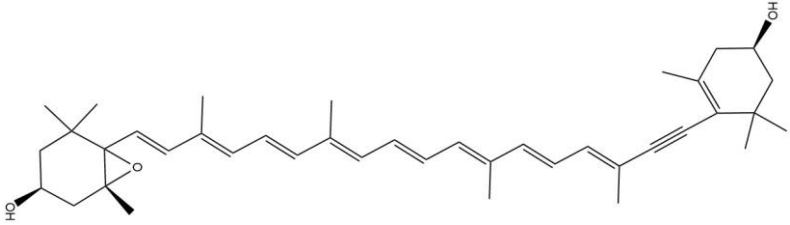
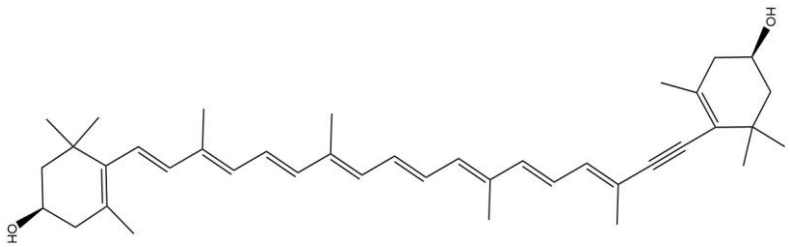
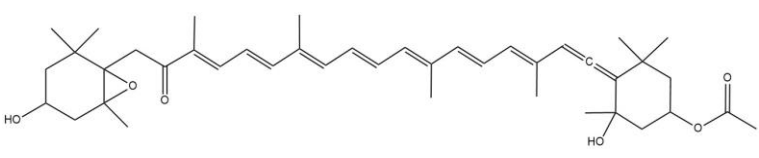
Appendix 1: Summary of DHI pigment standards

Table 13 - Summary of pigments from DHI-mix sample. Name, molecular formula, monoisotopic mass and molecular structure of each pigment is displayed.

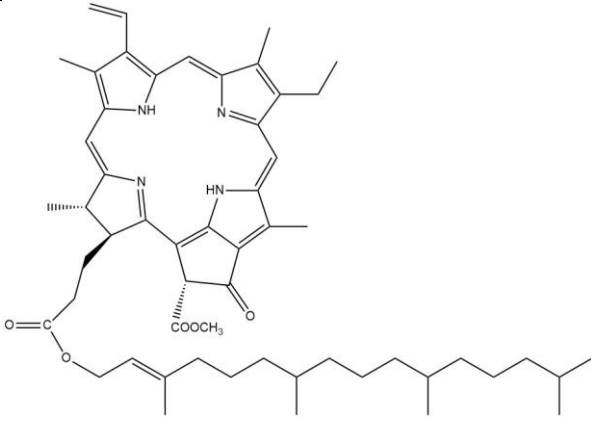
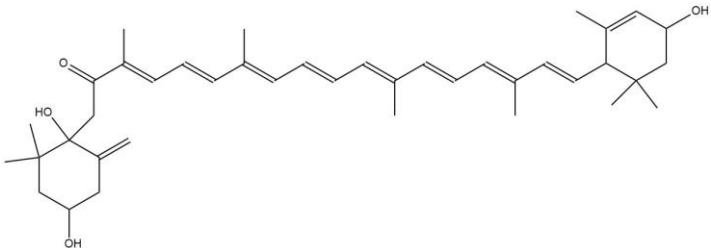
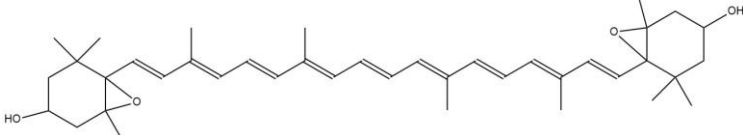
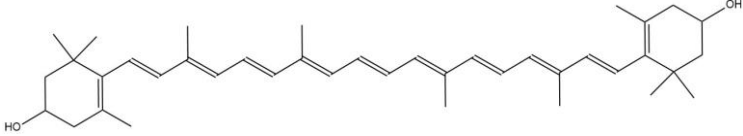
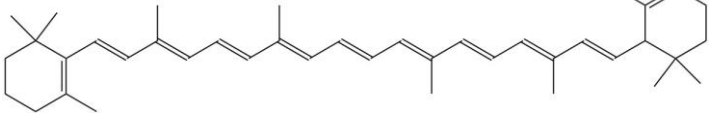
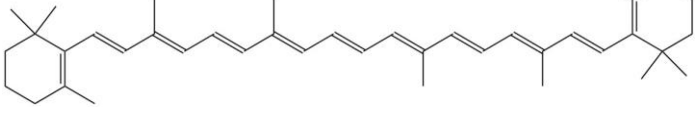
Pigment	Molecular formula	Monoisotopic mass (Da)	Molecular structure
Alloxanthin	C ₄₀ H ₅₂ O ₂	596.387	
Astaxanthin	C ₄₀ H ₅₂ O ₄	564.396	
Chlorophyll <i>a</i>	C ₅₅ H ₇₂ MgN ₄ O ₅	892.545	

<p>DV chlorophyll <i>a</i></p>	<p>$C_{55}H_{70}MgN_4O_5$</p>	<p>890.519</p>	 <p>The structure shows a central magnesium atom coordinated to four nitrogen atoms in a porphyrin-like ring. The ring is substituted with a vinyl group, a methyl group, and a phytyl ester chain. A methyl ester group (H₃COOC) is attached to the ring. The phytyl chain is a long, branched hydrocarbon chain with methyl groups at the 2, 6, 10, and 14 positions.</p>
<p>Chlorophyllide <i>a</i></p>	<p>$C_{35}H_{34}MgN_4O_5$</p>	<p>614.238</p>	 <p>The structure is similar to DV chlorophyll a, but the phytyl ester chain is replaced by a propionic acid group (-CH₂CH₂COOH). The central magnesium atom is coordinated to four nitrogen atoms in a porphyrin-like ring, which is substituted with a vinyl group, a methyl group, and a methyl ester group (H₃COOC).</p>
<p>Chlorophyll <i>b</i></p>	<p>$C_{55}H_{70}MgN_4O_6$</p>	<p>906.515</p>	 <p>The structure is similar to DV chlorophyll a, but the central magnesium atom is coordinated to five nitrogen atoms. The ring is substituted with a vinyl group, a methyl group, and a phytyl ester chain. A methyl ester group (H₃COOC) and an aldehyde group (-CHO) are also attached to the ring. The phytyl chain is a long, branched hydrocarbon chain with methyl groups at the 2, 6, 10, and 14 positions.</p>

<p>DV chlorophyll <i>b</i></p>	<p>$C_{55}H_{68}MgN_4O_6$</p>	<p>904.499</p>	 <p>The structure shows a central magnesium atom coordinated to four nitrogen atoms in a porphyrin-like ring. The ring is substituted with methyl groups and vinyl groups. A long phytol side chain is attached to the propionate group at the C3 position via an ester linkage. A methyl ester group is also present at the C2 position.</p>
<p>Chlorophyll <i>c</i>₂</p>	<p>$C_{35}H_{28}MgN_4O_5$</p>	<p>608.191</p>	 <p>The structure shows a central magnesium atom coordinated to four nitrogen atoms in a porphyrin-like ring. The ring is substituted with methyl groups and vinyl groups. A propionic acid side chain is attached to the propionate group at the C3 position. A methyl ester group is also present at the C2 position.</p>
<p>Chlorophyll <i>c</i>₃</p>	<p>$C_{36}H_{28}MgN_4O_7$</p>	<p>652.181</p>	 <p>The structure shows a central magnesium atom coordinated to four nitrogen atoms in a porphyrin-like ring. The ring is substituted with methyl groups and vinyl groups. A propionic acid side chain is attached to the propionate group at the C3 position. A methyl ester group is also present at the C2 position. An additional methoxy ester group is attached to the ring at the C5 position.</p>

DV protochloro- phyllide <i>a</i> (Mg- DVP)	$C_{35}H_{30}MgN_4O_5$	610.953	
Crocoxanthin	$C_{40}H_{54}O$	550.417	
Diadinoxanthin	$C_{40}H_{54}O_3$	582.407	
Diatoxanthin	$C_{40}H_{54}O_2$	566.412	
Fucoxanthin	$C_{42}H_{58}O_6$	658.423	

19'-but-fucoxanthin	$C_{46}H_{64}O_8$	744.997	
19'-hex-fucoxanthin	$C_{48}H_{68}O_8$	772.491	
Lutein	$C_{40}H_{56}O_2$	568.428	
Neoxanthin	$C_{40}H_{56}O_4$	600.418	
Peridinin*	$C_{39}H_{50}O_7$	630.356	

Pheophytin <i>a</i>	$C_{55}H_{74}N_4O_5$	870.566	
Prasinoxanthin	$C_{40}H_{56}O_4$	600.418	
Violaxanthin	$C_{40}H_{56}O_4$	600.418	
Zeaxanthin	$C_{40}H_{56}O_2$	568.428	
α -carotene	$C_{40}H_{56}$	536.438	
β -carotene	$C_{40}H_{56}$	536.438	

*Peridinin also have an isomer in the DHI-mix standard sample

Appendix 2: Wavelengths of light conditions

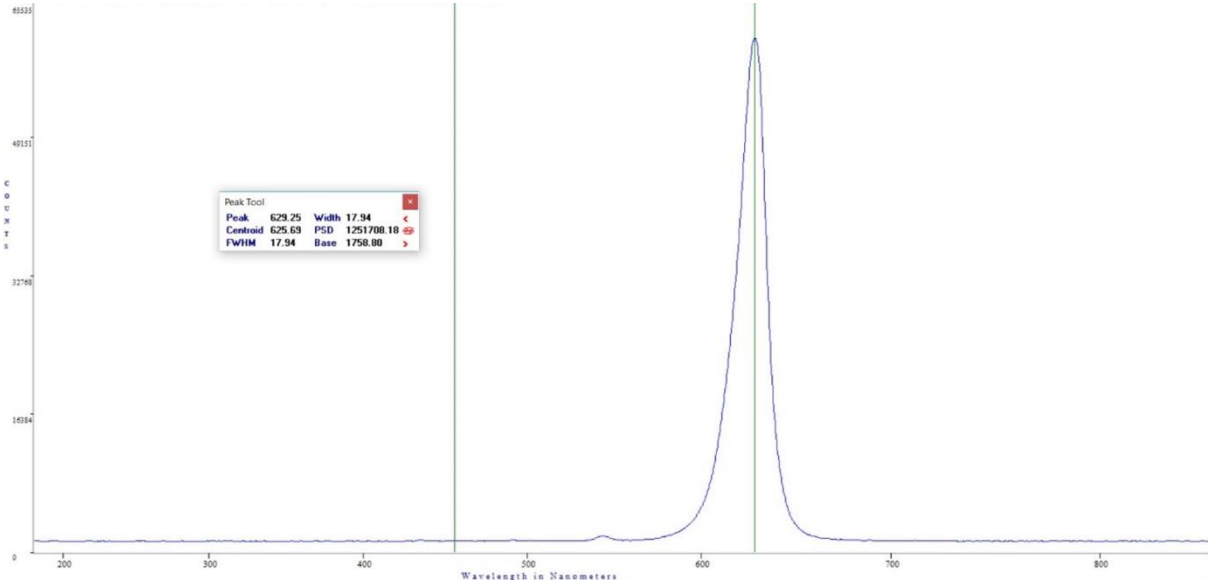


Figure 49 - Wavelength of red light regime (580~650 nm).

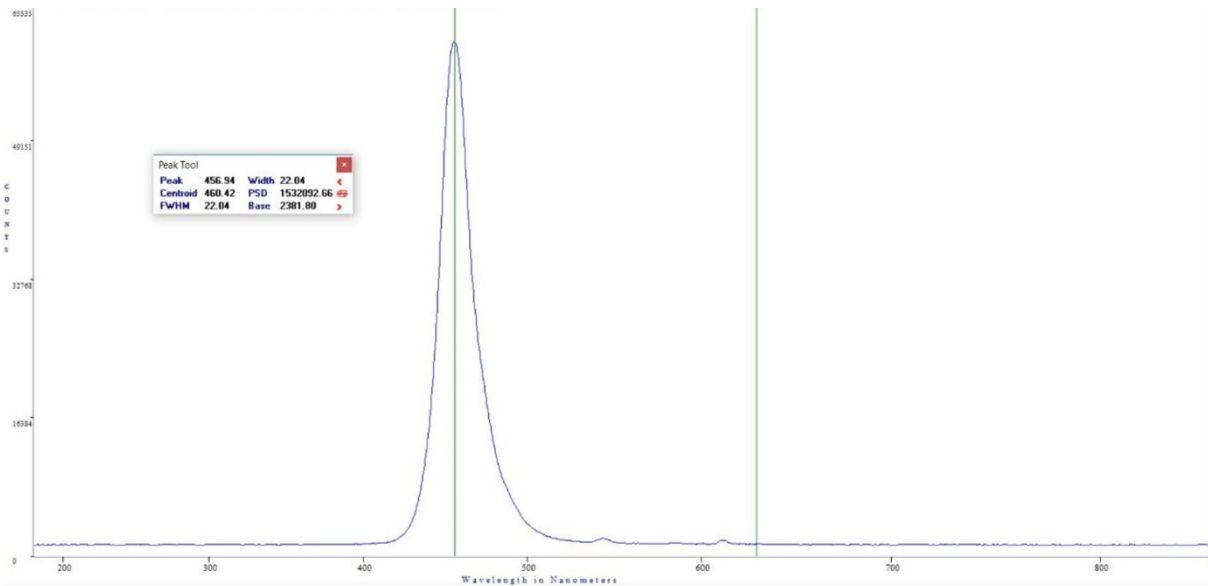


Figure 50 - Wavelength of blue light regime (420~500 nm).

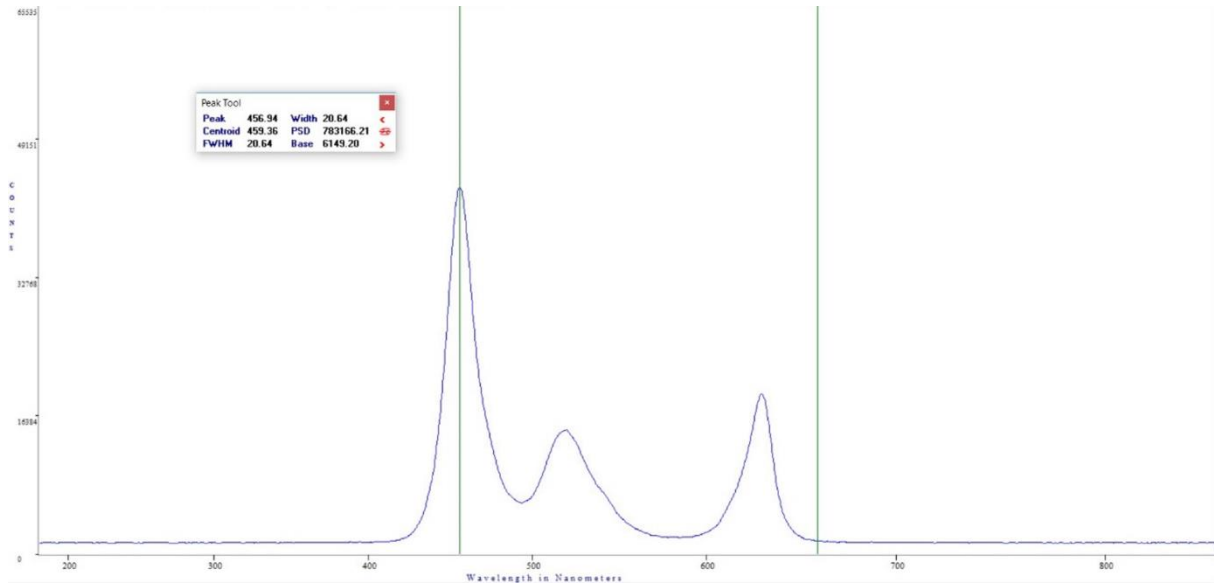


Figure 51 - Wavelength of white light regime (400~650 nm).

Appendix 3: Extraction test *P. glacialis*

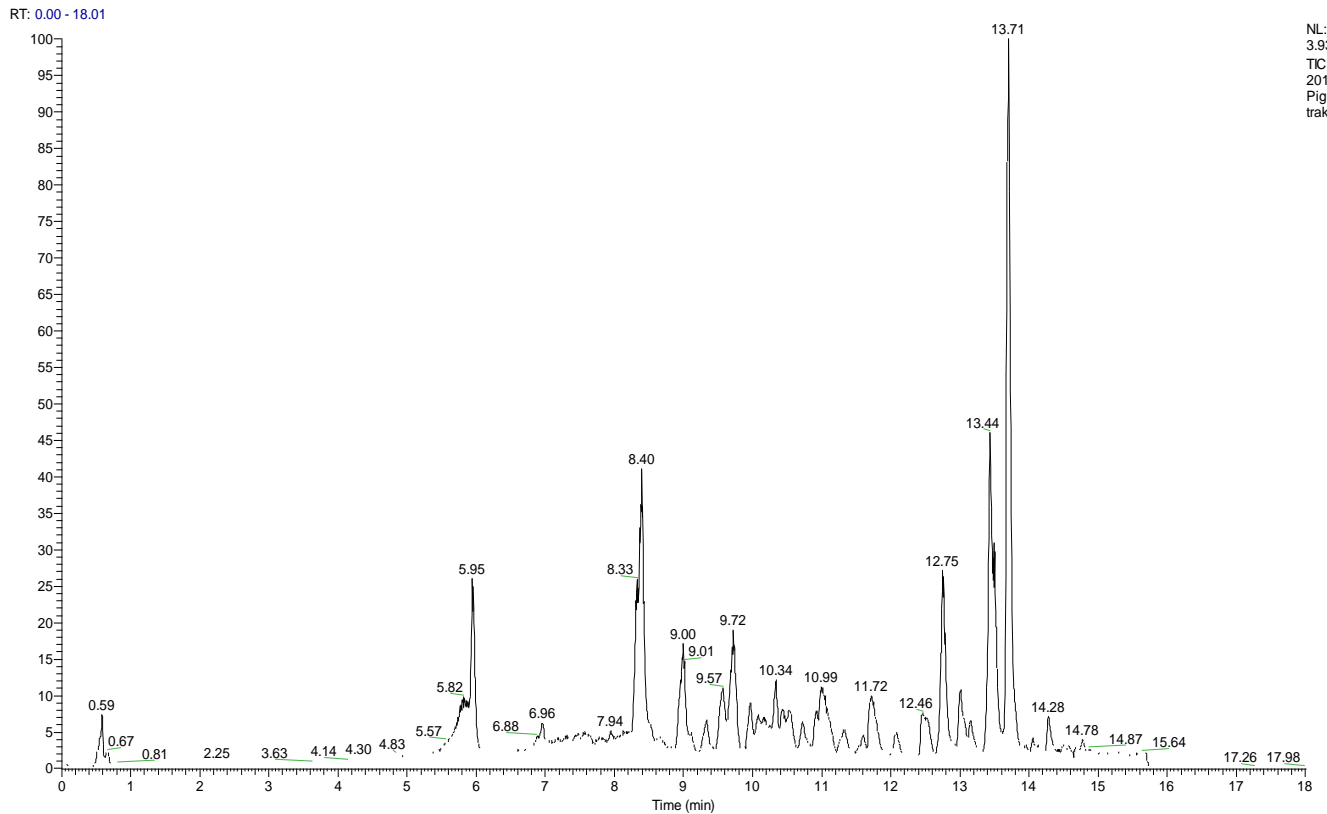


Figure 52 – Total ion current chromatogram of the first extraction of *P. glacialis*.

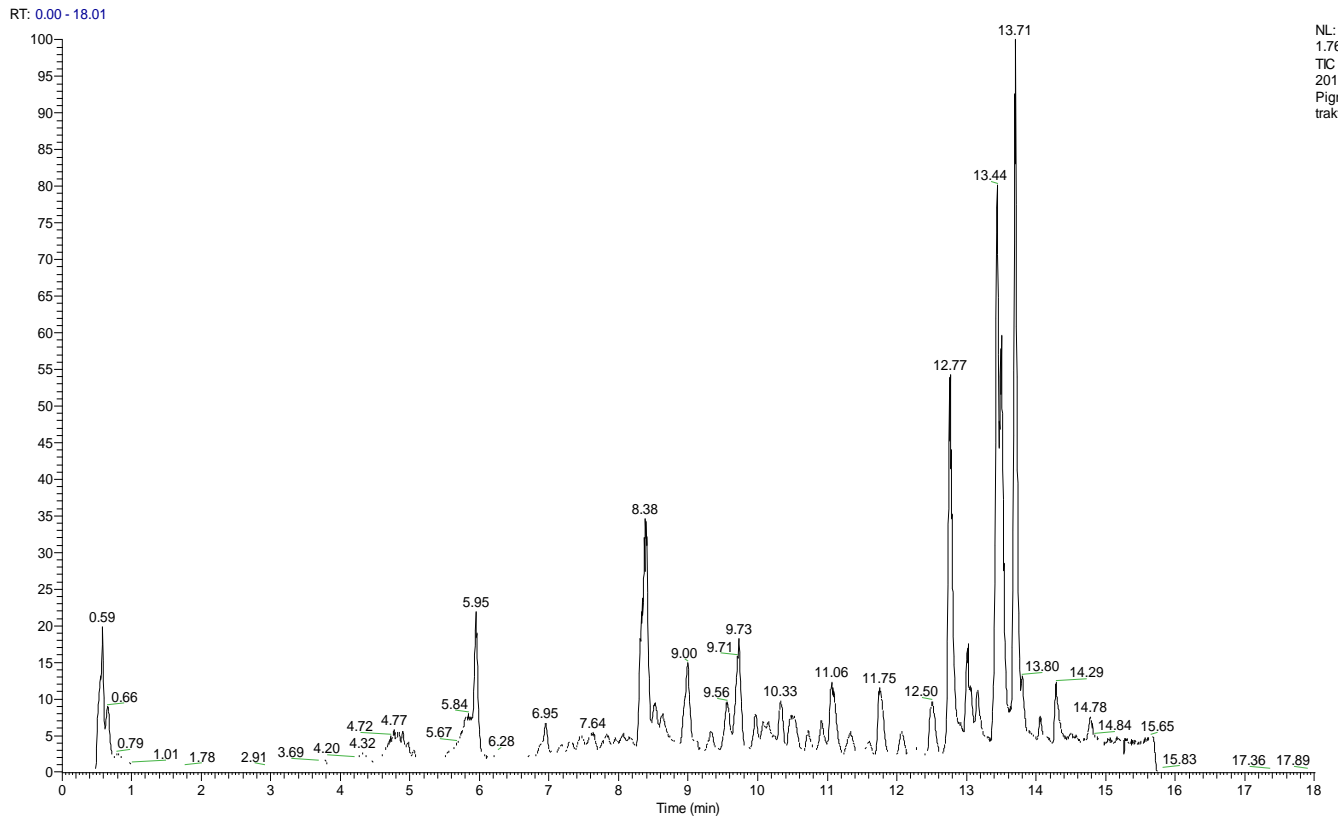


Figure 53 – Total ion current chromatogram of the second extraction of *P. glacialis*.

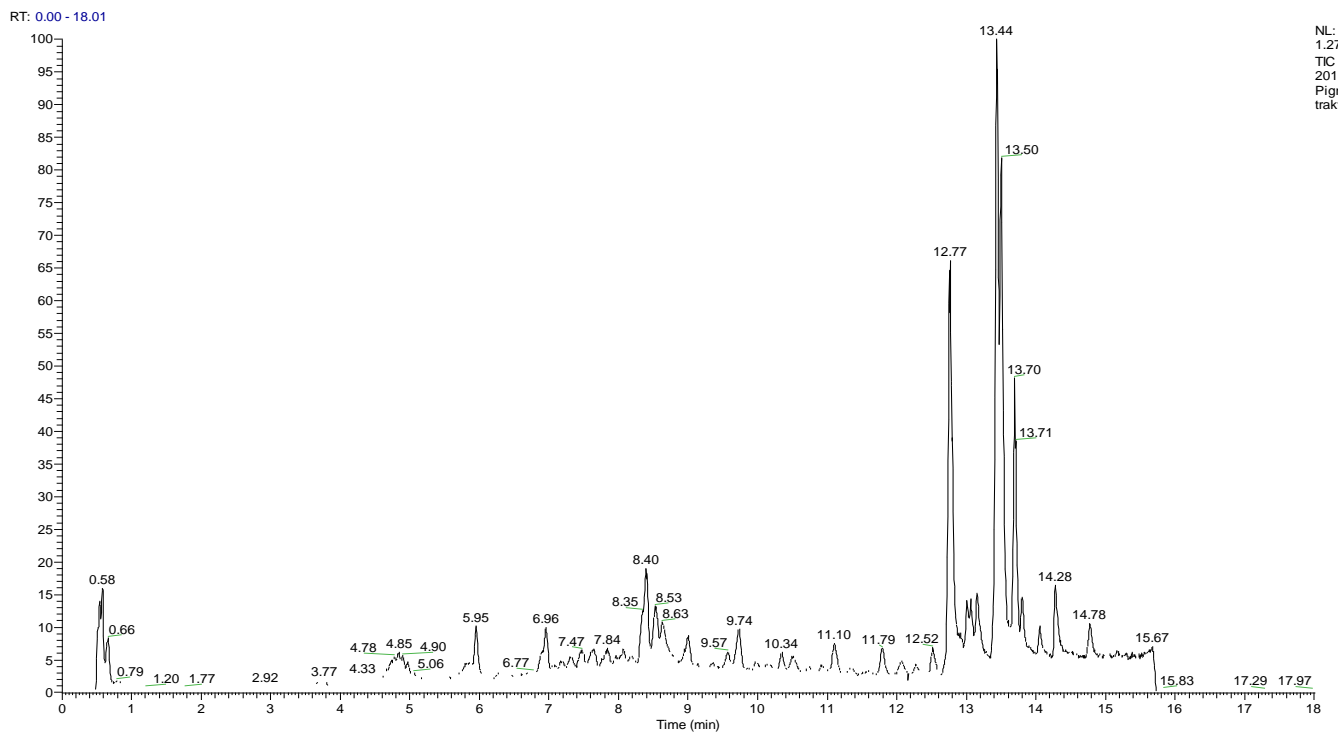


Figure 54 – Total ion current chromatogram of the third extraction of *P. glacialis*.

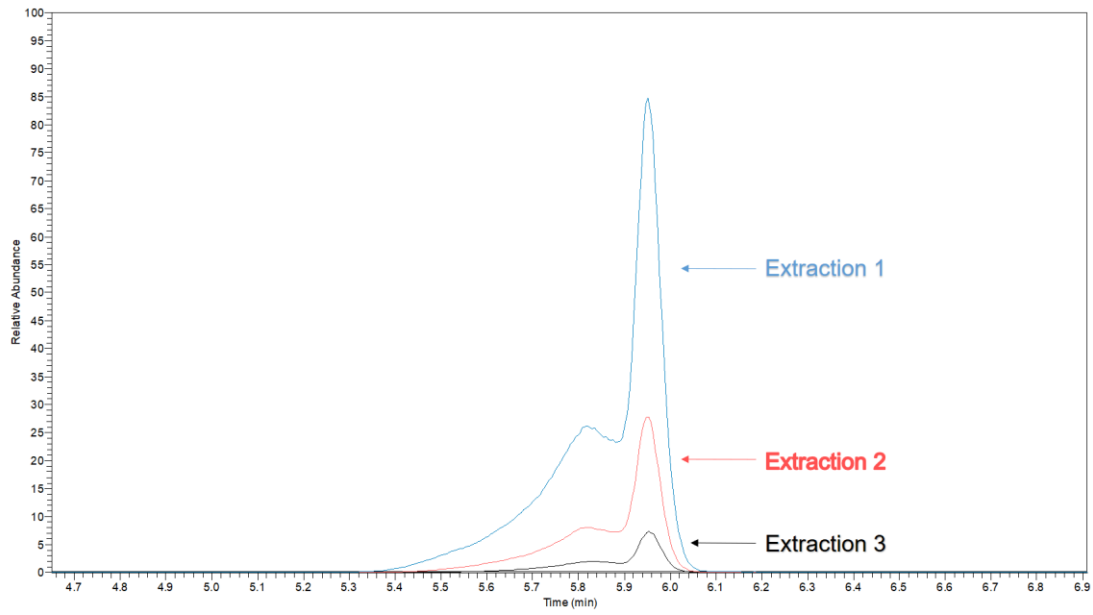


Figure 55 - Extracted ion chromatogram of fucoxanthin in extraction 1-3 from *P. glacialis*.

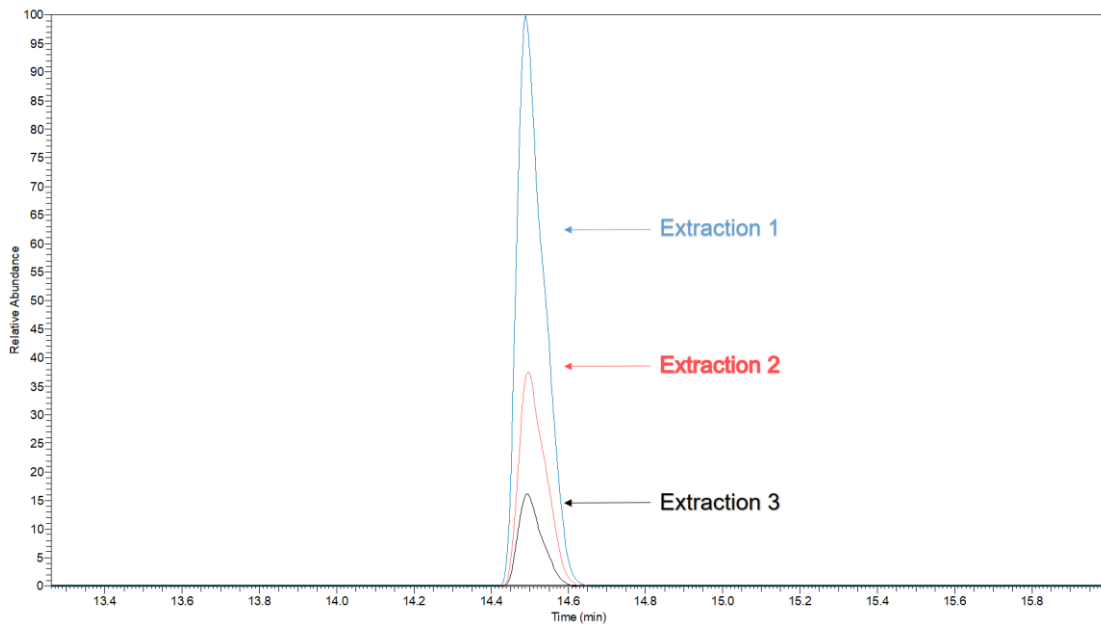


Figure 56 - Extracted ion chromatogram of carotene in extraction 1-3 from *P. glacialis*.

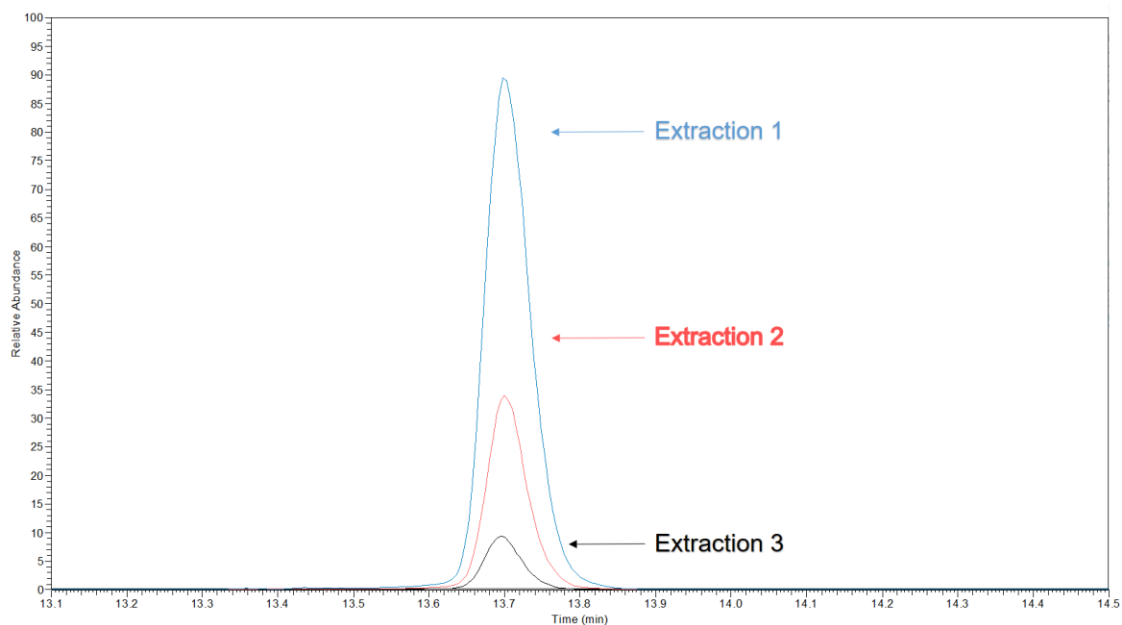


Figure 57 - Extracted ion chromatogram of pheophytin a in extraction 1-3 from *P. glacialis*.

Appendix 4: Preparation of standard solutions

Table 14 – Preparation of standard solution for chlorophyll a in DHI-mix.

Dilution number	Concentration (µg/mL)	Volume from dilution (µL)	Volume acetone:MeOH (µL)
1	33.1000		100
2	16.5500	50 from number 1	50
3	3.3100	20 from number 2	80
4	1.6550	50 from number 3	50
5	0.3310	20 from number 4	80
6	0.0331	10 from number 5	90

Table 15 – Preparation of standard solution for astaxanthin.

Dilution number	Concentration (µg/mL)	Volume from dilution (µL)	Volume acetone:MeOH (µL)
1	10.00	10 from stock 2	4500
2	5.00	500 from number 1	500
3	1.00	200 from number 1	1800
4	0.50	50 from number 1	950
5	0.10	10 from number 1	990
6	0.05	50 from number 3	950
7	0.01	10 from number 3	990

Appendix 5: Calibration curves

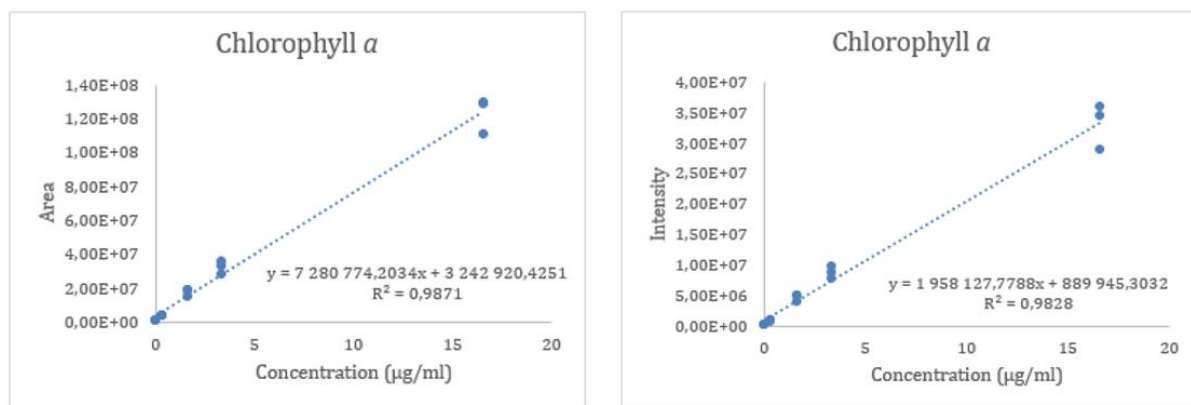


Figure 58 - Calibration curve for chlorophyll a based on peak area (left) and peak intensity (right).

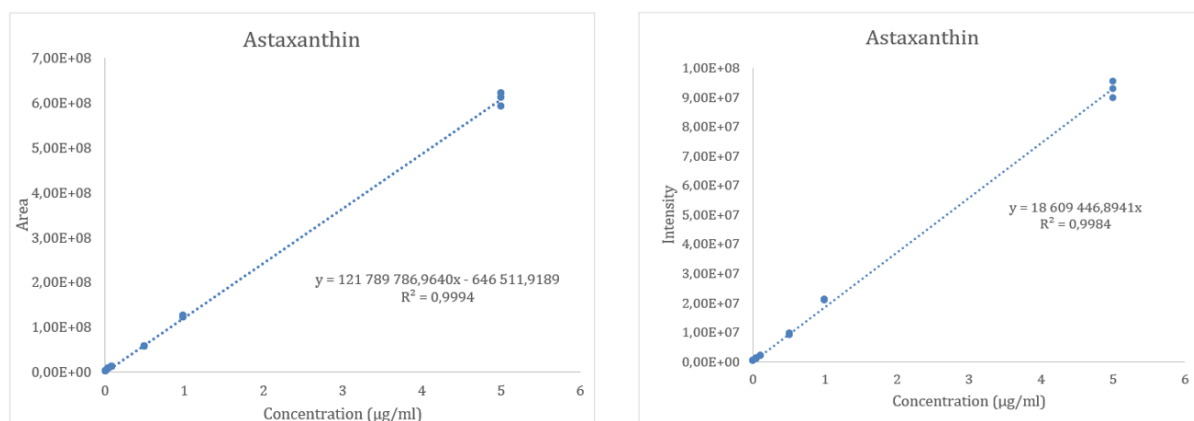


Figure 59 - Calibration curve for astaxanthin based on peak area (left) and peak intensity (right).

Appendix 6: t-SIM inclusion list

Table 16 - Inclusion list for t-SIM method. The MS parameters for the method is displayed in Table 9.

Pigment	Chemical formula	Mass (<i>m/z</i>)	Retention window (min)
Chlorophyll <i>c</i> ₂	C35H28MgN4O5	609.1998	4.26-4.86
Chlorophyllide <i>a</i>	C35H34MgN4O5	615.2458	12.44-13.04
Peridinin	C39H50O7	631.3638	3.80-4.40
Fucoxanthin	C42H58O6	659.4308	4.98-5.58
Neoxanthin, prasinoxanthin and violaxanthin	C40H56O4	600.4180	5.45-6.05
Astaxanthin	C40H52O4	597.3948	5.91-6.51
Diadinoxanthin	C40H54O3	583.4148	5.45-6.05
Alloxanthin	C40H52O2	565.4048	6.90-7.50
Diatoxanthin	C40H54O2	566.4120	7.21-7.81
Zeaxanthin and lutein	C40H56O2	569.4358	13.01-13.61
DV chlorophyll <i>b</i>	C55H68MgN4O6	905.5067	11.24-11.84
Chlorophyll <i>b</i>	C55H70MgN4O6	907.5228	11.24-11.84
Crococanthin	C40H54O	551.4248	7.70-8.30
DV chlorophyll <i>a</i>	C55H70MgN4O5	891.5196	12.37-12.97
Chlorophyll <i>a</i>	C55H72MgN4O5	893.5428	12.44-13.04
Pheophytin <i>a</i>	C55H74N4O5	871.5738	13.24-13.84
Carotene	C40H56	537.4458	14.00-14.60

Appendix 7: Extraction efficiency

Table 17 - Extraction efficiency of chlorophyll a from extraction one to extraction two and from extraction one to extraction three. Diluted sample is diluted 1:20. Values are means, SD and RSD (%) of triplicate samples injected three times on UPLC-MS.

Chl a	Area			EE (%) 1 to 2			EE (%) 1 to 3		
	Average	SD	RSD (%)	Average	SD	RSD (%)	Average	SD	RSD (%)
Red light	380600281.44	44782483	11.77	42.11	2.27	5.38	6.35	1.66	26.21
Red light diluted	69812826.78	15078212	21.60	16.21	1.56	9.60	1.79	0.47	26.03
Blue light	405315810.44	34764462	8.58	41.65	3.51	8.43	8.57	2.09	24.36
Blue light diluted	78420733.11	8192154	10.45	14.84	2.58	17.36	2.32	0.72	31.28
White light	413257682.67	46217557	11.18	48.73	3.03	6.22	9.79	0.92	9.44
White light diluted	88348355.22	11126644	12.59	18.00	1.17	6.48	2.54	0.33	12.93

Table 18 - Extraction efficiency of fucoxanthin from extraction one to extraction two and from extraction one to extraction three. Diluted sample is diluted 1:20. Values are means, SD and RSD (%) of triplicate samples injected three times on UPLC-MS.

Fucoxanthin	Area			EE (%) 1 to 2			EE (%) 1 to 3		
	Average	SD	RSD (%)	Average	SD	RSD (%)	Average	SD	RSD (%)
Red light	1061976736	286643057	26.99	15.36	0.71	4.63	1.48	0.13	8.66
Red light diluted	80501674	28690392	35.64	13.19	0.27	2.03	1.12	0.08	7.02
Blue light	919976640	16396957	1.78	18.60	0.26	1.39	2.24	0.10	4.48
Blue light diluted	60263348	1314220	2.18	15.48	0.23	1.50	1.52	0.02	1.57
White light	902810704	49534692	5.49	18.50	0.35	1.89	2.92	0.14	4.93
White light diluted	56873218	1689089	2.97	15.34	0.13	0.82	2.04	0.05	2.52

Appendix 8: Chromatograms of standard samples

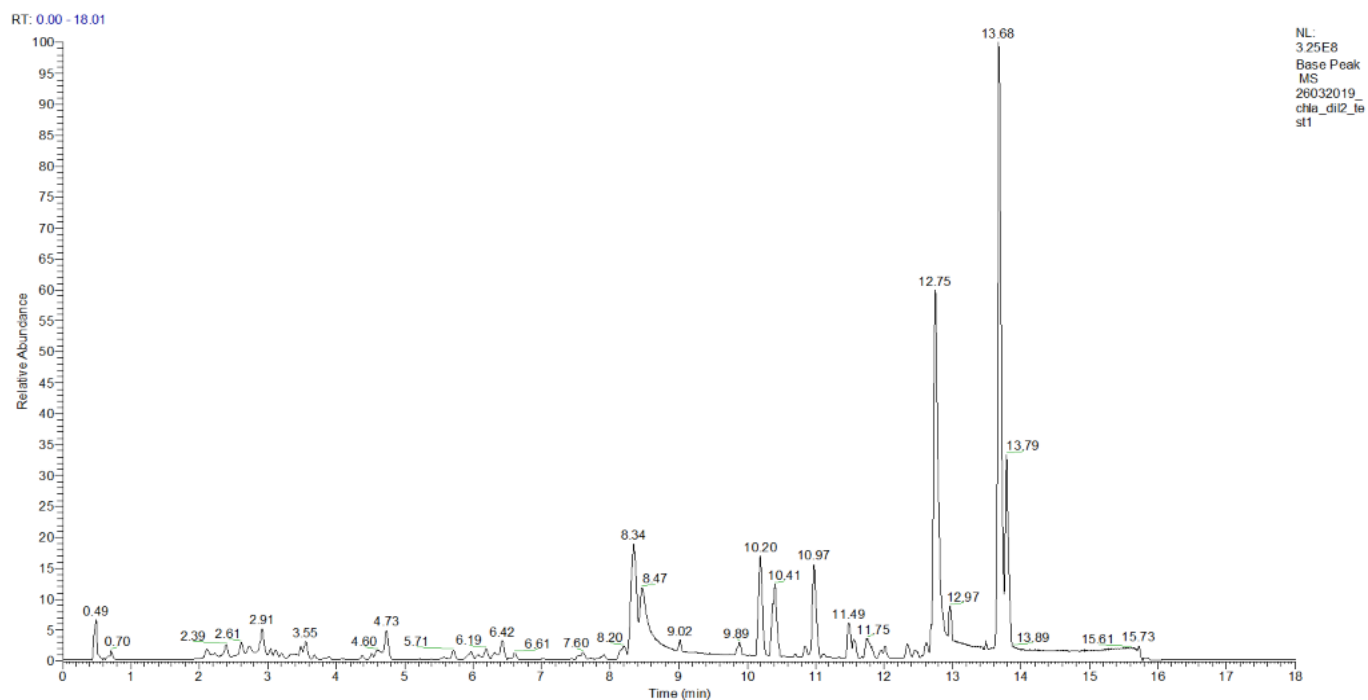


Figure 60 – Base peak chromatogram of standard sample (16.55 µg/mL chlorophyll a) from DHI with resolution of 70 000. Ion source: ESI

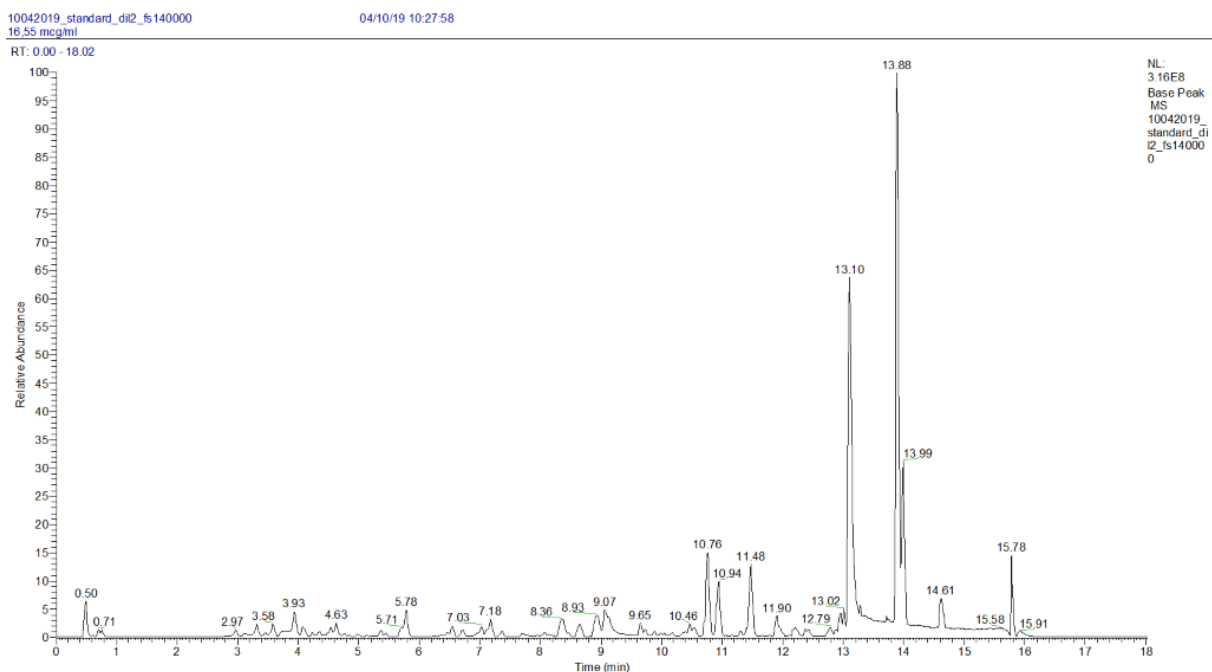


Figure 61 - Base peak chromatogram of standard sample (16.55 µg/mL chlorophyll a) from DHI with resolution of 140 000. Ion source: ESI.

Appendix 9: Chromatograms of pigment extract

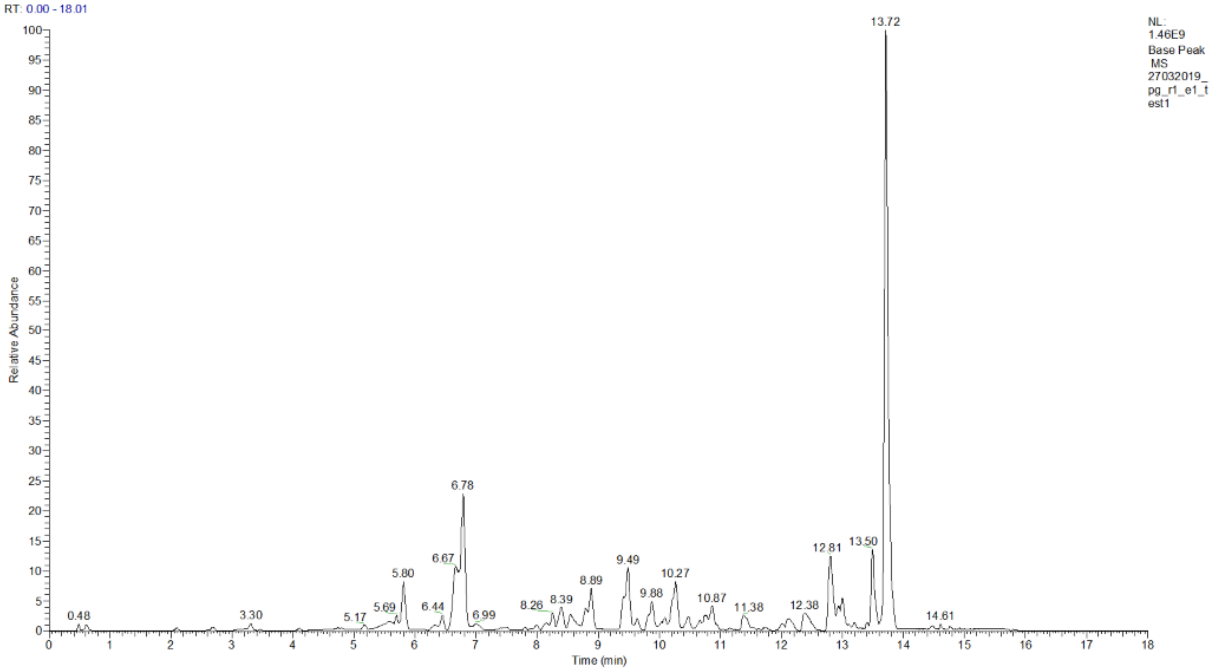


Figure 62 - Base peak chromatogram of *P. glacialis* illuminated with red light, extraction one. Resolution: 70 000 and ions source: ESI

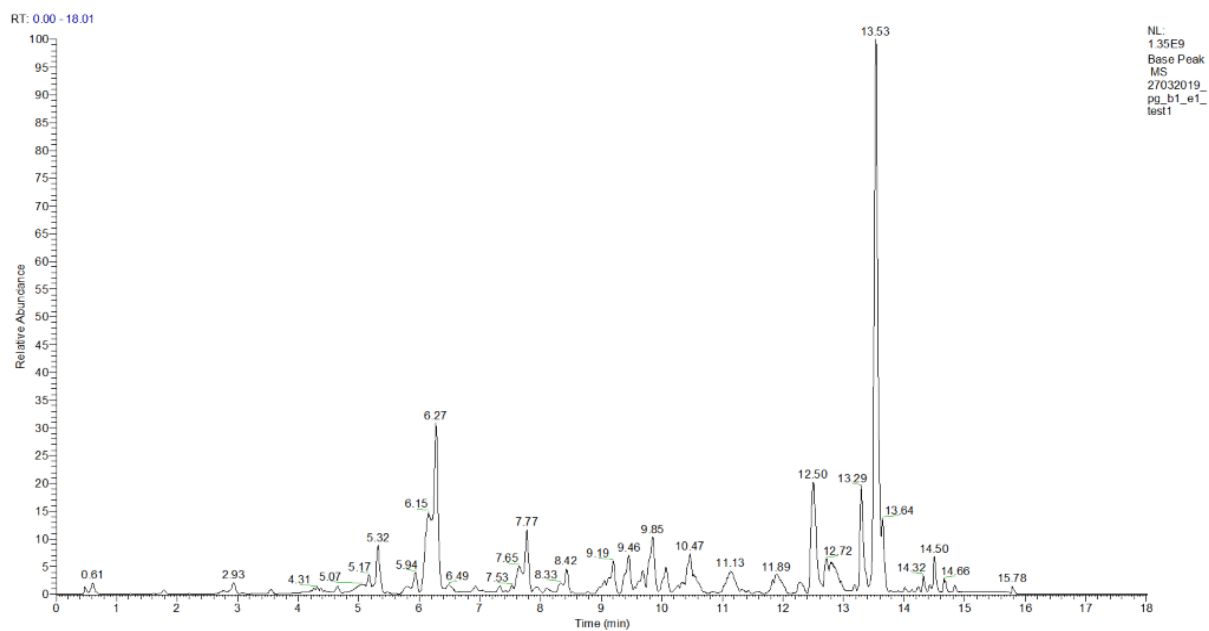


Figure 63 - Base peak chromatogram of *P. glacialis* illuminated with blue light, extraction one. Resolution: 70 000 and ions source: ESI

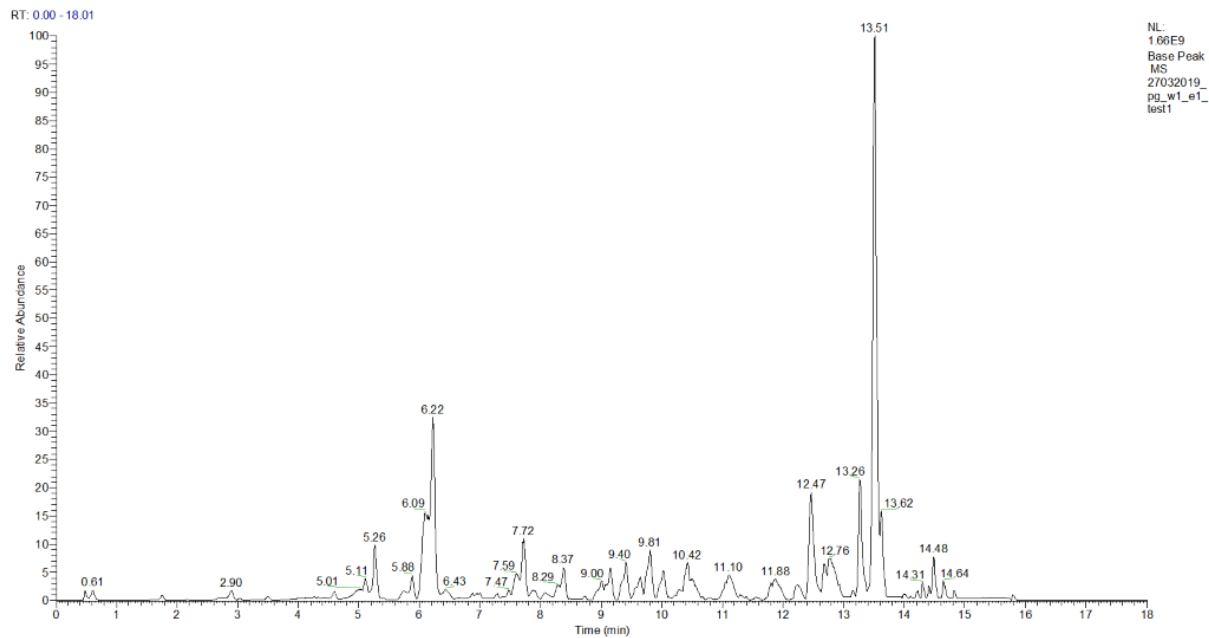


Figure 64 - Base peak chromatogram of *P. glacialis* illuminated with white light, extraction one. Resolution: 70 000 and ions source: ESI

Appendix 10: Chromatogram and mass spectra (t-SIM)

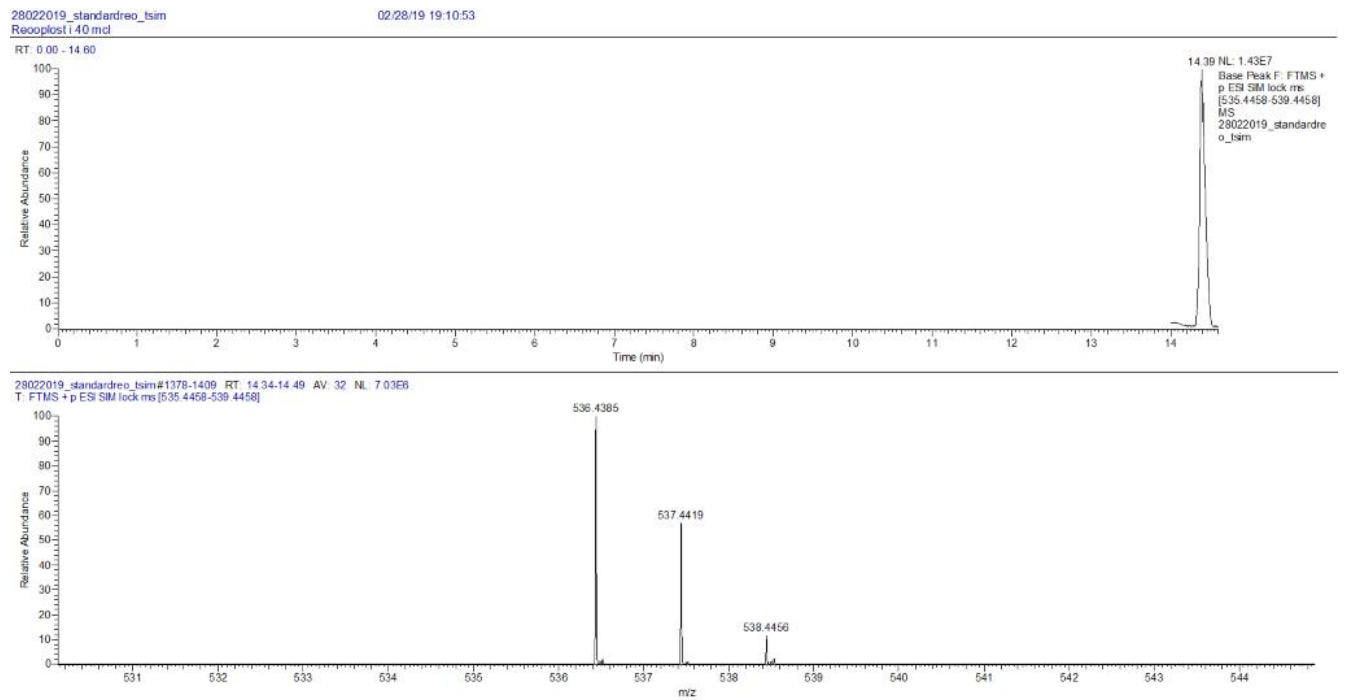


Figure 65 – Chromatogram and mass spectra of carotene in standard sample from DHI (33.1 µg/mL chlorophyll a)

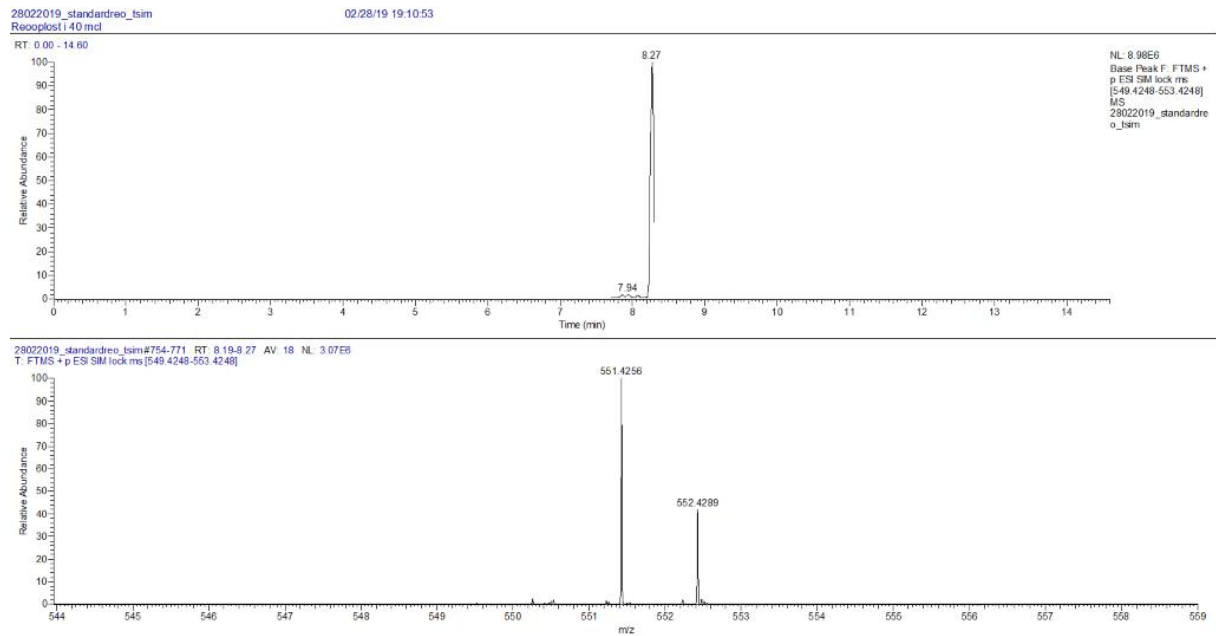


Figure 66 - Chromatogram and mass spectra of crocoxanthin in standard sample from DHI (33.1 µg/mL chlorophyll a)

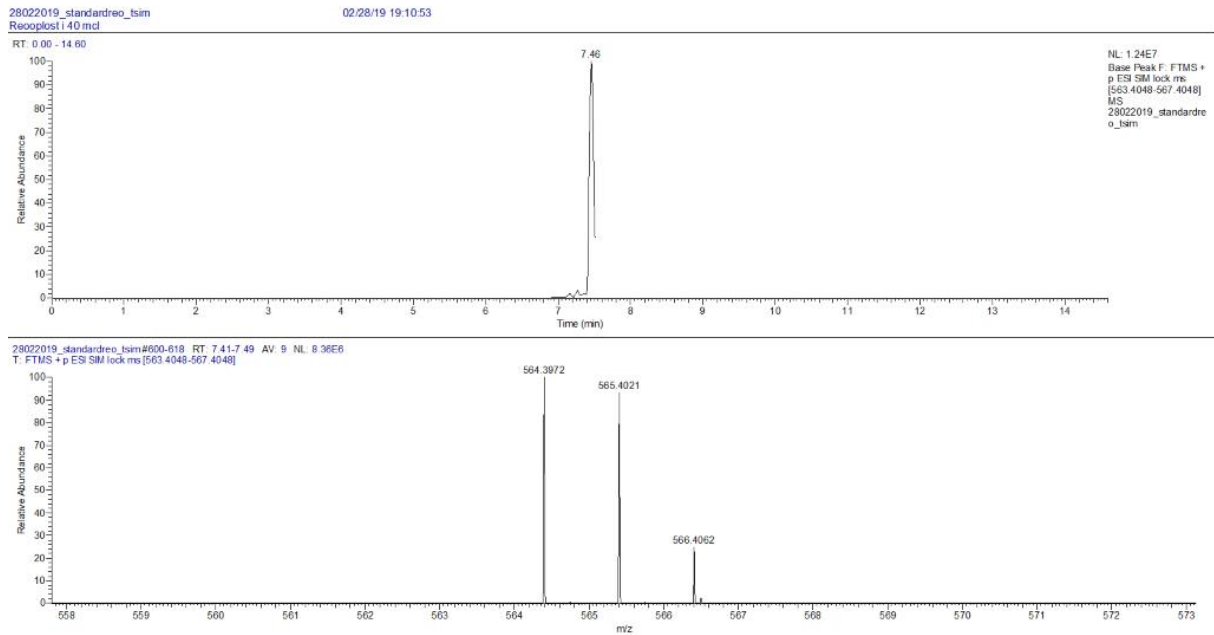


Figure 67 - Chromatogram and mass spectra of alloxanthin in standard sample from DHI (33.1 $\mu\text{g/mL}$ chlorophyll a)

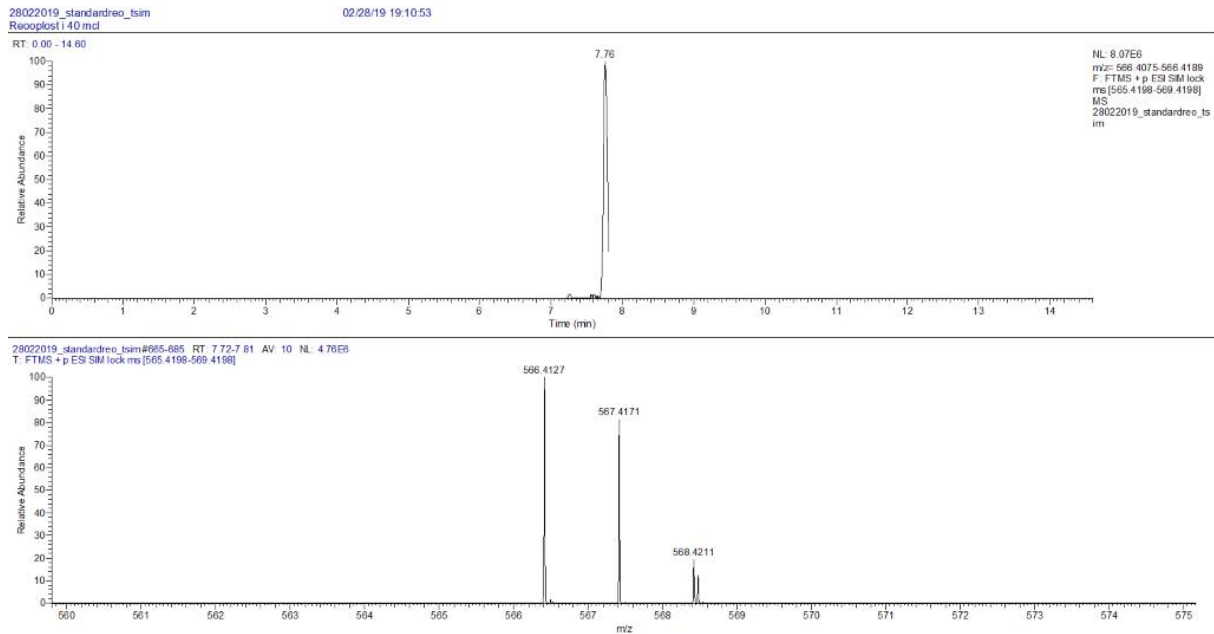


Figure 68 - Chromatogram and mass spectra of diatoxanthin in standard sample from DHI (33.1 $\mu\text{g/mL}$ chlorophyll a).

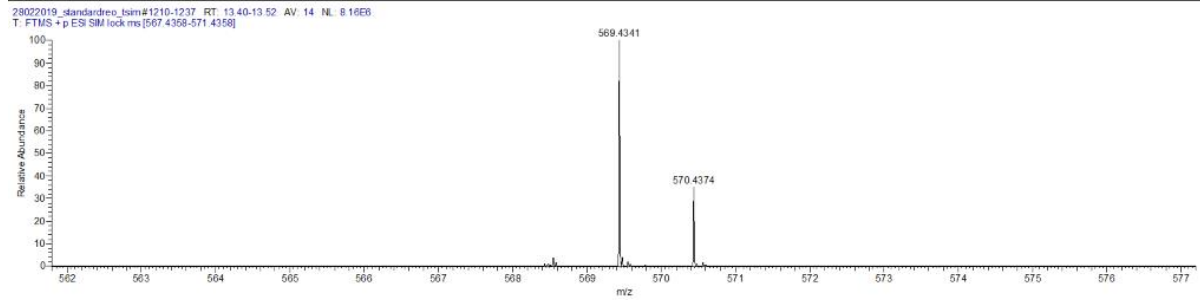
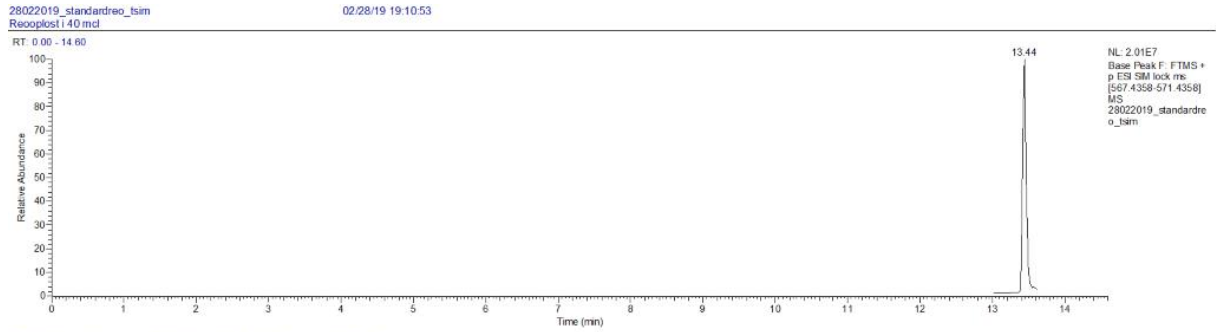


Figure 69 - Chromatogram and mass spectra of lutein in standard sample from DHI (33.1 $\mu\text{g/mL}$ chlorophyll a).

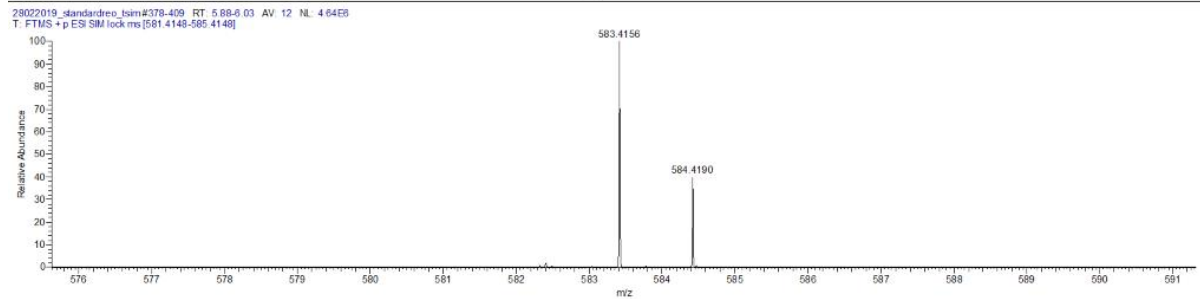
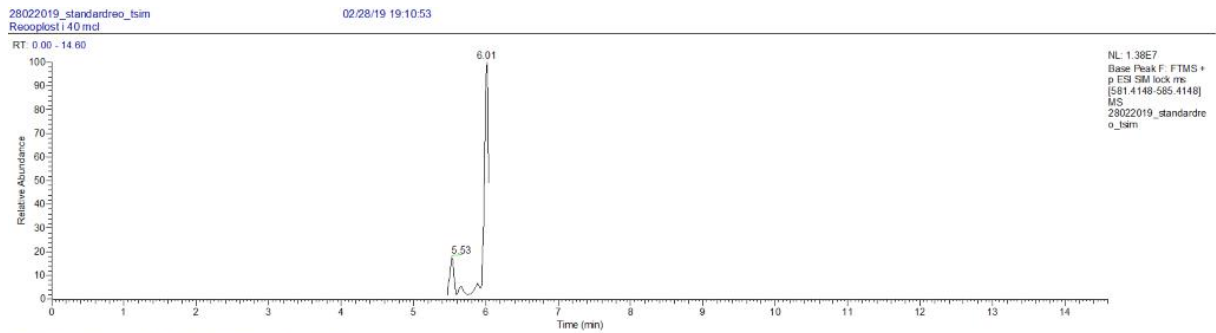


Figure 70 - Chromatogram and mass spectra of diadinoxanthin in standard sample from DHI (33.1 $\mu\text{g/mL}$ chlorophyll a).

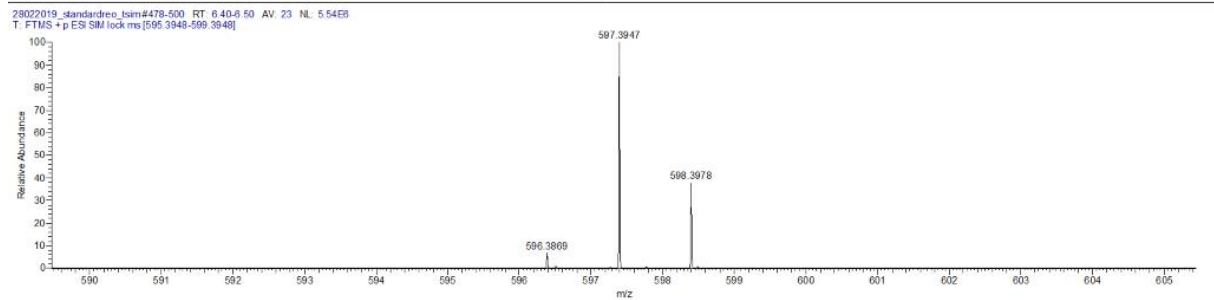
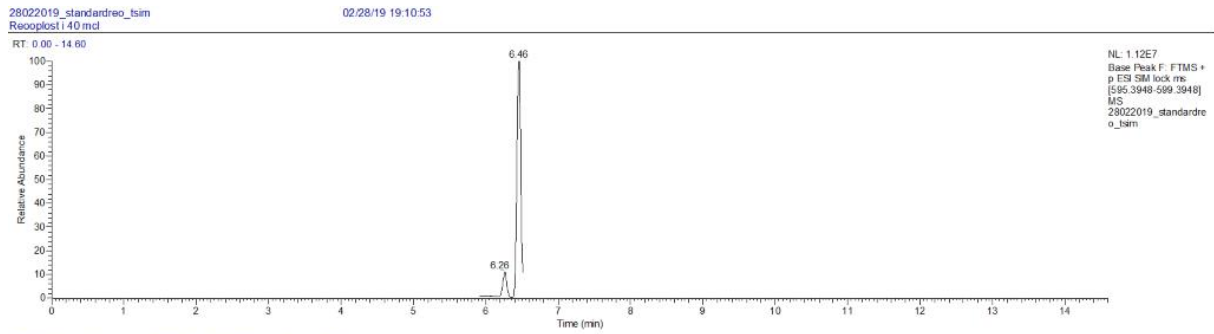


Figure 71 - Chromatogram and mass spectra of astaxanthin in standard sample from DHI (33.1 $\mu\text{g/mL}$ chlorophyll a).

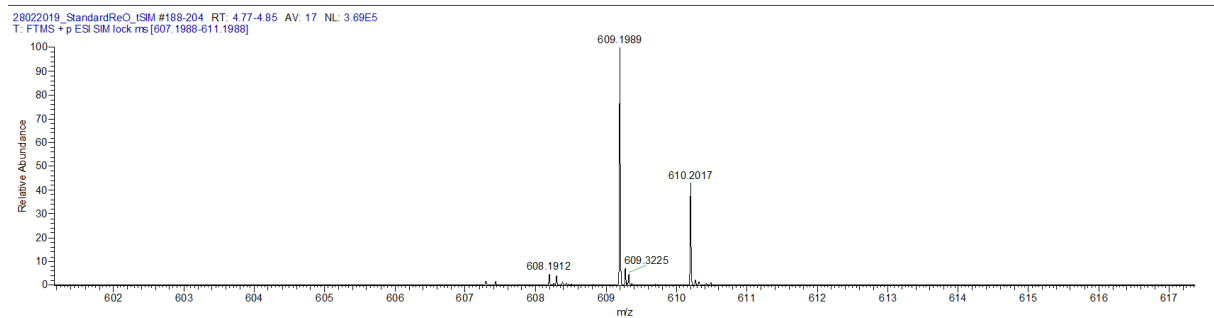
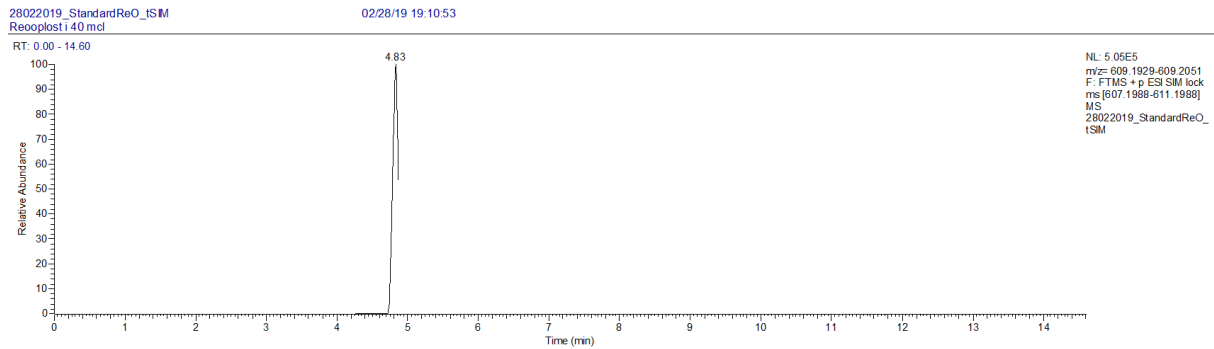


Figure 72 - Chromatogram and mass spectra of chlorophyll c_2 in standard sample from DHI (33.1 $\mu\text{g/mL}$ chlorophyll a).

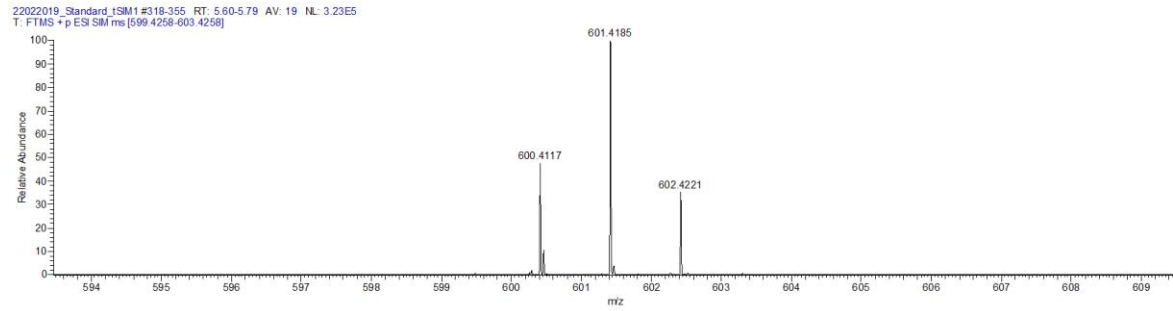
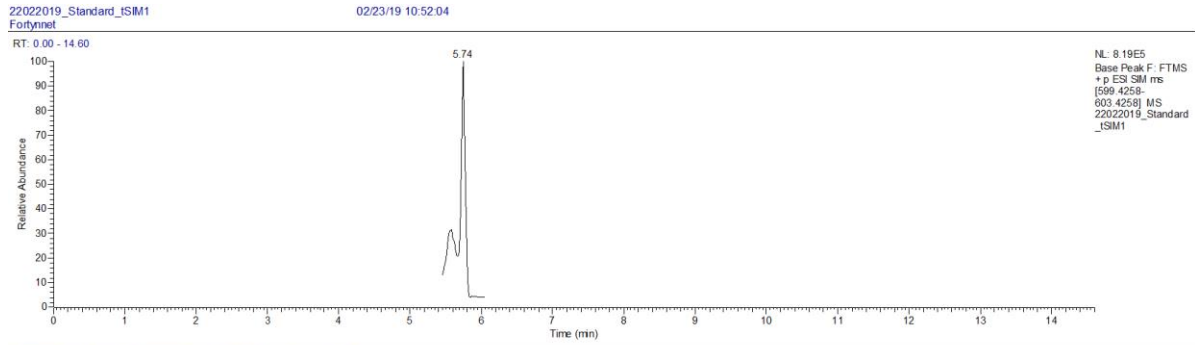


Figure 73 - Chromatogram and mass spectra of neoxanthin/Prasinoxanthin/violaxanthin in standard sample from DHI (33.1 $\mu\text{g}/\text{mL}$ chlorophyll a).

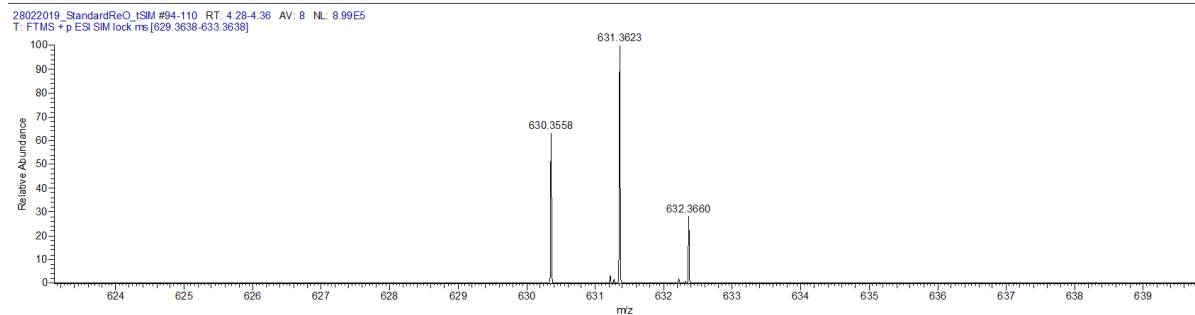
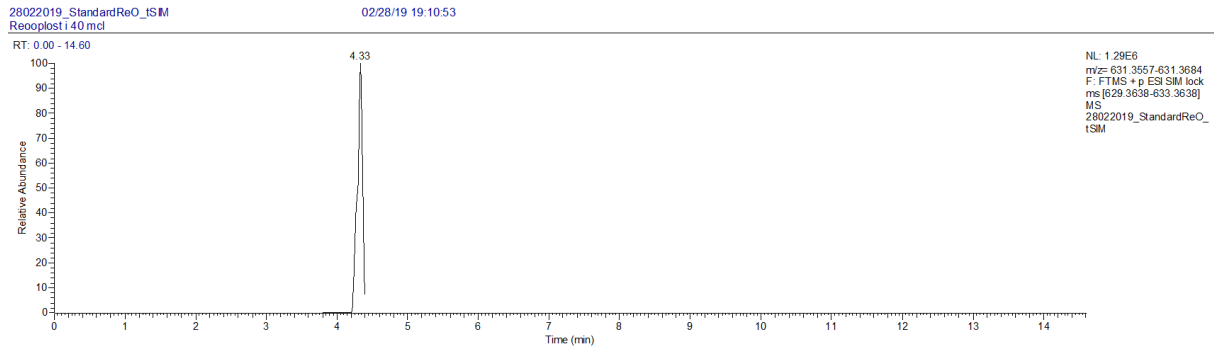


Figure 74 - Chromatogram and mass spectra of peridinin in standard sample from DHI (33.1 $\mu\text{g}/\text{mL}$ chlorophyll a).

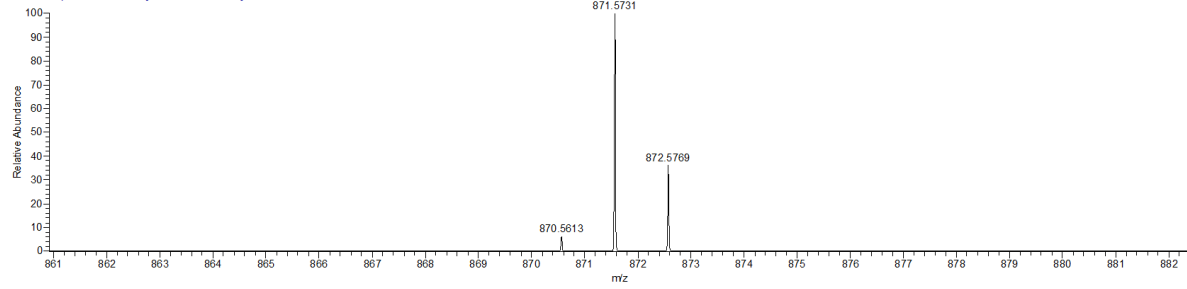
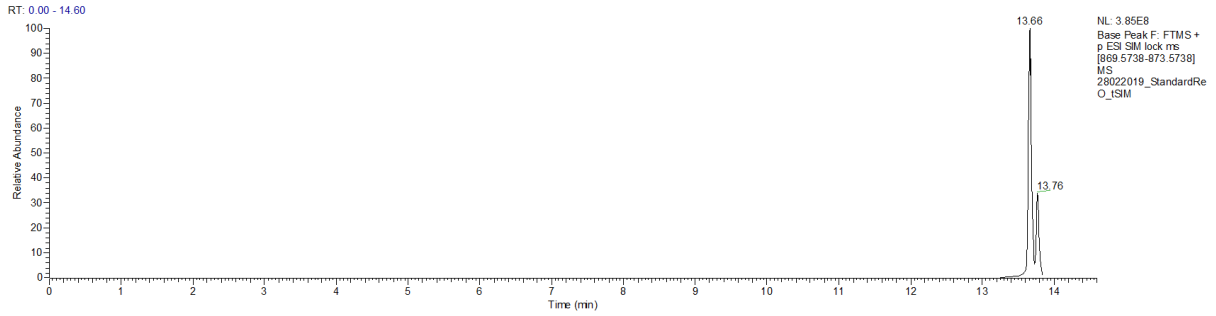


Figure 75 - Chromatogram and mass spectra of pheophytin a in standard sample from DHI (33.1 µg/mL chlorophyll a).

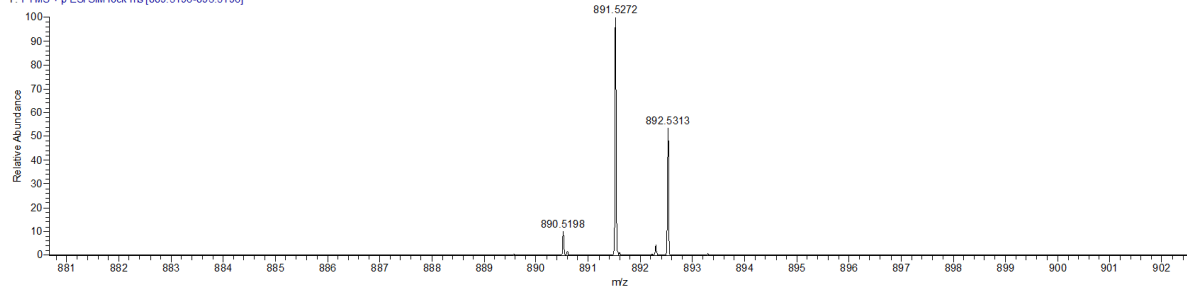
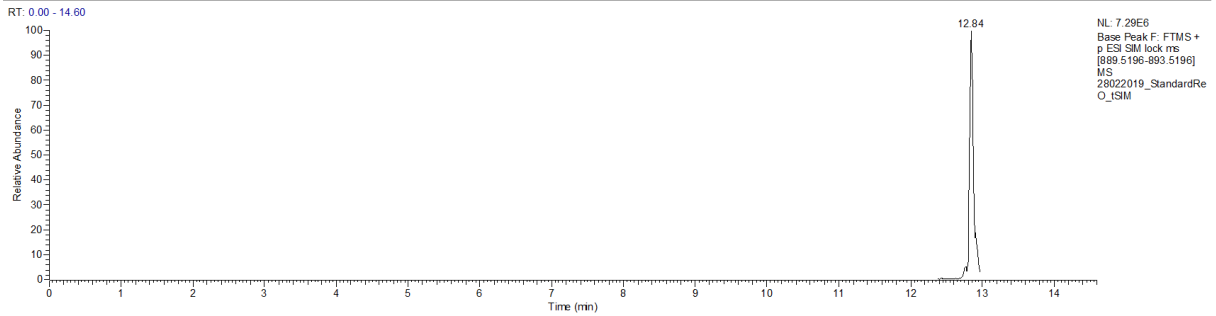


Figure 76 - Chromatogram and mass spectra of DV chlorophyll a in standard sample from DHI (33.1 µg/mL chlorophyll a).

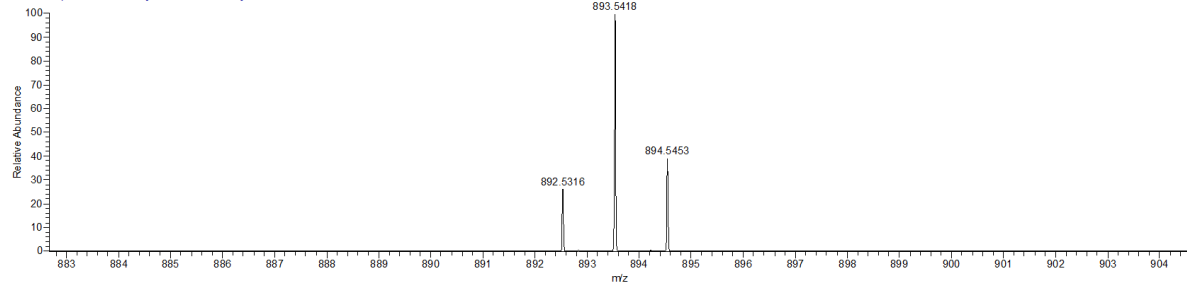
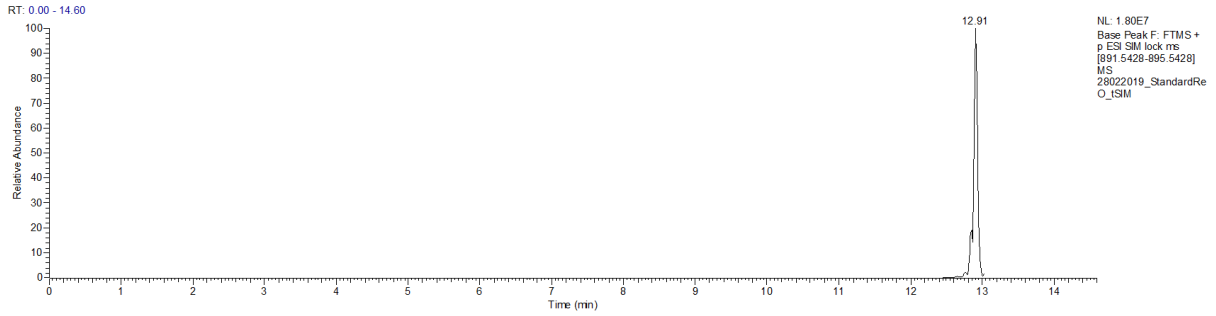


Figure 77 - Chromatogram and mass spectra of chlorophyll a in standard sample from DHI (33.1 µg/mL chlorophyll a).

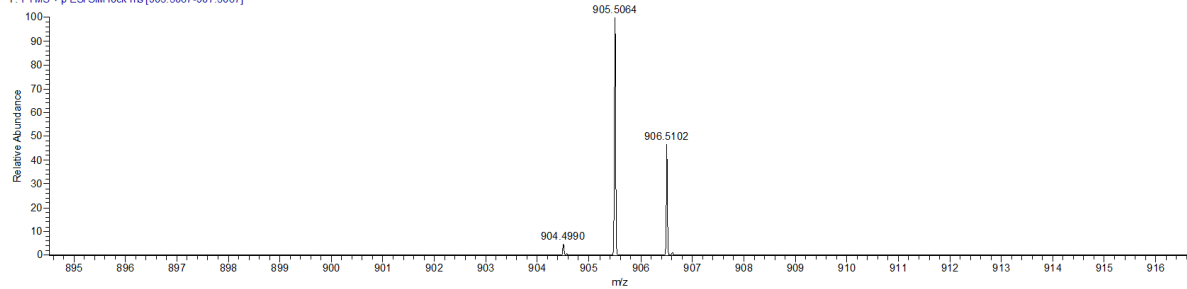
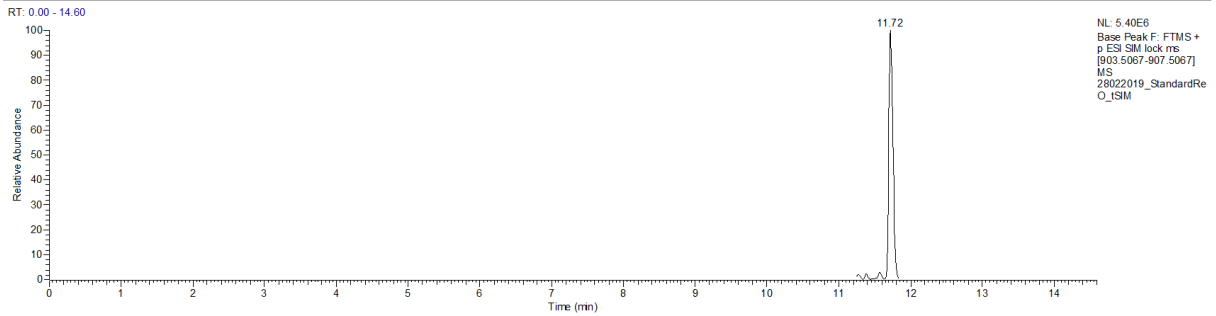


Figure 78 - Chromatogram and mass spectra of DV chlorophyll b in standard sample from DHI (33.1 µg/mL chlorophyll a).

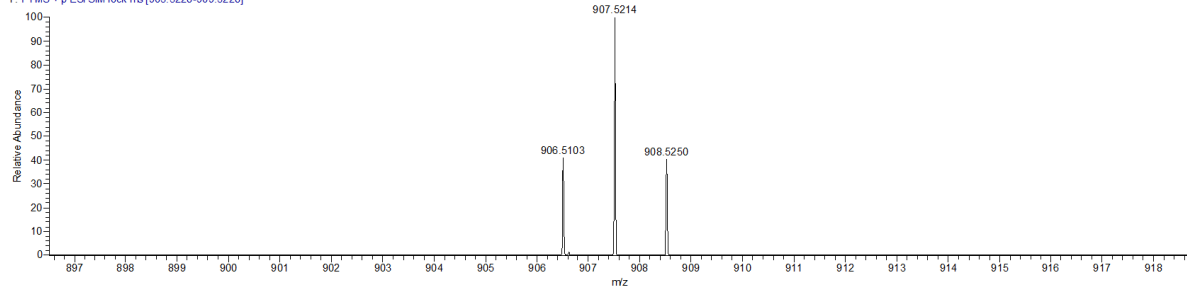
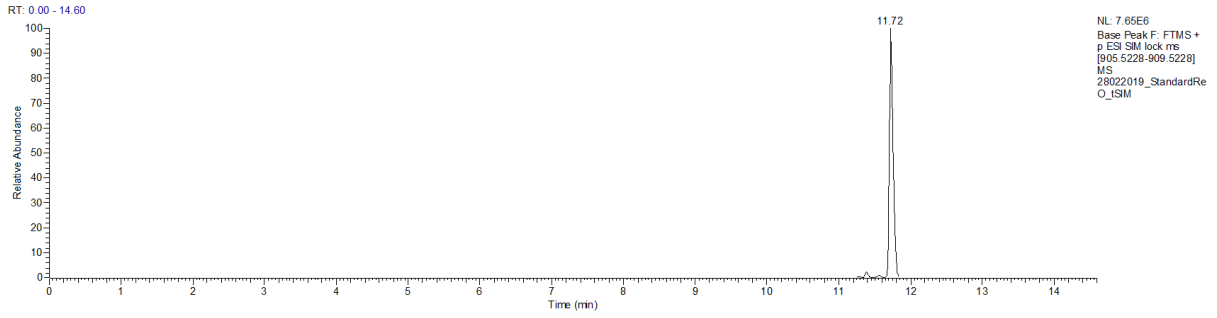


Figure 79 - Chromatogram and mass spectra of chlorophyll b in standard sample from DHI (33.1 $\mu\text{g/mL}$ chlorophyll a).

Appendix 11: MS/MS of chlorophyll a

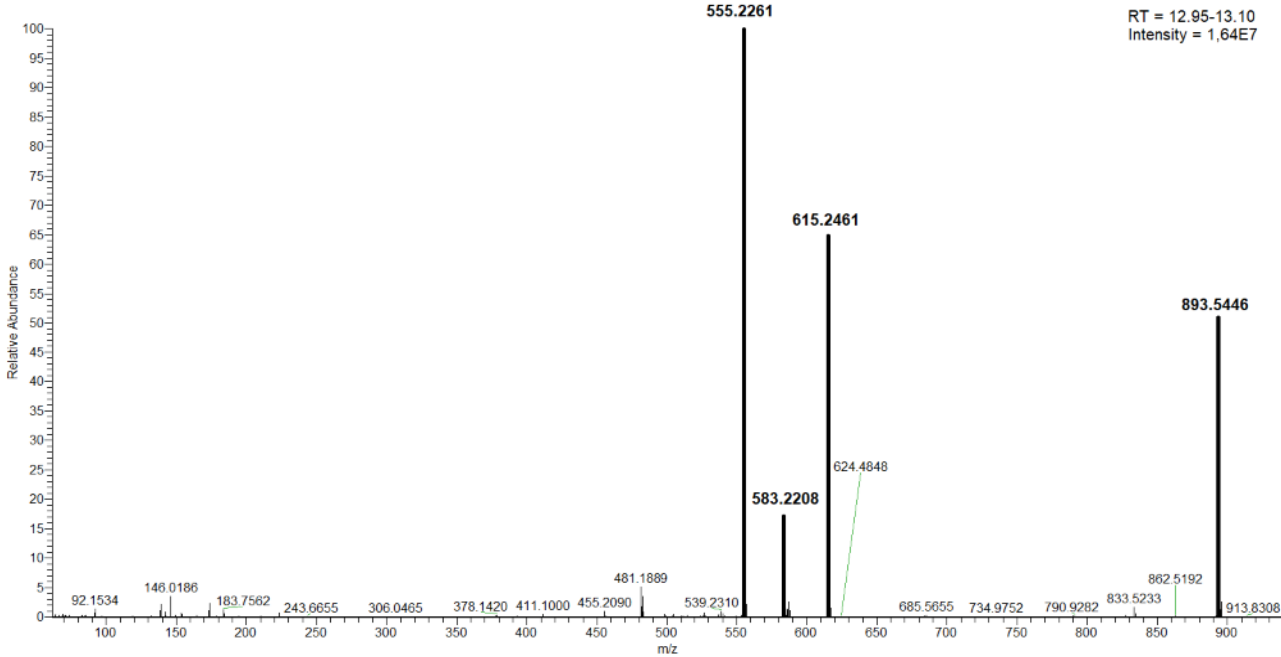


Figure 80 – MS/MS spectrum of chlorophyll a from samples of *P. glacialis* cultivated under red light (DDA).

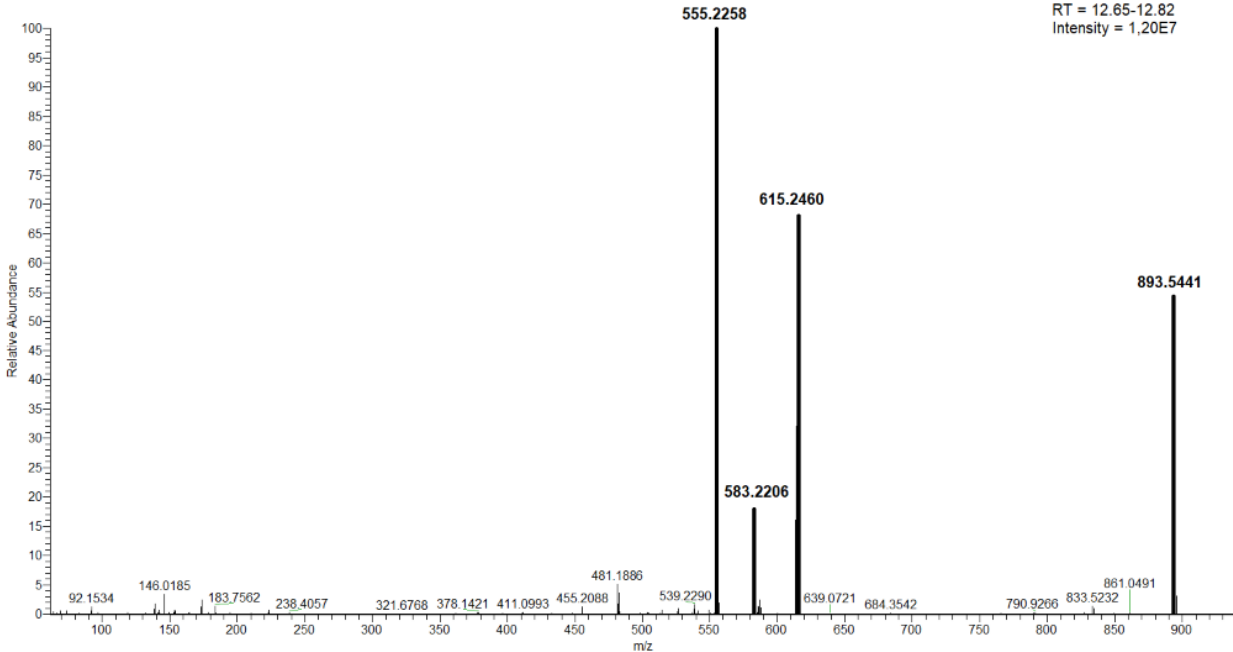


Figure 81 - MS/MS spectrum of chlorophyll a from samples of *P. glacialis* cultivated under blue light (DDA).

Appendix 12: MS/MS of astaxanthin like compound

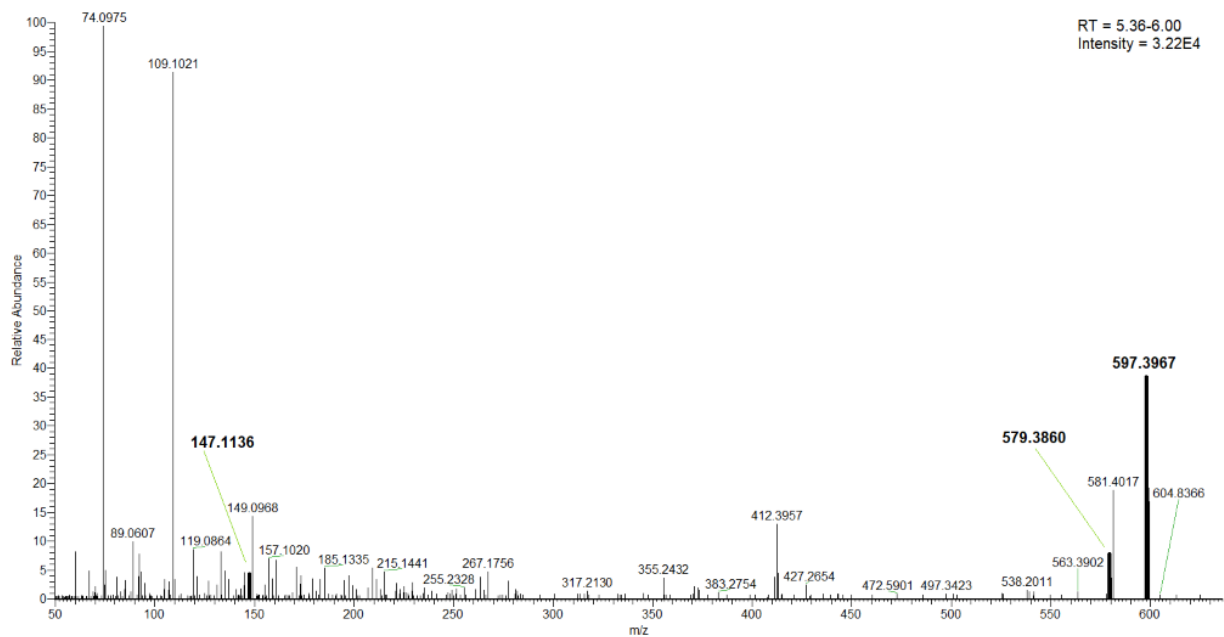


Figure 82 – MS/MS spectrum of something similar to astaxanthin from samples cultivated under red light (DDA).

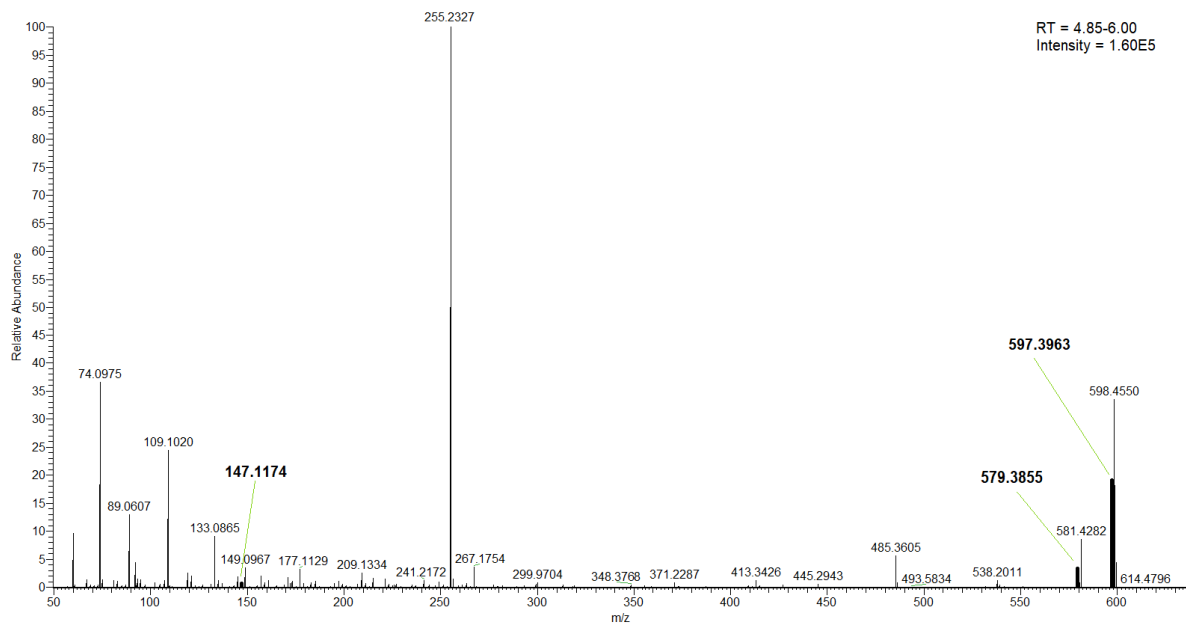


Figure 83 - MS/MS spectrum of something similar to astaxanthin cultivated under blue light (DDA).

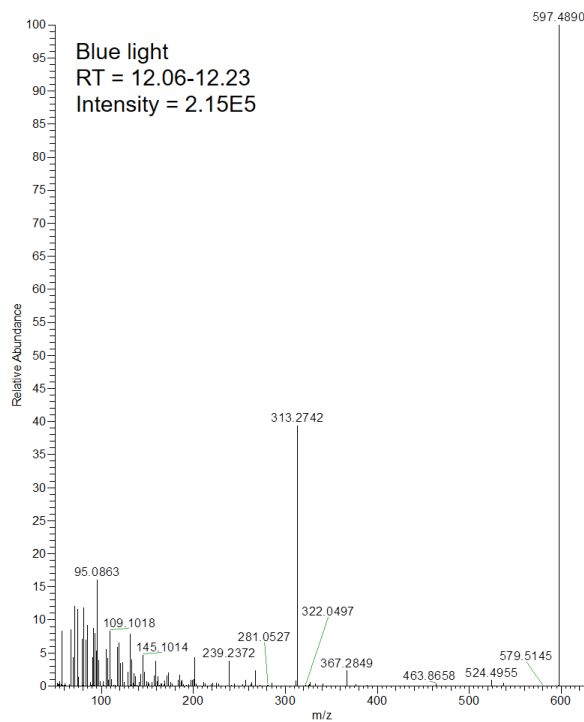
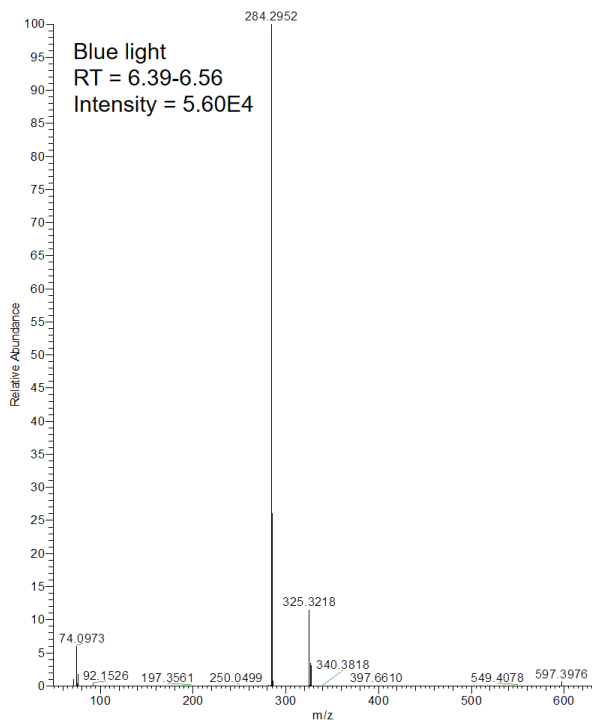


Figure 84 - MS/MS spectrum of two different peaks (retention time: 6.39-6.56 and 12.06-12.23) with masses similar to astaxanthin from samples cultivated under blue light (PRM).

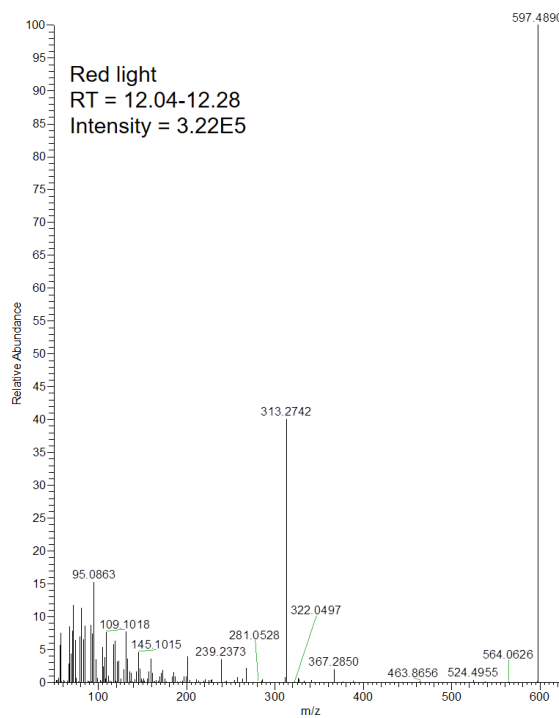
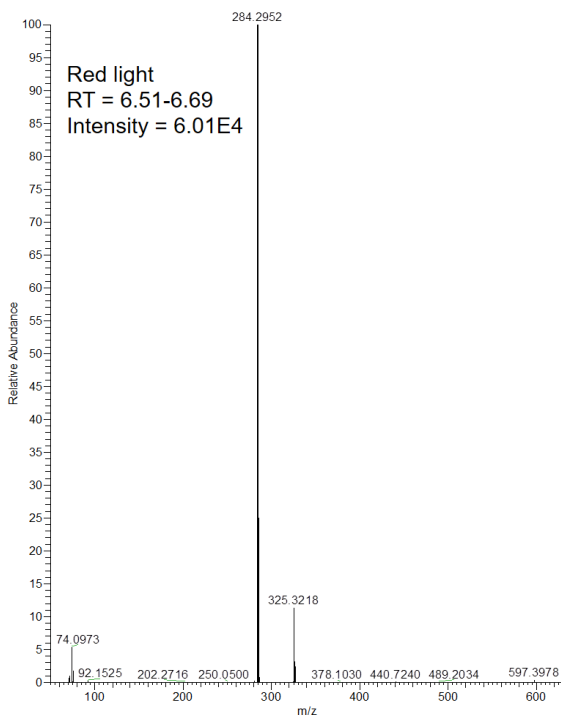


Figure 85 - MS/MS spectrum of two different peaks (retention time: 6.51-6.69 and 12.04-12.28) with masses similar to astaxanthin from samples cultivated under red light (PRM).

Appendix 13: MS/MS of pigments

Table 19 - UPLC-MS/MS of standard sample (DHI) and of algae sample. The theoretical masses of parent ion and masses of major fragments (theoretical, standard (DHI) and from algae samples) are presented.

Pigment	[M+H] or M ⁺	Fragments (m/z)			References
		Theoretical	Standard (DHI)	<i>P. glacialis</i>	
Chlorophyll c2	609.1	549.2 and 591.3	-	549.2, 591.2	(36, 39)
fucoxanthin	659.4 and 681.2**	641, 581 and 527.3	527.3**	581.4, 641.4 and 527.3**	(36, 55)
Astaxanthin	597.3	579.4, 561.4 and 147.1	579.4, 561.4 and 147.1	579.4 and 147.1*	(56)
Diadinoxanthin	583.4	221.2	221.2	221.2	(57)
Alloxanthin	564.4	549.4	549.4*	549.4*	(36)
Diatoxanthin	566.4	119.1	119.1*	119.1	
Zeaxanthin	568.4	476.6 and 283.2	476.4 and 283.2	476.4 and 283.2	(58)
Lutein	569.4	476.6 and 283.2	-	-	(58)
DV chlorophyll a	891.5	613.2	613.3 and 581.2	-	(36)
Chlorophyll a	893.5	615.2, 583.2 and 555.2	615.2, 583.2 and 555.2	615.2, 583.2 and 555.2	(38)
Pheophytin a	871.6	593.3 and 533.3	593.3 and 533.3	593.3 and 533.3	(36)
Carotene	536.4	444.4, 69.0, 177.4, 137.4	444.4, 177.2, 137.1 and 69.1	444.2, 177.2, 137.1 and 69.1	(22, 58)
Mg-DVP	611.2	-	285.2	285.2	

*Low signal, could be just noise. **Na-adduct

Appendix 14: Q-test chlorophyll a

Table 20 – Q-test on chlorophyll a concentrations based on peak area and peak intensity (n=9). Reject if calculated Q-value is over 0.493 (95% CI, n=9) and 0.526 (95% CI, n=8). *Denotes parallel one injection two.

Red area (n=9)	Testing	Q-value	Red area (n=8)	Testing	Q-value
147.2	289.3	0.728	147.2	147.2	0.398
162.6	147.2	0.108	162.6	185.9	0.190
165.9			165.9		
166.1			166.1		
173.9			173.9		
176.4			176.4		
178.6			178.6		
185.9			185.9		
289.3*					
Blue area (n=9)	Testing	Q-value	Blue area (n=8)	Testing	Q-value
153.7	239.3	0.271	203.3	239.3	0.645
203.3	153.7	0.580	205.5		
205.5			207.2		
207.2			208.1		
208.1			212.7		
212.7			212.8		
212.8			216.1		
216.1			239.3		
239.3*					
White area (n=9)	Testing	Q-value	White area (n=8)	Testing	Q-value
212.2	309.9	0.646	212.2	246.8	0.402
214.1	212.2	0.019	214.1		
215.1			215.1		
218.6			218.6		
226.5			226.5		
228.3			228.3		
232.9			232.9		
246.8			246.8		
309.9*					
Red intensity (n=9)	Testing	Q-value	Red intensity (n=8)	Testing	Q-value
143.0	283.8	0.717	143.0	182.8	0.077
155.2	143.0	0.087	155.2	143.0	0.308
159.3			159.3		
160.3			160.3		
167.4			167.4		
170.5			170.5		

179.7			179.7		
182.8			182.8		
283.8*					
Blue intensity (n=9)	Testing	Q-value	Blue intensity (n=8)	Testing	Q-value
133.8	208.3	0.192	181.7	208.3	0.538
181.7	133.8	0.644	181.7		
181.7			186.8		
186.8			187.9		
187.9			193.0		
193.0			194.0		
194.0			194.0		
194.0			208.3		
208.3*					
White intensity (n=9)	Testing	Q-value	White intensity (n=8)	Testing	Q-value
187.9	270.5	0.593	187.9	221.5	0.455
187.9	187.9	0.000	187.9		
189.9			189.9		
194.0			194.0		
195.0			195.0		
202.1			202.1		
206.2			206.2		
221.5			221.5		
270.5*					

Table 21 – Q-test on chlorophyll a concentrations in each parallel (p) for peak area and peak intensity. Reject if calculated Q-value is over 0.970 (95% CI, n=3).

Red area p.1	Testing	Q-value	Red area p.2	Testing	Q-value	Red area p.3	Testing	Q-value
147.2	289.3	0.728	162.6	173.9	0.706	166.1	178.6	0.171
185.9	147.2	0.272	165.9	162.6	0.294	176.4	166.1	0.829
289.3			173.9			178.6		
Blue area p.1	Testing	Q-value	Blue area p.2	Testing	Q-value	Blue area p.3	Testing	Q-value
153.7	239.3	0.375	203.3	208.1	0.543	212.7	216.1	0.981
207.2	153.7	0.625	205.5	203.3	0.457	212.8	212.7	0.019
239.3			208.1			216.1		
White area p.1	Testing	Q-value	White area p.2	Testing	Q-value	White area p.3	Testing	Q-value
212.2	309.9	0.646	226.5	232.9	0.725	214.1	218.6	0.763
246.8	212.2	0.354	228.3	226.5	0.275	215.1	214.1	0.237
309.9			232.9			218.6		
Red intensity p.1	Testing	Q-value	Red intensity p.2	Testing	Q-value	Red intensity p.3	Testing	Q-value
143.0	283.8	0.717	155.2	170.5	0.733	160.3	179.7	0.632
182.8	143.0	0.283	159.3	155.2	0.267	167.4	160.3	0.368
283.8			170.5			179.7		
Blue intensity p.1	Testing	Q-value	Blue intensity p.2	Testing	Q-value	Blue intensity p.3	Testing	Q-value
133.8	208.3	0.356	181.7	194.0	0.083	186.8	194.0	0.857
181.7	133.8	0.644	193.0	181.7	0.917	187.9	186.8	0.143
208.3			194.0			194.0		
White intensity p.1	Testing	Q-value	White intensity p.2	Testing	Q-value	White intensity p.3	Testing	Q-value
187.9	270.5	0.593	195.0	206.2	0.364	187.9	194.0	0.667
221.5	187.9	0.407	202.1	195.0	0.636	189.9	187.9	0.333
270.5			206.2			194.0		